UNITED STATES DEPARTMENT OF THE INTERIOR

GEOLOGICAL SURVEY

Geological and geochemical studies in the Wadi Bidah district, Kingdom of Saudi Arabia

by

C. W. Smith, B. C. Waters 1/, M. Naqvi, R. G., Worl 2/,

A. M. Helaby, V. J. Flanigan 2/, H. Sadek, and R. M. Samater

Open-File Report 83-672

Prepared for Ministry of Petroleum and Mineral Resources,
Deputy Ministry for Mineral Resources
Jiddah, Kingdom of Saudi Arabia

This report is preliminary and has not been reviewed for conformity with U.S. Geological Survey editorial standards and stratigraphic nomenclature.

1/ Consolidated Mining Company, Vancouver, British Colombia

2/ U.S. Geological Survey, Denver, Colorado

1983

CONTENTS

Page

ILLUSTRATIONS

[Plates are in pocket]

TABLES

GEOLOGICAL AND GEOCHEMICAL STUDIES IN THE WADI BIDAH DISTRICT, KINGDOM OF SAUDI ARABIA

by

C. W. Smith, B. C. Waters[1], M. Naqvi, R. G. Worl[2],

A. M. Helaby, V. J. Flanigan[2], H. Sadek, and R. M. Samater

ABSTRACT

Geological and geochemical followup studies of airborne electromagnetic anomalies in the Wadi Bidah district, southwestern Saudi Arabia, did not reveal metals of economic grade.

Investigation of an anomaly enclosing the Rabathan ancient mine disclosed tightly folded and sheared Proterozoic tuffaceous rocks interlayered mostly with chert, dolomite, carbonaceous rocks, and volcanic wacke including cherty iron-manganese formations slightly anomalous in copper and zinc. Three drill holes placed to test anomalies within these formations yielded negative results.

Studies of a long, narrow anomaly north of the Rabathan area indicated a similar geological environment. This northern area also contains limited zones that are highly anomalous in copper and zinc and extensive zones that are slightly anomalous in those metals. Drilling was not undertaken in this area.

The Bilajimah airborne electromagnetic anomaly west of Wadi Bidah coincides with a broad synclinorium of layered felsic tuffs and gossans. Geochemical studies indicated slightly anomalous copper, zinc, and silver values in gossans within the anomaly area. Two drill holes intersected carbonaceous rock that contained approximately 15 percent pyrrhotite and traces of sphalerite and chalcopyrite.

Two geophysically anomalous areas west of Wadi Bidah surround ancient mines at Mahawiyah and Khayal al Masna'ah. Results of geochemical sampling at these workings were positive. An airborne electromagnetic anomaly located in the Assifar area in the southwestern corner of the Wadi Bidah district is underlain principally by metasedimentary rocks that include large linear zones of cherty iron-manganese formation and a few gossans containing secondary base metal minerals.

[1] Consolidated Mining Company, Vancouver, British Columbia

[2] U.S. Geological Survey, Denver, Colorado

Detailed mapping and sampling of the Mulhal ancient mine, located west of Wadi Bidah, revealed two types of polymetallic gossans: (1) stratiform deposits interlayered with ignimbrites and mafic volcanic rocks and (2) barite-bearing gossanous material in shear zones that grade into hydrothermally altered shear zones and extend beyond the mine area. The gossans and gossanous shear zones contain anomalous amounts of gold, silver, lead, copper, zinc, barium, and selenium.

Two gossans west of Wadi Bidah were mapped and sampled in detail; both gossans are interlayered with siliceous volcanic rocks. Although the gossan at Jabal Mohr covers a large area, it contains low amounts of precious and base metals. The gossan at Mulhal No. 2 contains moderate to high amounts of gold, silver, copper, lead, and zinc.

INTRODUCTION

The center of the Wadi Bidah district, Kingdom of Saudi Arabia, is located approximately at lat 20°30' N., long 41°20' E., and the main geographic feature of the district is a large north-draining wadi (figs. 1-3). The reader is referred to Kiilsgaard and others (1978) for a description of the geography of the Wadi Bidah district.

Numerous scientists have studied the Wadi Bidah district, and a brief chronology of both previous and present investigations is presented below. Impetus for the present study was the selection of the Wadi Bidah district as one of the areas to be covered in an airborne electromagnetic survey in 1977. Numerous anomaly areas were delineated during the survey (fig. 2), and Wynn and Blank (1979) outlined methods for appraisal of these areas. Subsequent ground electromagnetic and self-potential geophysical surveys further delineated zones of interest in anomaly areas B-13, B-25, B-26, B-29, and B-24 (Flanigan and others, 1981, 1982). Rock-chip sampling indicated isolated and very small copper and zinc anomalies. Drilling tested the best geophysical and geochemical anomalies in the B-29 (Rabathan, MODS 02701) and B-25 and B-26 (Bilajimah, MODS 02703) areas.

During the present investigation of the Wadi Bidah area, a detailed study was conducted of a gossan named Jabal Mohr (MODS 02827), which is located approximately 1.75 km southeast of the Sha'ab at Tare prospect (MODS 00464; fig. 3) and was discovered by the Riofinex Geological Mission (1979). During helicopter reconnaissance work, C. W. Smith discovered another gossan located 2.5 km southeast of the Mulhal ancient mine and informally named it Mulhal No. 2 (MODS 02702; fig. 3); detailed geological, geochemical, and geophysical surveys were later conducted.

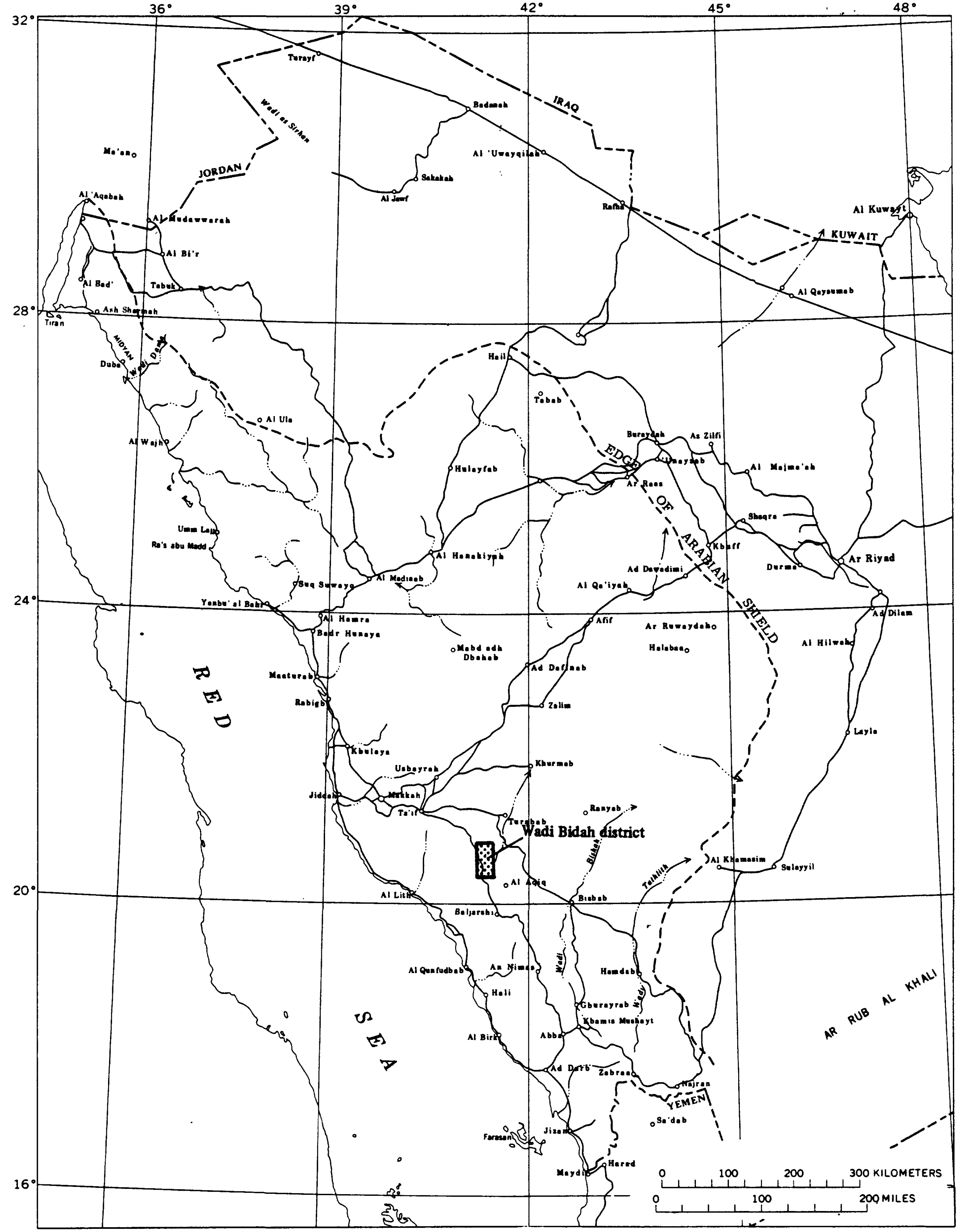

Figure 1.--Index map of western Saudi Arabia showing the location of the Wadi Bidah district.

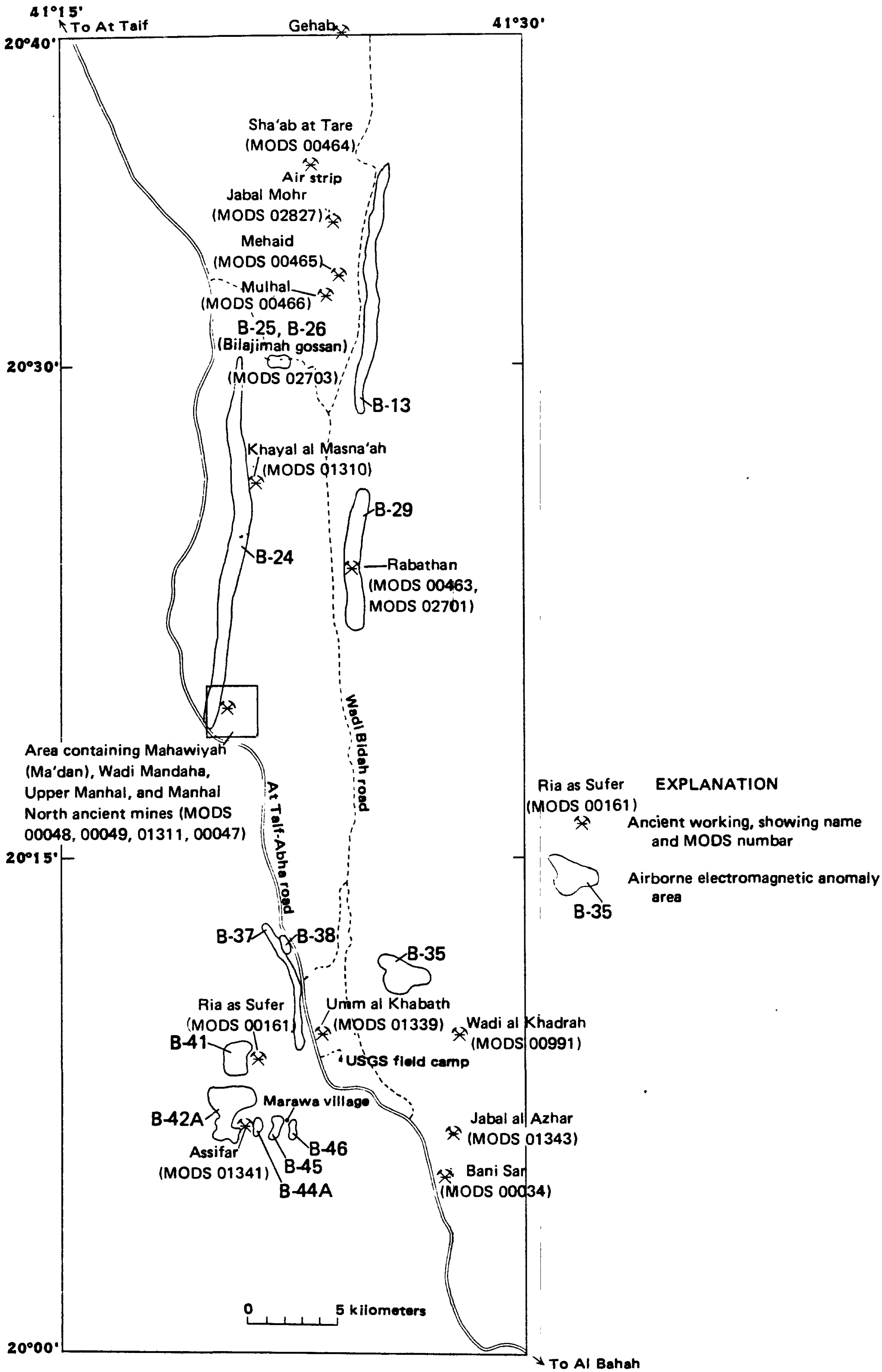

Figure 2.—Map of the Wadi Bidah district showing the locations of airborne electromagnetic anomalies and ancient mine workings.

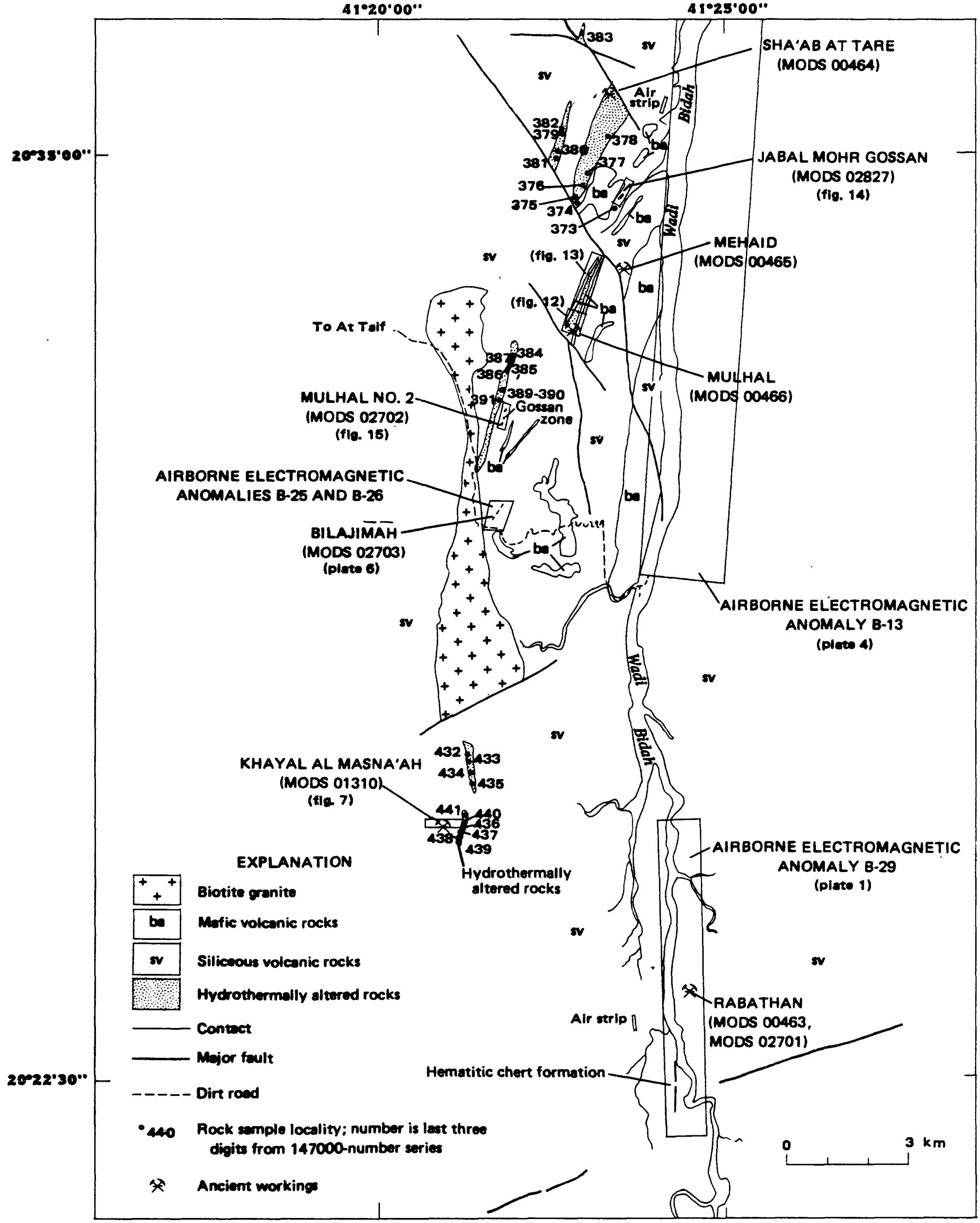

Figure 3.--Map of the northern part of the Wadi Bidah district showing reconnaissance geology, airborne electromagnetic anomalies, ancient workings, and sample locations.

The Mulhal ancient mine (MODS 00466) was restudied with emphasis on sampling for precious metal content. The ancient mine was mapped and sampled at a scale of 1:1,000, and a zone of rock alteration extending 1.8 km north of the ancient mine was mapped and sampled at a scale of 1:12,500.

Previous investigations

1936

T. P. Larken (1936), Saudi Arabian Mining Syndicate, examined an ancient mine at Jabal Azhar, which is the distance of a 3-hour northerly walk from the village of Bani Sar. He also examined and reported on As Sufer (MODS 01341), Ria As Sufer (MODS 00161), Bani Sar (MODS 00034), and Maadan (Mahawiyah) (MODS 00048).

1957

W. H. MacLean (1957), Saudi Arabian Directorate General of Mineral Resources (DGMR), visited and briefly reported on the Wadi Mandaha (MODS 00049) and Maadan ancient workings near the village of Al Mahawiyah.

1961-62, 1965-66

A shieldwide airborne magnetometer survey included the Wadi Bidah district. The survey was completed by a consortium including Aero Service Corporation, Hunting Geology and Geophysics Limited, Lockwood Survey Limited, and Arabian Geophysical and Surveying Company (ARGAS). The U.S. Geological Survey (USGS) analyzed the data (Hase, 1970).

1963

C. W. Smith and J. H. Kouther, DGMR, conducted a mineral reconnaissance survey and made a reconnaissance geologic map of a large part of the Wadi Bidah district. A 1:50,000-scale map shows the location of ancient workings at Mahawiyah, Khayal al Masna'ah (MODS 01310), Upper Manhal (Umm al Mahel) (MODS 01311), Rabathan (MODS 00463), Mehaid (MODS 00465), and Mulhal. All of the mines were cursorily sampled, and assay results and brief descriptions were given (Smith, 1963a). Smith and Kouther (Smith, 1963b) also mapped and sampled in detail the ancient workings at Wadi Mandaha.

The 1:500,000-scale geologic map of the Southern Hijaz quadrangle (including the Wadi Bidah district) was published (Brown and others, 1963).

1964

C. W. Smith (1964a), DGMR, mapped the geology of the area including the Mulhal and Sha'ab at Tare prospects.

C. W. Smith (1964b) also made a mineral reconnaissance survey of the Wadi Bidah district and produced a 1:50,000-scale map showing locations of the Izhab (Gehab) (MODS 00468) and Jabal Malas (Mulgatah; MODS 00467) workings, as well as those of the ancient mines that were located in 1963.

1964-65

R. Goldsmith, USGS, and J. H. Kouther, DGMR, conducted reconnaissance rock sampling and reported briefly on mines at Mulgatah, Ria As Saifer (Ria as Sufer), Mehaid, Mulhal, As Sut, Rabathan, Manhal, Manhal North (MODS 00047), Mandaha South, Mahawiyah, As Saifer (As Sufer), and Bani Sar. A mineral resources map showing most of the locations of known mineral deposits was prepared (Goldsmith, 1971).

1965

W. E. Davis and R. V. Allen (1970), USGS, conducted magnetometer, electromagnetic dip angle, and horizontal coil surveys at the Mehaid, Mulhal, Asut (As Sut), Mahawiyah, Mandaha, and Mandaha South workings and at the Kamden anomaly.

1966

V. A. Trent, USGS, and G. H. Sultan, DGMR, examined and reported on an airborne magnetic anomaly (Kamden anomaly) in the southeastern part of the Wadi Bidah district (Trent and Sultan, 1968).

L. Gonzalez (1970), USGS, panned alluvium samples in the Rabathan area in a test for gold content.

1966-69

R. L. Earhart and M. M. Mawad (1970), USGS, mapped the geology of a large part of the Wadi Bidah district at a scale of 1:50,000 and mapped in detail the geology of the Mulgatah, Gehab, Sha'ab at Tare, Mulhal, and Rabathan ancient mines. One hole was drilled at Mulgatah, five at Gehab, three at Sha'ab at Tare, and eight at Rabathan.

1967

An Austrian Geological Mission team including K. Metz, V. Ertl, F. Fehleissen, H. Litscher, and H. Petschnigg studied the structural geology of the Wadi Bidah-Mahawiyah area and made small-scale geologic maps of the region (Metz and others, 1971)

1968

G. H. Allcott (1969), USGS, conducted a geochemical survey of the Ma'dan (Mahawiyah) ancient mine area and made a brief report.

A helicopter-borne electromagnetic and magnetic survey by Sanders Geophysics Company included a narrow zone along the northern part of Wadi Bidah (Sanders, unpublished data).

1968-69

B. Jackaman (1972), Ph.D. candidate of the Imperial College of Science and Technology, London, mapped the geology of Wadi Bidah from the Gehab ancient mine southward to a region south of the Rabathan workings. He refined the stratigraphy of the area by using Earhart's classification (Earhart and Mawad, 1970), made laboratory studies of sulfides from drill-core samples, and studied geochemistry of layered rocks.

1969

H. H. Kazzaz (1969), DGMR, conducted Turam electromagnetic surveys at the Sha'ab at Tare and Gehab ancient mines.

1970

V. J. Flanigan, USGS, and H. Merghelani, DGMR, conducted a Turam electromagnetic survey over the Ma'dan (Mahawiyah) ancient workings (Flanigan, 1970).

G. H. Allcott (1970), USGS, drilled three holes at the Ma'dan (Mahawiyah) ancient mine.

L. Gonzalez, USGS, mapped part of the Wadi Shuqub quadrangle (sheet 20/41 A) at 1:100,000 scale; this quadrangle includes the northern two-thirds of the Wadi Bidah district (Greene and Gonzalez, 1980).

A. R. Abo-Rashid (1971), DGMR, mapped the geology of an area east of the village of Al Mahawiyah that includes the Mahawiyah ancient mine.

1970-71

W. R. Greenwood (1975), USGS, mapped the geology of the Jabal Ibrahim quadrangle at 1:100,000 scale. In the same report, R. G. Worl tabulated various mineral deposits of the quadrangle, including those of Wadi Bidah. Greenwood classified the layered rocks of Wadi Bidah as belonging to the Baish Group.

1972

T. H. Kiilsgaard and R. J. Roberts, USGS, reexamined the known sulfide deposits in Wadi Bidah and recommended additional exploration work. W. R. Greenwood and R. J. Roberts mapped the geology of the Rabathan mine at 1:500 scale. Greenwood also mapped in detail the ancient workings at Gehab and revised the mapping of Earhart and Mawad (1970).

V. J. Flanigan, USGS, and H. H. Kazzaz, DGMR, conducted self-potential geophysical surveys at the Sha'ab at Tare and Gehab ancient mines. They also made magnetic and gravity profiles across the southern end of the Rabathan ancient mine and an electromagnetic survey over the southern end of the Gehab deposit.

All of the above work is described in Kiilsgaard and others (1978).

1973

H. M. Merghelani, DGMR, conducted self-potential and electromagnetic surveys at Mulgatah (Kiilsgaard and others, 1978).

Two holes were drilled by the USGS at Sha'ab at Tare, four at Gehab, and six at Rabathan (Kiilsgaard and others, 1978).

R. G. Worl (1978), USGS, made a mineral reconnaissance study of various deposits in Wadi Bidah.

1973-74

V. J. Flanigan, USGS, and H. Merghelani, DGMR, conducted self-potential and Turam electromagnetic surveys over the ancient workings at Umm al Kabath (MODS 01339) (Worl, 1978).

W. R. Greenwood, R. J. Roberts, T. H. Kiilsgaard, W. Puffet, and I. M. Naqvi, USGS, summarized the types of sulfide deposits in Wadi Bidah and commented on their origin (Greenwood and others, 1974).

1974

One hole was drilled at Mulgatah by the USGS (Kiilsgaard and others, 1978).

Three holes were drilled at Umm al Khabath by the USGS (Worl, 1978).

1974-75

Z. Al Koulak (unpub. data), USGS, mapped the Mahawiyah (Ma'dan) ancient mine area in detail and conducted a geochemical survey.

1976

R. J. Roberts and H. R. Blank, USGS, made a field survey of the sulfide deposits of Wadi Bidah to plan the limits of a proposed airborne geophysical survey (ARGAS, 1978).

1977

Geoterrex conducted airborne electromagnetic and magnetometer surveys in the Wadi Bidah district (ARGAS, 1978).

R. C. Greene, USGS, completed the mapping of the Wadi Shuqub quadrangle begun by Gonzalez. Greene and Gonzalez (1980) classified layered rocks in the quadrangle in numerical order from east to west.

M. M. Mawad (1980), USGS, made a detailed geologic map and conducted a geochemical survey at the Wadi Mandahah ancient mine. Three diamond drill holes were completed.

H. M. Merghelani, DGMR, conducted self-potential and Turam electromagnetic surveys over the the Wadi Mandahah ancient mine (Mawad, 1980).

1978

J. C. Wynn and H. R. Blank (1979), USGS, examined and classified the geophysical anomalies in Wadi Bidah.

The Riofinex Geological Mission (1979) mapped geology in the northern part of Wadi Bidah district, discovered a gossan-bearing base metal deposit at Wadi Leif (MODS 02013), and drilled two angled holes to test the gossan. It also made prospect evaluations of Mulgatah, Gehab, Sha'ab at Tare, Rabathan, and Wadi Leif.

ARGAS (1978) conducted preliminary ground electromagnetic and self-potential surveys over nine airborne electromagnetic anomaly areas in the Wadi Bidah district.

R. G. Worl and V. J. Flanigan (oral commun., 1978), USGS, made a ground evaluation of a number of airborne electromagnetic anomaly areas.

1979

ARGAS field crews conducted electromagnetic and self-potential ground geophysical surveys in the Wadi Bidah airborne electromagnetic anomaly areas B-29, B-13, B-25, B-26, B-24, and B-35 and in the Khadrah area.

Present investigations

1979

R. G. Worl and J. C. Wynn mapped and sampled in detail an area that includes the ancient mines at Khadrah (MODS 00991) in the southeastern part of the Wadi Bidah district (Worl and Wynn, unpublished data).

V. J. Flanigan acted as the USGS field representative for geophysical ground surveys conducted by ARGAS in Wadi Bidah. In addition, he conducted independent ground magnetic surveys and produced interpretational maps from geophysical data.

C. W. Smith and A. M. Helaby conducted rock-chip sample geochemical surveys along geophysical survey lines at Wadi Bidah airborne electromagnetic anomaly areas B-29, B-13, B-25, B-26, and B-24 (northern end). Smith and Helaby also mapped the geology of area B-29.

B. C. Waters, consultant for USGS, mapped in detail the geology of anomaly areas B-25 and B-26 (Bilajimah) and B-13.

1979-80

The USGS drilled three holes at anomaly area B-29 and two holes at anomaly areas B-25 and B-26.

1980

T. H. Kiilsgaard (1982) mapped and sampled in detail anomaly area B-35 in the southeastern part of Wadi Bidah.

C. W. Smith and M. Naqvi mapped and sampled in detail the Jabal Mohr gossan (MODS 02827) and the Mulhal No. 2 gossan (MODS 02702) and remapped and sampled the Mulhal ancient mine. Smith also mapped and sampled a hydrothermally altered zone extending north from the Mulhal ancient mine.

V. J. Flanigan and C. L. Tippens conducted postdrilling geophysical surveys at anomaly area B-29. Both electromagnetic and self-potential methods were used. Similar surveys were conducted at the Jabal Mohr gossan (Flanigan and others, 1982).

V. J. Flanigan, C. W. Smith, and H. Sadek made reconnaissance studies of anomaly areas B-44A, B-45, B-42A, and B-37.

ARGAS crews conducted ground electromagnetic and self-potential surveys in anomaly areas B-44A, B-45, B-42A, and B-37 and at Mulhal No. 2. They conducted induced potential surveys at anomaly areas B-25, B-26, B-44, and B-45 and at Khadrah.

M. Naqvi and Mir Amjed Hussein sampled and mapped anomaly areas B-44A and B-42A. These areas are about 10 km west of the At Taif-Bisha highway and were the final areas to be studied in the ground-followup phase.

STRATIGRAPHY AND STRUCTURE OF THE WADI BIDAH DISTRICT

Stratigraphy

Previous studies

The first attempt to define the stratigraphy of the layered rocks in the Wadi Bidah district was by Earhart and Mawad (1970), who classified the basalt-andesite assemblage on the eastern side of the wadi as "Older Volcanic Rocks," all layered rocks in the wadi bottom as "Metasedimentary Rocks," and the generally felsic assemblage on the western side of the wadi as "Younger Volcanic Rocks." They proposed a north-trending anticlinal axis about 2 km east of the wadi; according to this interpretation, unless complicated by faulting, the layered rocks are progressively younger toward the west. Jackaman (1972) mapped approximately the same area as Earhart and Mawad and closely agreed with their stratigraphic succession. He maintained more or less the same stratigraphic divisions, naming them the Sharq, Bidah, and Gharb Groups, respective to the divisions of Earhart and Mawad. According to Jackaman's stratigraphy also, younger layered rocks are to the west.

In 1978, geologists of the Riofinex Geological Mission (1979) mapped mostly in the northern part of Wadi Bidah, their work being concentrated on the western slopes of the wadi. They postulated an anticlinorium having north-trending axes lying west of the ancient mines at Mulhal and Gehab; the core of the anticlinorium was intruded by small granitic plutons. Consequently, according to their theory, layered rocks become progressively younger to the east. This relationship is in agreement with our experience that layered rocks in the region generally dip steeply east.

W. R. Greenwood (1975), USGS, mapped the Jabal Ibraham quadrangle, which includes the southern part of the Wadi Bidah district, and classified all of the layered rocks in Wadi Bidah as belonging to the Baish Group; this assignment makes the rocks of Wadi Bidah among the oldest layered rocks in the Arabian Shield. Kiilsgaard and others (1978) maintained this classification. The Wadi Shuqub quadrangle, which includes the northern part of the Wadi Bidah district, was mapped by Greene and Gonzalez (1980), who did not assign the layered rocks to any group and stated "the true stratigraphic order of the units, however, is uncertain."

Table 1 (following) is taken in entirety from the report of the Riofinex Geological Mission (1979) and succinctly presents the stratigraphic succession according to five independent studies.

Table 1.--Stratigraphic nomenclature of Proterozoic metavolcanic and metasedimentary rocks, Wadi Bidah district

Earhart and Mawad (1970)	Jackaman (1972)	Greenwood (1975); Kiilsgaard and others (1978)	Riofinex (1979)
Younger Volcanic Rocks	Gharb Group	Baish Group	Sharq group
Metasedimentary Rocks	Bidah Group	Baish Group	Bidah group
Older Volcanic Rocks	Sharq Group	Baish Group	Gharb group

Present studies

The stratigraphic succession in the Wadi Bidah district is very difficult to determine because isoclinal folding, shearing, and metamorphism have destroyed many of the original rock textures. In most cases, therefore, whatever evidence is gathered concerning successive layering must necessarily be of the indirect type. However, Waters suggests in the present report that section tops are to the west, on the basis of direct evidence from mapping in the B-13 area. The senior author closely examined the lower shale unit mapped by Waters in the B-13 area. This unit is finely laminated and is one of the best exposures of bedding in Wadi Bidah. Truncated crossbedding within the shale indicates that the top of the section is toward the west in this particular area. Detailed mapping (plate 1) by the senior author in the B-29 (Rabathan) area gave no direct evidence concerning stratigraphic succession. Only the east to west progression of volcanic layered rocks from mafic to silicic indicates that stratigraphic tops are probably toward the west in this area. Waters' detailed map of the B-25 and B-26 (Bilajimah) areas shows a broad syncline that has an amplitude of about 250 m; this syncline is clearly marked by the extensively layered gossan. However, the senior author's detailed mapping of the Jabal Mohr and Mulhal No. 2 gossans to the north (fig. 3) indicates tight isoclinal folding and extensive shearing. Detailed mapping at the Mulhal ancient mine (fig. 3) indicates highly sheared, siliceous volcanic rocks that generally dip steeply east.

Such evidence gives very little assurance that observations in one place may pertain to all of the region. However, most evidence suggests that the layered rocks become younger toward the west. Greenwood (1975) mapped a syncline west of the town of Al Bahah in which Bahah group metasedimentary rocks overlie Baish group volcanic rocks. On the basis of this evidence, he placed Bahah group rocks stratigraphically above Baish group rocks. This relationship agrees with the hypothesis that progressively younger layered rocks crop out in a westerly direction because the majority of Bahah group rocks crop out west of the Wadi Bidah district and are in contact with Baish group rocks (Greenwood, 1975).

Because the present study entailed detailed mapping of small, widely dispersed areas, no attempt was made to correlate layered rocks from one area to another, except in areas B-29 (Rabathan) and B-13 (fig. 3). In these areas, layered rock units, especially a very distinctive lapilli tuff bearing stubby pyroxene crystals, may be traced along Wadi Bidah for a distance of more than 4 km. The lapilli tuff was also noted just west of the At Taif-Abha highway, near the USGS camp and approximately 2 km northwest of anomaly areas B-42A and B-44A (fig. 2). Another marker horizon in the district is a hematitic chert layer, the northern end of which is in the Rabathan area (plate 1, fig. 3); this chert layer extends far to the south of the index map area. This unit may correlate with other mapped chert units west of Wadi Bidah (Greenwood, 1975), but such a relationship is tenuous at best. Much more traversing and mapping in directions normal to the north-trending fold axes in the area are needed to truly understand the general stratigraphic sequence in the region.

Structure

Isoclinal folding about north-trending axes is typical of the general area. In many places in the district, especially in the Wadi Bidah valley bottom, folding has progressed to such an extent that the rocks have sheared. Graphitic schists are the loci of shear zones in most places along the valley bottom. These shear zones are extensive and many indicate right-lateral movement. Some are as wide as 20 m; most are vertical or subvertical. The shear zones are distinguished by their weathering and erosional characteristics and commonly form topographic saddles underlain by soil consisting of iron-stained sericite and clay. Rocks in the Wadi Bidah valley bottom range in competency from massive dolomite to graphitic schist, and shearing has occurred in all except the most competent rocks. Ordinarily the dolomite lenses are boudinized. Detailed mapping shows that the folding is complex and that the rocks have been refolded by varying directional stress components.

Smith does not agree with Waters' model (presented herein) of the Wadi Bidah valley bottom in which he depicts sedimentary rocks folded into a syncline. Smith's most important objection is that the layered rocks do not correlate from limb to limb. A very distinctive and easily identifiable layer of pyroxene-bearing crystal tuffaceous rock extends along the western side of the valley where Waters mapped. In Water's cross sections he depicts a facies change between the western and eastern sides of the wadi, in which pyroxene tuff interfingers with andesite-dacite flow rocks. The pyroxene tuff is widespread in extent and it would be coincidental if this facies change did take place along the valley bottom. Smith's mapping in the valley bottom indicates extremely tight isoclinal folding and shearing with no recognizable repetition of layered rocks either east or west.

A general comparison of rock types between areas B-29 and B-13 shows a lateral facies change from fine-grained tuffaceous rocks in the B-29 area to more shaly rocks in the B-13 area. The simplified stratigraphic sections in table 2 are used to compare two authors' lithologic interpretations.

Table 2.--Simplified stratigraphic sections for two mapped areas in the Wadi Bidah valley bottom

	B-29 area	B-13 area
Gharb group	Pyroxene crystal tuff	
Bidah group	Dolomite Cherty iron-manganese formation Calcareous quartz schist	Silty limestone Cherty iron-manganese rocks
Sharq group	Basaltic and andesitic flow rocks, tuffs, and breccias	Pyroxene crystal tuff Lower shale Lower andesite

Structural details of the Wadi Bidah district have been described by many authors and will not be repeated here.

B-29 ANOMALY AREA, RABATHAN

The B-29 anomaly area, which includes the Rabathan ancient mine, is a long, slender, north-trending belt of rocks that lies along the Wadi Bidah valley (plate 1). The eastern side of the valley is very steep, and in many places valley walls are nearly vertical where more massive rocks of the basalt-andesite assemblage form fault scarps. Slopes on the western side of the valley are more gradual, except at the southern end of the valley. The Wadi Bidah riverbed and alluvium and colluvium cover nearly half of the surface area.

Layered rocks

Sharq group

Basaltic and andesitic flow rocks, tuffs, and breccias.--Basaltic and andesitic flow rocks, tuffs, and breccias are thought to be the oldest layered rocks in the mapped area (plate 1). They crop out on the eastern side of the valley and are in faulted contact with the metasedimentary-metavolcanic rocks to the west. They are composed partly of amygdaloidal flow rocks and also include thick sections of pyroclastic rocks ranging from tuff to breccia. They are more massive and less foliated than the adjacent layered rocks to the west. Because they do not contain sulfide deposits, they were not studied in detail.

Bidah group

Calcareous quartz schist.--Gray-green, fine-grained calcareous quartz schist crops out over much of the valley floor in the area (plate 1). This unit was named by Kiilsgaard and others (1978) during their detailed work at the Rabathan ancient mine area. The origin of these rocks is difficult to determine. Locally they have thin carbonaceous seams, fine-grained quartz aligned with foliation, and perhaps layering. They also show faint feldspar relicts in some places. These rocks probably represent subaerial ashfall tuffs that locally grade into mudstone and are interlayered with dolomite, carbonaceous layers, cherty iron-manganese formations, and gossans.

Carbonaceous-tuffaceous schist.--The carbonaceous-tuffaceous schist unit is difficult to recognize in outcrop and most certainly underlies more of the mapped area than is shown (plate 1). The schist weathers to sericite and clay and is iron stained and moderately friable. Fresh rock displays alternating thin layers, 2-4 mm thick, of cream-colored siliceous tuff and carbonaceous material. Within the tuff, pyrite is ordinarily aligned along the layers. These schists form topographic saddles in many places in the wadi valley and probably grade into the easily recognizable carbonaceous schist unit.

Cherty iron-manganese formation.--Ferruginous and manganiferous cherts occur as lenticular-shaped layers within the calcareous quartz schist and, in many places, are adjacent to dolomitic lenses (plate 1). They were mapped on the basis of their contrasting texture and color, as compared with the enclosing rocks. Some lenses grade into carbonaceous schist or pure gray layered chert. The cherts are predominantly siliceous and locally contain pockets of goethite and jarosite or manganese oxide. Hematite is pervasive throughout much of the rock. The cherty lenses have been fragmented enough in some areas to allow the deposition of stockworklike systems of milky quartz stringers. The cherts are dark gray and have a slightly brecciated appearance on fresh surfaces. They have a dark-brown to black, shiny luster on weathered surfaces. They contain thin contorted wisps of carbonaceous material and pyrite, which varies in form from very fine disseminations to fracture fillings to patches as much as 2 cm in diameter. The manganiferous pods at the surface are dark gray to black, massive, friable, and earthy. The manganiferous mineral was determined to be mostly pyrolusite (MnO_2).

Throughout the length of the mapped area, the cherty lenses are found within the calcareous quartz schist. Individual lenses are as long as 200 m and ordinarily are from 10 to 20 m wide. A hematitic chert layer extending along the western side of the area from 900 N to 2300 N (plate 1) is included within this unit in the mapped area. This layer very closely resembles a chert layer that extends to the south for many kilometers (fig. 3) and is probably a different chert horizon from those previously described. In contrast to the cherty iron-manganese lenses, this chert layer stands in bold relief and appears to be more or less continuous. On weathered surfaces it is medium brown. It has a slightly brecciated appearance in most places; in some areas it is cut by milky quartz veins, and it probably has an average thickness of 15 m.

Gossan.--Outcrops of gossan are small and usually have unclear stratigraphic positions. In the well-documented case of the Rabathan ancient mine, the gossan and underlying sulfides are between dolomite or calcareous rock and carbonaceous-tuffaceous schist. The sulfide lens intersected by drill hole R-2 (plate 1) is enclosed by siliceous, limey, and chloritic pyroclastic rocks and by siliceous carbonate rocks, as described by Earhart and Mawad (1970). These rocks correspond to the calcareous quartz schist, as defined in the present report, and do not appear to be associated with either cherty or dolomitic layers. Drill hole R-3 (near 5100 N, plate 1) undercut a typical cherty iron-manganese layer and, on a steeply east dipping projection, intersected 4.3 m of massive to richly disseminated base metal-bearing sulfides. These relationships suggest that somewhere between the surface and the drill hole intersection the cherty iron-manganese formation grades into massive sulfides. In surface mapping of an area adjacent to the East fault, a facies change was noted between 5100 N and 6100 N (plate 1), and, at several localities within this area, cherty iron-manganese rocks grade laterally into goethite-hematite gossans. These gossans are only a few meters long and very narrow and were not mapped on plate 1. At 500 N, 200 W, a gossan at the contact between calcareous quartz schist and graywacke is as thick as 2 m, siliceous, and massive and contains no visible copper staining. This gossan disappears under alluvium to the north and pinches out to the south, although other pods were mapped on strike several hundred meters to the south. The gossan, which is undoubtedly the weathering product of sulfides, is positioned in an almost totally different environment from those just described.

Results of mapping show that most gossans and related sulfides are not confined to any specific stratigraphic horizon within the Rabathan area, although they are generally located in calcareous quartz schist. In the stratigraphic column on plate 1, the gossan unit has been placed between the cherty iron-manganese formation and a buff-colored dolomite because the majority of lenses were found in that position.

Dolomite.--Buff-colored dolomite lenses were found within the calcareous quartz schist in close association with cherty iron-manganese rocks and carbonaceous schist (plate 1). In general, the dolomite is massive and forms ridges. Individual dolomite lenses are less than 40 m wide and from 2 to 300 m long. The dolomite is not bedded, and on many fresh surfaces bright-green chlorite resembles malachite. In places, contacts between the dolomite and graphitic material are gradational; isolated dolomite lenses are a few centimeters long and gradually increase in size toward a dolomite outcrop. Jackaman (1972) stated that the dolomite contains phosphate in varying amounts.

Calcareous quartz schist is commonly replaced by dolomite for several centimeters along both sides of fractures, a fact which suggests that at least part of the unit was deposited by metasomatic processes. These fractures generally cross the dolomite, and replacement has occurred where the fractures extend into the schistose rocks. The metasomatism may represent a local form of diagenesis in which some of the dolomite has been remobilized and reprecipitated along fractures.

Carbonaceous schist.--Although carbonaceous schist lenses generally crop out west of the cherty iron-manganese lenses and dolomite, they may be higher in the stratigraphic section but still lie within the calcareous quartz schist unit (plate 1). The schist lenses are easily recognizable in outcrop, being dark gray, black, or brown. Some of the lenses are composed of nearly pure carbon, and the lenses may also have gradational contacts with the calcareous quartz schist. Although the lenses are usually only a few meters wide and vertical, in the northern part of the map area they extend for long distances.

Graywacke.--The graywacke consists of lithic fragments cemented by fine sericite and clay (plate 1). It is poorly sorted and grades from very fine grained, barely visible individual grains to coarse-grained angular fragments as much as 2 mm in diameter. Individual grains consist mainly of quartz and plagioclase. The mafic minerals have been completely altered to epidote or chlorite, and in many places the graywacke has been mapped on the basis of high epidote content. Because the graywacke is less schistose than the calcareous quartz schist and weathers to more massive forms, it is distinguishable in many places on aerial photographs. In much of the area, lenses of graywacke are as thick as 160 m and are enclosed by calcareous quartz schist. However, because the graywacke also crops out in contact with dacitic lapilli tuff and dacitic pyroclastic breccia, it has been shown separately in the stratigraphic column.

There is no evidence that the graywacke is comprised of poorly sorted volcanic fragments deposited by stream action into a rapidly subsiding basin. Instead, the graywacke may have been deposited as lithic ash or tuff, and, in some places, especially on the west bank of Wadi Bidah, it exhibits a general westward increase in fragment size. Regardless of origin, the unit contains rocks of volcanic derivation closely related to most other layered rocks in the area.

Gharb group

Dacitic lapilli tuff.--The dacitic lapilli tuff is gray green on weathered surfaces and characteristically contains black pyroxene crystals as long as 1 cm (plate 1). It is very schistose and in places contains pink orthoclase crystals. The matrix of the tuff displays little structure and is composed mainly of platelets of chlorite and sericite. The unit is as thick as 50 m and may grade into dacitic pyroclastic breccia, these two units having been separated mainly on the basis of clast size. The tuff is definitely of pyroclastic origin and is a very good marker bed.

Dacitic pyroclastic breccia or tuff lava.--The dacitic pyroclastic breccia contains angular fragments as long as 30 cm and from 10 to 15 cm thick (plate 1). In some places the fragments are clearly distinguishable from the matrix because of their lighter gray color. Both fragments and matrix contain stubby black pyroxene crystals. The matrix of the dacitic pyroclastic breccia contains sporadically abundant pink orthoclase crystals, consists mainly of chlorite, quartz, and sericite, and is practically featureless. The unit includes a few thin, discontinuous flows of pillow basalt. The dacitic breccia is clearly of pyroclastic origin and its average thickness is nearly 40 m.

Amygdaloidal andesite and basalt.--Amygdaloidal andesite and basalt were mapped only in the northwestern corner of the area (plate 1). The rocks are dark green, massive, and probably flow banded and contrast sharply with adjacent layered rocks. Pillow basalts occur locally within this unit.

Intrusive rocks

Syntectonic quartz diorite-microdiorite crops out on both sides of the valley in elongate belts parallel to schistosity and layering (plate 1). On the western side of the Wadi Bidah valley, the diorite contains large areas of chilled margins. In its interior, away from the chilled margins, the rock is a medium-grained hornblende quartz diorite.

Structure

The eastern side of the Wadi Bidah valley is bounded by a major fault zone named the East fault by Earhart and Mawad (1970) (plate 1). The eastern wall of the valley is a fault scarp along which basalt and andesite flow rocks and tuffs are relatively free of foliation and shearing. Because the fault offsets no marker horizons, neither horizontal nor vertical displacement can be measured. However, wide zones extending out from the fault have been affected by drag folding. In some areas displacement along numerous faulted segments has left isolated wedges of dolomite and calcareous quartz schist within basaltic and andesitic flow rocks and tuffs. Fracturing appears to have occurred mostly in carbonaceous-tuffaceous schist west of the fault, the carbonaceous seams having acted as lubricants.

Related faulting may be found in other parts of the valley. From 5100 N to 6300 N, a major shear zone centered on carbonaceous-tuffaceous schist is in contact with graywacke (plate 1). This shear zone, which is 20 m wide in drill hole RAB-2, can be traced for long distances at the surface and is undoubtedly directly related to the East fault. Probably much of the Wadi Bidah riverbed is the locus of a fault plane, as suggested by Jackaman (1972). Rocks west of the wadi strike into the riverbed at a low angle and then appear to be faulted out.

Layered rocks have been isoclinally folded and sheared to such an extent that their stratigraphic position within the B-29 area can only be generally ascertained. Buff dolomite, chert, and graphitic schist are repeated on both eastern and western walls of the wadi valley in the southern part of the mapped area, but it is not known if these rocks are exposures of the same formation or only segments of similar formations. In general, layered rocks are not repeated from east to west across the valley. Instead, they show an east to west progression from massive andesites and basalts through a metasedimentary series to siliceous pyroclastic rocks. All contacts are nearly vertical, and the only repeated layer is a thin andesite-basalt layer in contact with siliceous volcanic ejecta in the extreme northwestern part of the map area. There is no evidence to suggest that this thin andesite-basalt layer is stratigraphically related to the thick andesite-basalt sections on the eastern side of the Wadi Bidah valley.

Detailed geology of four areas within the B-29 anomaly area

Four areas within the B-29 anomaly area were mapped at 1:1,000 scale to provide more detail concerning the geology and structure of the region. Three of the areas include drill holes RAB-1, -2, and -3, and a fourth includes the area between 6050 N to 6350 N, from 350 E to 400 E (plates 1 and 2).

Geology of the area surrounding drill hole RAB-1

Most of the area surrounding drill hole RAB-1 is covered by a thin veneer of alluvium and colluvium, and in general only cherty iron-manganese and dolomite crop out (plate 2). From north to south the cherty iron-manganese unit grades from banded gray chert to siliceous hematite-bearing zones containing local pockets of goethite and jarosite, some of which are cellular boxworks containing cubic voids after pyrite. Buff-brown, streaky dolomite is in contact with the cherty unit. A fine-grained, calcareous, chloritized quartz schist west of the chert unit is seen in drill core to be a green mudstone interbedded with thin layers of green chert. East of the largest cherty outcrop, rocks exposed on the surface are intensely weathered and iron stained; weathering products include sericite and clay. Fresh drill core beneath these rocks consists of alternating thin bands of gray tuff and carbonaceous rock (plate 2); cubic pyrite aligned along folia is distributed throughout.

All of the units have been folded several times and therefore are now intensely folded. Layering and fold axes dip easterly and plunge north-northeasterly. The drill-hole area may center on a tight isoclinal synclinal fold. Shearing is widespread in the general area and is distinguished mainly by the presence of milky quartz veinlets in stockworks. Several fault breccias were intersected in the drill hole (plate 2).

Because of the intense folding and shearing, surface geology and drill-core results could be correlated only very generally. The cherty iron-manganese layer mapped at the surface was not intersected by the drill hole; a sharp synclinal fold may be present (plate 2).

Geology of the area surrounding drill hole RAB-2

The area around drill hole RAB-2 is distinguished by nearly vertical north-trending chert horizons that have been unaffected by small-scale folding (plate 2); most chert horizons are gray, some are green. Fine-grained mudstones range from gray to greenish gray. The mudstones and cherts very much resemble those intersected in drill hole RAB-1. Because of their fine-grained nature, the mudstones are generally difficult to distinguish in surface mapping; they weather to a fine-grained rock bearing chlorite and sericite and are very similar to calcareous quartz schist.

The shear zone intersected by drill hole RAB-2 is composed of 80 percent or more carbonaceous material, and small-scale folding is prevalent throughout the zone (plate 2). At the surface, the zone is an erosional trough formed by differential weathering. Although most of the sheared rock is covered by alluvium, iron-sericite-clay alteration obscures its carbonaceous nature where it is exposed. Drag folding on both sides of the shear zone indicates that both the east and west sides of the fault moved south relative to the shear zone. To the west the shear zone is in contact with an epidotized, massive graywacke.

Geology of the area surrounding drill hole RAB-3

In the area around drill hole RAB-3, a north-trending ridge is underlain by carbonaceous-tuffaceous schist, buff dolomite, cherty iron-manganese formation, and a calcareous quartz schist that weathers light green (plate 2). Surface exposures of the carbonaceous-tuffaceous schist are difficult to identify because much of the rock weathers to a fine-grained gray-green schist that is indistinguishable from the calcareous quartz schist. Layering was not observed in surface exposures of this rock. Massive dolomite lenses in the area are typical of dolomite lenses found elsewhere in the valley. On fresh dolomite surfaces a fine network of bright-green chlorite resembles malachite. Contacts between dolomite and carbonaceous-tuffaceous schist are gradational in many places. The cherty iron-manganese rocks range from typical brown- to black-weathering lenses on the western side of the ridge to gray, banded, pure cherts on the southeastern side.

Rocks within the map area are tightly and complexly folded. Two very sharp and nearly contiguous north-trending anticlines were mapped (plate 2). In places at the southern end of the ridge, the structure is well exposed. In these areas, cherts are both complexly folded about flat-lying, north-trending axes and folded in another plane having nearly vertical axes, as illustrated by the sinuous nature of cherty iron-manganese outcrops. Two shear couples were necessary for such folding to have occurred: one in a west-trending vertical plane and the other in a north-trending horizontal plane. The structure in this area is typical of that throughout Wadi Bidah, in that rocks have been affected by more than one stage of folding.

Geology of the area between lines 6100 N and 6300 N

This area between lines 6100 N and 6300 N (plate 2) is underlain by calcareous-quartz schist, cherty iron-manganese formation, and buff dolomite. These rocks are similar to those in other areas mapped in detail, except that the cherty iron-manganese formation contains more hematite and goethite than do most such rocks in the area.

The predominant structure is a tight anticlinal fold that was mapped at the northern end of a long north-trending ridge (plate 2). Other folding shown on plate 2 indicates the complexity of the folding about north-trending axes, a complexity typical of layered rocks in the Wadi Bidah valley bottom. Wide north-trending shear zones are both east and west of the anticlinal ridge (the western shear zone is not shown on plate 2). Relatively closely spaced north-trending shears are typical of the structure in much of Wadi Bidah, and folding about nearly vertical axes is also common.

Geochemical studies in the B-29 anomaly area

Cherty iron-manganese formation

Detailed mapping and sampling of the cherty iron-manganese formation were conducted to examine the possibility that this formation grades laterally into sulfide deposits containing base and precious metals. Earhart and Mawad (1970) had previously shown that in at least one place in the Rabathan area there is a direct spatial relationship between cherty iron-manganese rocks and massive sulfides. Their drill hole R-3 intersected a massive base metal-pyrite lens some 60 m directly below a cherty iron-manganese outcrop that is indistinguishable by either geochemistry or appearance from other such outcrops.

Throughout the world numerous massive sulfide deposits grade laterally into or are overlain by cherty formations. These formations may be pyritic cherts, laminated pyrite-bearing siliceous sediments, ferruginous cherty sediments, jasper, banded iron formation, or cherty iron-manganese formation. The cherty formations are thought to be chemical precipitants formed during the exhalative phase of volcanic activity. In Japan, Tertiary sulfide deposits are associated with iron-manganese cherts, some of which have been mined for their manganese content (Imai, 1978). In the Spanish-Portugese pyrite belt, purple-red tuffaceous shales are interbedded with ferruginous jasper lenses and with primary manganese silicates and (or) carbonates, and Strauss and others (1970, p. 69) stated that "the manganese formation is mostly later than the sulfide facies. Laterally it may replace the sulfide facies or even precede it."

Geochemical sample locations are shown on plate 1, and gold, silver, copper, lead, and zinc values, as determined by atomic absorption methods, are given in table 3. Copper values were as high as 300 ppm and zinc values were as high as 200 ppm. The highest silver value was 4.8 ppm, the highest gold 0.12 ppm. Semiquantitative spectrographic methods determined only trace amounts of 30 other elements (table 3).

Although the results of this sampling program are inconclusive, the mapping of the cherty iron-manganese formation shows that in places these cherty lenses grade laterally into true hematite-goethite gossans, if only on a very small scale.

Detailed rock geochemistry

The bedrock in the B-29 Rabathan area was sampled along a geophysical grid having stations at 25-m intervals. Sample-line intervals were 200 m, except in areas of special interest, where they were 100 m (plate 1).

Copper values have been contoured at 50, 100, 200, and 300 ppm intervals, and the copper distribution map of the B-29 Rabathan area (plate 1) indicates very spotty, moderate copper values. Known copper deposits such as the Rabathan prospect have very small primary geochemical dispersion zones, and hydrothermal alteration is noticeably limited in the area. The highest copper values were obtained from ancient workings where copper is visible, and most of the moderate values correlate with cherty iron-manganese or carbonaceous rocks. A gossan at 500 N, 200 W (plate 1), contained 3,500 ppm copper. It contained no secondary copper minerals, and primary dispersion of copper or zinc was almost totally absent. Scattered one-sample anomalies are erratically distributed throughout the area sampled and in places are projected between sample lines, a distance of 200 m. Only more detailed sampling between lines could ascertain the accuracy of these projections.

Zinc values have been contoured at 50, 100, 200, and 300 ppm intervals on plate 1. The zinc response is less than that of copper; only a few moderate, one-sample anomalies are in the Rabathan area, and these do not appear to represent

Table 3.--Semiquantitative spectrographic and atomic absorption assay values for samples from cherty iron-manganese formations, B-29 anomaly area, Wadi Bidah

[Results in parts per million unless otherwise indicated. S indicates semiquantitative spectrographic assay; AA indicates atomic absorption assay. G indicates element found in greater amount than value given; N indicates element not detected at value given; L indicates element detected but in amount less than value given. For atomic absorption assays, T following element indicates sample preparation included total digestion of sample, P indicates partial digestion of sample]

SAMPLE	S-FE %	S-MG %	S-CA %	S-TI %	S-MN	S-AG	S-AS	S-AU	S-B	S-BA
141446	15.0000	0.1500	3.0000	0.1500	5000.0000G	0.5000N	200.0000	10.0000N	10.0000L	70.0000
141447	15.0000	0.2000	3.0000	0.0500	5000.0000	0.5000N	200.0000L	10.0000N	10.0000L	70.0000
141448	15.0000	0.3000	3.0000	0.0700	5000.0000G	0.5000N	700.0000	10.0000N	10.0000L	150.0000
141449	15.0000	0.3000	3.0000	0.1500	5000.0000G	0.5000N	700.0000	10.0000N	15.0000	30.0000
141450	15.0000	1.5000	5.0000	0.1500	5000.0000G	0.5000N	200.0000N	10.0000N	10.0000L	150.0000
141451	7.0000	2.0000	7.0000	0.5000	5000.0000G	0.5000N	200.0000N	10.0000N	100.0000	150.0000
141452	15.0000	0.7000	3.0000	0.1500	5000.0000G	0.5000N	200.0000N	10.0000N	10.0000L	500.0000
141453	15.0000	0.1000	1.5000	0.0700	5000.0000G	0.5000N	200.0000N	10.0000N	10.0000L	150.0000
141454	15.0000	0.1500	3.0000	0.0700	5000.0000G	0.5000N	200.0000N	10.0000N	10.0000L	100.0000
141468	7.0000	0.7000	7.0000	0.1500	5000.0000G	0.5000N	200.0000N	10.0000N	10.0000	150.0000
141470	7.0000	1.0000	0.7000	0.3000	5000.0000G	0.5000N	200.0000N	10.0000N	10.0000	150.0000
141471	7.0000	1.5000	0.2000	0.3000	1500.0000	0.5000N	200.0000N	10.0000N	10.0000	20.0000
141472	15.0000	1.5000	1.5000	0.3000	5000.0000G	0.5000N	200.0000N	10.0000N	10.0000	70.0000
141473	15.0000	1.5000	1.5000	0.1500	5000.0000G	0.5000N	200.0000N	10.0000N	10.0000L	150.0000
141490	20.0000G	0.5000	3.0000	0.1500	5000.0000G	0.5000N	200.0000N	10.0000N	10.0000L	150.0000
141491	15.0000	0.7000	7.0000	0.0300	5000.0000G	0.5000N	200.0000N	10.0000N	10.0000L	150.0000
141492	10.0000	0.7000	1.5000	0.1500	5000.0000G	0.5000N	200.0000N	10.0000N	10.0000L	300.0000
141493	15.0000	1.5000	3.0000	0.1500	5000.0000G	0.5000N	200.0000N	10.0000N	10.0000L	70.0000
141494	7.0000	3.0000	7.0000	0.3000	5000.0000G	0.5000N	200.0000N	10.0000N	10.0000L	70.0000
141495	20.0000	1.0000	0.7000	0.1500	5000.0000G	0.5000N	200.0000N	10.0000N	10.0000L	30.0000
141496	20.0000G	1.5000	1.5000	0.1500	5000.0000G	0.5000N	200.0000N	10.0000N	10.0000L	20.0000N
141497	20.0000	0.5000	2.0000	0.1500	5000.0000G	0.5000N	200.0000N	10.0000N	10.0000	100.0000
141498	15.0000	0.7000	3.0000	0.0300	5000.0000G	0.5000N	200.0000N	10.0000N	10.0000L	20.0000L
141499	7.0000	0.3000	5.0000	0.1500	5000.0000G	0.5000N	200.0000N	10.0000N	20.0000	200.0000
141501	15.0000	0.3000	7.0000	0.0500	5000.0000G	0.5000N	200.0000N	10.0000N	10.0000	300.0000
141502	20.0000	0.5000	2.0000	0.0500	1000.0000	0.5000N	200.0000N	10.0000N	10.0000L	20.0000L
141503	15.0000	0.7000	3.0000	0.1000	5000.0000G	0.5000N	200.0000N	10.0000N	10.0000L	30.0000
141504	20.0000	1.5000	0.3000	0.1500	5000.0000G	0.5000N	200.0000N	10.0000N	10.0000L	20.0000
141505	20.0000	0.7000	3.0000	0.1000	5000.0000G	0.5000N	200.0000N	10.0000N	10.0000L	300.0000
141506	7.0000	5.0000	7.0000	1.0000G	5000.0000G	0.5000N	200.0000N	10.0000N	10.0000L	70.0000
141507	15.0000	2.0000	2.0000	0.3000	5000.0000G	0.5000N	200.0000N	10.0000N	10.0000L	20.0000L
141508	10.0000	0.2000	7.0000	0.0500	5000.0000G	0.5000N	200.0000N	10.0000N	10.0000L	20.0000
141509	15.0000	0.3000	3.0000	0.0700	5000.0000G	0.5000N	200.0000N	10.0000N	10.0000	20.0000
141510	20.0000	0.2000	3.0000	0.0500	5000.0000G	0.5000N	200.0000N	10.0000N	10.0000L	50.0000
141512	20.0000G	0.3000	0.7000	0.1000	5000.0000	0.5000N	200.0000N	10.0000N	10.0000	20.0000
141513	15.0000	0.2000	0.0500	0.0500	5000.0000G	0.5000N	200.0000N	10.0000N	10.0000	100.0000
141515	20.0000G	0.0500	1.0000	0.0700	5000.0000G	0.5000N	200.0000N	10.0000N	10.0000L	150.0000
141516	20.0000G	0.5000	2.0000	0.1500	5000.0000G	0.5000N	200.0000N	10.0000N	10.0000L	20.0000
141517	20.0000	0.2000	2.0000	0.0700	5000.0000G	0.5000N	200.0000N	10.0000N	10.0000	200.0000
141518	20.0000G	0.1000	3.0000	0.3000	5000.0000G	0.5000N	500.0000	10.0000N	10.0000	20.0000
141519	7.0000	0.7000	1.0000	0.1000	5000.0000G	0.5000N	200.0000N	10.0000N	10.0000L	20.0000L
141520	20.0000G	3.0000	5.0000	0.3000	5000.0000G	0.5000N	200.0000N	10.0000N	10.0000L	20.0000L

Table 3.--Semiquantitative spectrographic and atomic absorption assay values for samples from cherty iron-manganese formations, B-29 anomaly area, Wadi Bidah-Continued

SAMPLE	S-BE	S-BI	S-CD	S-CO	S-CR	S-CU	S-LA	S-MO	S-NB	S-NI
141446	1.0000N	10.0000N	20.0000N	7.0000	200.0000	30.0000	20.0000	5.0000N	20.0000L	70.0000
141447	1.0000	10.0000N	20.0000N	7.0000	70.0000	70.0000	20.0000	5.0000N	20.0000L	70.0000
141448	3.0000	10.0000N	20.0000N	20.0000	50.0000	70.0000	20.0000	5.0000N	20.0000L	70.0000
141449	1.0000	10.0000N	20.0000N	30.0000	150.0000	150.0000	50.0000	5.0000N	20.0000L	150.0000
141450	1.0000N	10.0000N	20.0000N	30.0000	70.0000	300.0000	20.0000	5.0000N	20.0000L	100.0000
141451	1.0000N	10.0000N	20.0000N	30.0000	70.0000	200.0000	20.0000	5.0000N	20.0000N	100.0000
141452	1.5000	10.0000N	20.0000N	20.0000	150.0000	150.0000	20.0000N	5.0000N	20.0000N	150.0000
141453	1.0000N	10.0000N	20.0000N	20.0000	100.0000	150.0000	20.0000	5.0000N	20.0000N	150.0000
141454	2.0000	10.0000N	20.0000N	30.0000	150.0000	200.0000	20.0000	5.0000N	20.0000N	150.0000
141468	1.5000	10.0000N	20.0000N	30.0000	150.0000	200.0000	20.0000	5.0000	20.0000N	70.0000
141470	1.5000	10.0000N	20.0000N	20.0000	150.0000	100.0000	20.0000	5.0000N	20.0000N	100.0000
141471	1.0000N	10.0000N	20.0000N	20.0000	150.0000	70.0000	20.0000N	5.0000N	20.0000N	70.0000
141472	1.0000N	10.0000N	20.0000N	30.0000	70.0000	200.0000	20.0000N	5.0000N	20.0000N	200.0000
141473	2.0000	10.0000N	20.0000N	70.0000	70.0000	300.0000	50.0000	5.0000N	20.0000N	300.0000
141490	1.0000N	10.0000N	20.0000N	50.0000	70.0000	150.0000	70.0000	5.0000N	20.0000N	150.0000
141491	2.0000	10.0000N	20.0000N	15.0000	70.0000	100.0000	30.0000	15.0000	20.0000N	70.0000
141492	3.0000	10.0000N	20.0000N	20.0000	70.0000	300.0000	20.0000	7.0000	20.0000N	70.0000
141493	1.0000N	10.0000N	20.0000N	30.0000	100.0000	200.0000	50.0000	5.0000N	20.0000N	150.0000
141494	1.0000N	10.0000N	20.0000N	20.0000	150.0000	150.0000	20.0000N	5.0000N	20.0000N	70.0000
141495	1.0000N	10.0000N	20.0000N	30.0000	150.0000	70.0000	30.0000	5.0000N	20.0000N	150.0000
141496	1.0000N	10.0000N	20.0000N	20.0000	150.0000	150.0000	20.0000	5.0000N	20.0000N	150.0000
141497	1.0000L	10.0000N	20.0000N	10.0000	100.0000	150.0000	20.0000N	5.0000N	20.0000N	100.0000
141498	1.0000L	10.0000N	20.0000N	50.0000	70.0000	150.0000	20.0000N	5.0000N	20.0000N	100.0000
141499	1.0000L	10.0000N	20.0000N	10.0000	200.0000	100.0000	20.0000N	5.0000N	20.0000N	70.0000
141501	1.0000N	10.0000N	20.0000N	10.0000	100.0000	150.0000	20.0000N	5.0000N	20.0000N	70.0000
141502	1.0000N	10.0000N	20.0000N	5.0000	100.0000	200.0000	20.0000N	5.0000N	20.0000N	70.0000
141503	1.0000N	10.0000N	20.0000N	5.0000	150.0000	150.0000	20.0000N	5.0000N	20.0000N	70.0000
141504	1.0000N	10.0000N	20.0000N	20.0000	70.0000	200.0000	20.0000N	5.0000N	20.0000N	150.0000
141505	1.0000	10.0000N	20.0000N	5.0000	100.0000	150.0000	30.0000	5.0000N	20.0000N	70.0000
141506	1.0000	10.0000N	20.0000N	30.0000	50.0000	30.0000	20.0000N	5.0000N	20.0000	50.0000
141507	1.0000N	10.0000N	20.0000N	20.0000	50.0000	100.0000	20.0000N	5.0000N	20.0000N	70.0000
141508	1.5000	10.0000N	20.0000N	10.0000	50.0000	150.0000	20.0000N	5.0000N	20.0000N	50.0000
141509	1.5000	10.0000N	20.0000N	10.0000	50.0000	150.0000	20.0000N	5.0000N	20.0000N	70.0000
141510	1.5000	10.0000N	20.0000N	50.0000	70.0000	150.0000	20.0000N	5.0000N	20.0000N	70.0000
141512	1.0000N	10.0000N	20.0000N	20.0000	150.0000	200.0000	20.0000N	5.0000N	20.0000N	100.0000
141513	1.0000N	10.0000N	20.0000N	20.0000	50.0000	150.0000	50.0000	5.0000N	20.0000N	100.0000
141515	1.0000N	10.0000N	20.0000N	5.0000	150.0000	70.0000	20.0000N	5.0000N	20.0000N	50.0000
141516	1.0000N	10.0000N	20.0000N	5.0000	70.0000	150.0000	20.0000N	5.0000N	20.0000N	100.0000
141517	1.0000	10.0000N	20.0000N	5.0000	150.0000	150.0000	20.0000N	5.0000N	20.0000N	70.0000
141518	2.0000	10.0000N	20.0000N	20.0000	200.0000	300.0000	20.0000N	5.0000	20.0000N	200.0000
141519	1.0000N	10.0000N	20.0000N	10.0000	200.0000	150.0000	20.0000N	5.0000N	20.0000N	100.0000
141520	1.0000N	10.0000N	20.0000N	70.0000	200.0000	500.0000	20.0000N	5.0000N	20.0000N	300.0000

Table 3.--Semiquantitative spectrographic and atomic absorption assay values for samples from cherty iron-manganese formations, B-29 anomaly area, Wadi Bidah-Continued

SAMPLE	S-PB	S-SB	S-SC	S-SN	S-SR	S-V	S-W	S-Y	S-ZN	S-ZR
141446	30.0000	100.0000N	7.0000	10.0000N	150.0000	300.0000	50.0000N	30.0000	200.0000L	70.0000
141447	30.0000	100.0000N	5.0000	10.0000N	100.0000	300.0000	50.0000N	30.0000	200.0000L	20.0000
141448	30.0000	100.0000N	5.0000	10.0000N	200.0000	300.0000	50.0000N	30.0000	200.0000L	30.0000
141449	15.0000	100.0000N	15.0000	10.0000N	300.0000	300.0000	50.0000N	70.0000	200.0000L	70.0000
141450	100.0000	100.0000N	10.0000	10.0000N	100.0000	300.0000	50.0000N	70.0000	200.0000L	70.0000
141451	30.0000	100.0000N	15.0000	10.0000N	300.0000	150.0000	50.0000N	30.0000	200.0000L	100.0000
141452	10.0000	100.0000N	5.0000	10.0000N	300.0000	300.0000	50.0000N	30.0000	200.0000L	30.0000
141453	300.0000	100.0000N	5.0000	10.0000N	300.0000	150.0000	50.0000N	70.0000	200.0000L	15.0000
141454	30.0000	100.0000N	5.0000L	10.0000N	300.0000	150.0000	50.0000N	50.0000	200.0000L	15.0000
141468	10.0000	100.0000N	7.0000	10.0000N	300.0000	100.0000	50.0000N	30.0000	200.0000L	30.0000
141470	10.0000	100.0000N	15.0000	10.0000N	150.0000	150.0000	50.0000N	30.0000	200.0000L	100.0000
141471	10.0000N	100.0000N	15.0000	10.0000N	100.0000N	150.0000	50.0000N	10.0000	200.0000L	15.0000
141472	150.0000	100.0000N	15.0000	10.0000N	150.0000	300.0000	50.0000N	100.0000	200.0000L	100.0000
141473	70.0000	100.0000N	10.0000	10.0000N	300.0000	150.0000	50.0000N	70.0000	200.0000L	70.0000
141490	20.0000	100.0000N	7.0000	10.0000N	1000.0000	300.0000	50.0000N	70.0000	200.0000L	100.0000
141491	30.0000	100.0000N	5.0000L	10.0000N	700.0000	150.0000	50.0000N	70.0000	200.0000L	30.0000
141492	70.0000	100.0000N	7.0000	10.0000N	700.0000	200.0000	50.0000N	70.0000	200.0000L	30.0000
141493	30.0000	100.0000N	10.0000	10.0000N	300.0000	200.0000	50.0000N	70.0000	200.0000L	70.0000
141494	30.0000	100.0000N	15.0000	10.0000N	150.0000	150.0000	50.0000N	30.0000	200.0000L	70.0000
141495	50.0000	100.0000N	15.0000	10.0000N	100.0000	300.0000	50.0000N	50.0000	200.0000L	70.0000
141496	100.0000	100.0000N	10.0000	10.0000N	100.0000	300.0000	50.0000N	70.0000	200.0000L	70.0000
141497	70.0000	100.0000N	5.0000	10.0000N	150.0000	300.0000	50.0000N	50.0000	200.0000L	50.0000
141498	30.0000	100.0000N	5.0000L	10.0000N	700.0000	300.0000	50.0000N	50.0000	200.0000L	10.0000
141499	15.0000	100.0000N	5.0000	10.0000N	200.0000	200.0000	50.0000N	30.0000	200.0000L	30.0000
141501	50.0000	100.0000N	5.0000L	10.0000N	100.0000	200.0000	50.0000N	20.0000	200.0000L	10.0000
141502	20.0000	100.0000N	5.0000L	10.0000N	200.0000	200.0000	50.0000N	50.0000	200.0000L	10.0000
141503	70.0000	100.0000N	5.0000L	10.0000N	100.0000	300.0000	50.0000N	20.0000	200.0000L	20.0000
141504	150.0000	100.0000N	7.0000	10.0000N	100.0000N	500.0000	50.0000N	15.0000	200.0000	50.0000
141505	70.0000	100.0000N	5.0000	10.0000N	150.0000	200.0000	50.0000N	50.0000	200.0000L	30.0000
141506	10.0000	100.0000N	15.0000	10.0000N	150.0000	300.0000	50.0000N	50.0000	200.0000L	100.0000
141507	10.0000	100.0000N	10.0000	10.0000N	100.0000L	300.0000	50.0000N	15.0000	200.0000L	20.0000
141508	20.0000	100.0000N	5.0000L	10.0000N	700.0000	200.0000	50.0000N	30.0000	200.0000L	10.0000
141509	50.0000	100.0000N	5.0000L	10.0000N	150.0000	200.0000	50.0000N	30.0000	200.0000L	10.0000
141510	10.0000L	100.0000N	5.0000L	10.0000N	1000.0000	200.0000	50.0000N	15.0000	200.0000L	10.0000
141512	10.0000L	100.0000N	5.0000L	10.0000N	100.0000L	500.0000	50.0000N	50.0000	200.0000L	15.0000
141513	50.0000	100.0000N	5.0000L	10.0000N	700.0000	300.0000	50.0000N	100.0000	200.0000L	10.0000
141515	30.0000	100.0000N	5.0000L	10.0000N	100.0000L	500.0000	50.0000N	20.0000	200.0000L	10.0000
141516	10.0000L	100.0000N	5.0000L	10.0000N	200.0000	200.0000	50.0000N	50.0000	200.0000L	50.0000
141517	50.0000	100.0000N	5.0000L	10.0000N	100.0000	200.0000	50.0000N	30.0000	200.0000L	20.0000
141518	70.0000	100.0000N	7.0000	10.0000N	1000.0000	700.0000	50.0000N	100.0000	200.0000L	70.0000
141519	20.0000	100.0000N	5.0000L	10.0000N	300.0000	300.0000	50.0000N	10.0000	200.0000L	30.0000
141520	70.0000	100.0000N	5.0000	10.0000N	200.0000	500.0000	50.0000N	70.0000	300.0000	70.0000

Table 3.--Semiquantitative spectrographic and atomic absorption assay values for samples from cherty iron-manganese formations, B-29 anomaly area, Wadi Bidah-Continued

SAMPLE	AA-AU-T	AA-AG-T	AA-CU-P	AA-PB-P	AA-ZN-P
141446	0.0500L	0.9000	90.0000	35.0000	30.0000
141447	0.0500L	1.5000	90.0000	40.0000	50.0000
141448	0.1000	2.0000	65.0000	50.0000	55.0000
141449	0.0600	1.6000	140.0000	30.0000	65.0000
141450	0.0600	1.6000	600.0000	140.0000	160.0000
141451	0.0500L	1.3000	165.0000	50.0000	115.0000
141452	0.1000	1.4000	190.0000	35.0000	50.0000
141453	0.1000	1.3000	105.0000	310.0000	120.0000
141454	0,0600	1.4000	190.0000	45.0000	95.0000
141468	0.0600	1.2000	225.0000	30.0000	35.0000
141470	0.0600	0.7000	110.0000	20.0000	130.0000
141471	0.0600	0.8000	85.0000	20.0000	100.0000
141472	0.1600	1.3000	165.0000	190.0000	140.0000
141473	0.0600	1.5000	220.0000	85.0000	155.0000
141490	0.0600	2.3000	105.0000	35.0000	100.0000
141491	0.0600	1.5000	300.0000	50.0000	95.0000
141492	0.0600	1.5000	300.0000	50.0000	85.0000
141493	0.0600	1.4000	160.0000	50.0000	110.0000
141494	0.0600	1.5000	115.0000	60.0000	95.0000
141495	0.0600	1.3000	60.0000	50.0000	160.0000
141496	0.0600	1.4000	165.0000	85.0000	250.0000
141497	0.0600	1.5000	110.0000	80.0000	140.0000
141498	0.1000	1.7000	115.0000	45.0000	95.0000
141499	0.0600	1.1000	90.0000	40.0000	100.0000
141501	0.0600	1.6000	100.0000	55.0000	60.0000
141502	0.0600	1.4000	205.0000	40.0000	100.0000
141503	0.1000	1.3000	110.0000	90.0000	125.0000
141504	0.0600	1.2000	220.0000	155.0000	200.0000
141505	0.1000	1.2000	100.0000	70.0000	100.0000
141506	0.0600	1.4000	25.0000	45.0000	125.0000
141507	0.1000	1.3000	75.0000	25.0000	80.0000
141508	0.0600	2.6000	110.0000	30.0000	50.0000
141509	0.0600	1.7000	85.0000	60.0000	100.0000
141510	0.0600	1.6000	90.0000	15.0000	65.0000
141512	0.0600	1.5000	130.0000	25.0000	120.0000
141513	0.0600	1.7000	85.0000	35.0000	105.0000
141515	0.0600	1.5000	75.0000	35.0000	75.0000
141516	0.1200	1.6000	75.0000	25.0000	80.0000
141517	0.0600	1.3000	115.0000	55.0000	75.0000
141518	0.1000	1.9000	210.0000	75.0000	55.0000
141519	0.0600	0.7000	60.0000	30.0000	145.0000
141520	0.0600	1.5000	250.0000	75.0000	300.0000

Table 3.--Semiquantitative spectrographic and atomic absorption assay values for samples from cherty iron-manganese formations, B-29 anomaly area, Wadi Bidah-Continued

SAMPLE	S-FE %	S-MG %	S-CA %	S-TI %	S-MN	S-AG	S-AS	S-AU	S-B	S-BA
141521	15.0000	3.0000	0.7000	1.0000G	5000.0000G	0.5000N	200.0000N	10.0000N	10.0000L	20.0000L
141522	20.0000G	1.0000	1.0000	0.1000	5000.0000G	0.5000N	200.0000N	10.0000N	10.0000L	200.0000
141523	20.0000G	0.7000	0.5000	0.2000	3000.0000	0.5000N	200.0000N	10.0000N	10.0000L	20.0000L
141524	20.0000G	1.5000	3.0000	0.3000	1500.0000	0.5000N	200.0000N	10.0000N	10.0000L	20.0000L
141525	20.0000G	0.3000	1.0000	0.1000	1000.0000	0.5000N	200.0000N	10.0000N	10.0000L	20.0000L
141526	15.0000	1.5000	3.0000	0.1000	5000.0000G	0.5000N	200.0000N	10.0000N	10.0000L	70.0000
141527	20.0000G	1.0000	1.5000	0.1500	10.0000	0.5000N	200.0000N	10.0000N	10.0000L	20.0000L
141528	20.0000G	0.2000	0.7000	0.1000	10.0000	0.5000N	200.0000N	10.0000N	10.0000L	20.0000L
141529	20.0000G	1.0000	5.0000	0.0500	10.0000	0.5000N	200.0000N	10.0000N	10.0000L	20.0000L
141530	20.0000G	1.0000	1.5000	0.2000	10.0000	0.5000N	200.0000N	10.0000N	10.0000L	200.0000
141531	20.0000G	0.7000	5.0000	0.0700	5000.0000G	3.0000	200.0000N	10.0000N	10.0000L	20.0000
141532	20.0000	0.3000	3.0000	0.3000	1500.0000	0.5000N	200.0000N	10.0000N	10.0000	150.0000
141533	15.0000	0.3000	3.0000	0.0700	5000.0000G	0.5000N	200.0000N	10.0000N	10.0000	70.0000
141534	20.0000	0.2000	3.0000	0.0300	1500.0000	0.5000N	200.0000N	10.0000N	10.0000L	30.0000
141535	20.0000	0.1500	5.0000	0.0300	2000.0000	0.5000N	200.0000N	10.0000N	10.0000	50.0000
141536	15.0000	0.1500	3.0000	0.0500	5000.0000G	0.5000N	200.0000N	10.0000N	10.0000	300.0000
141537	20.0000	0.1500	2.0000	0.0500	5000.0000	0.5000N	200.0000N	10.0000N	10.0000L	150.0000
141538	15.0000	0.3000	1.5000	0.1500	500.0000	0.5000N	200.0000N	10.0000N	10.0000	150.0000
141539	10.0000	0.3000	1.5000	0.0300	5000.0000G	0.5000N	200.0000N	10.0000N	10.0000L	30.0000
141540	15.0000	0.5000	1.5000	0.0500	5000.0000G	0.5000N	200.0000N	10.0000N	10.0000L	50.0000
141541	10.0000	0.7000	0.7000	0.1500	5000.0000G	0.5000N	200.0000N	10.0000N	10.0000L	30.0000
141542	7.0000	0.7000	1.5000	0.1000	5000.0000G	0.5000N	200.0000N	10.0000N	10.0000L	150.0000
141544	15.0000	0.1000	3.0000	0.0700	5000.0000G	0.5000N	200.0000N	10.0000N	10.0000	300.0000
141553	15.0000	0.7000	2.0000	0.0700	5000.0000	0.5000N	200.0000N	10.0000N	10.0000L	50.0000
141554	15.0000	0.3000	3.0000	0.1000	5000.0000G	0.5000N	200.0000N	10.0000N	10.0000L	150.0000
141555	3.0000	0.7000	3.0000	0.0050	5000.0000	0.5000N	200.0000N	10.0000N	10.0000L	70.0000
141556	20.0000	0.2000	3.0000	0.1500	5000.0000G	0.5000N	200.0000N	10.0000N	10.0000	150.0000
141557	15.0000	0.7000	3.0000	0.1500	5000.0000G	0.5000N	200.0000N	10.0000N	10.0000L	70.0000
141558	15.0000	0.5000	0.7000	0.2000	5000.0000	0.5000N	200.0000N	10.0000N	10.0000L	20.0000L
141559	7.0000	0.1500	7.0000	0.1000	1000.0000	0.5000N	200.0000N	10.0000N	10.0000L	150.0000
141560	10.0000	0.5000	3.0000	0.0500	5000.0000G	0.5000N	200.0000N	10.0000N	10.0000L	30.0000
141561	5.0000	0.0700	5.0000	0.0500	5000.0000G	0.5000N	200.0000N	10.0000N	10.0000L	150.0000
141562	7.0000	0.7000	0.7000	0.1000	2000.0000	0.5000N	200.0000N	10.0000N	10.0000	70.0000
141563	7.0000	0.1000	3.0000	0.0300	5000.0000G	0.5000N	200.0000N	10.0000N	10.0000	70.0000
141564	15.0000	0.0300	0.1500	0.2000	5000.0000	0.5000N	200.0000N	10.0000N	10.0000L	150.0000
141565	10.0000	0.3000	5.0000	0.1000	5000.0000G	0.5000N	200.0000N	10.0000N	10.0000	150.0000

Table 3.--Semiquantitative spectrographic and atomic absorption assay values for samples from cherty iron-manganese formations, B-29 anomaly area, Wadi Bidah-Continued

SAMPLE	S-BE	S-BI	S-CD	S-CO	S-CR	S-CU	S-LA	S-MO	S-NB	S-NI
141521	1.0000N	10.0000N	20.0000N	20.0000	100.0000	30.0000	20.0000N	5.0000N	20.0000N	100.0000
141522	1.0000N	10.0000N	20.0000N	10.0000	100.0000	300.0000	20.0000N	5.0000N	20.0000N	100.0000
141523	1.0000N	10.0000N	20.0000N	5.0000	200.0000	500.0000	20.0000N	5.0000N	20.0000N	200.0000
141524	1.0000N	10.0000N	20.0000N	5.0000L	100.0000	300.0000	20.0000N	5.0000N	20.0000N	100.0000
141525	1.0000N	10.0000N	20.0000N	5.0000L	300.0000	300.0000	20.0000N	5.0000N	20.0000N	70.0000
141526	1.5000	10.0000N	20.0000N	15.0000	100.0000	200.0000	20.0000N	5.0000N	20.0000N	100.0000
141527	1.0000N	10.0000N	20.0000N	10.0000	150.0000	200.0000	20.0000N	5.0000N	20.0000N	100.0000
141528	3.0000	10.0000N	20.0000N	10.0000	100.0000	150.0000	20.0000N	5.0000N	20.0000N	100.0000
141529	1.0000N	10.0000N	20.0000N	15.0000	200.0000	300.0000	20.0000N	5.0000N	20.0000N	200.0000
141530	1.0000N	10.0000N	20.0000N	50.0000	200.0000	200.0000	20.0000N	5.0000N	20.0000N	100.0000
141531	1.0000N	10.0000N	20.0000N	5.0000	150.0000	200.0000	20.0000N	5.0000N	20.0000N	100.0000
141532	1.0000N	10.0000N	20.0000N	15.0000	300.0000	150.0000	20.0000N	5.0000L	20.0000L	50.0000
141533	1.0000N	10.0000N	20.0000N	20.0000	300.0000	150.0000	20.0000N	5.0000	20.0000L	50.0000
141534	1.0000N	10.0000N	20.0000N	10.0000	150.0000	100.0000	20.0000N	5.0000N	20.0000L	70.0000
141535	1.0000N	10.0000N	20.0000N	10.0000	100.0000	50.0000	20.0000N	5.0000N	20.0000L	30.0000
141536	1.0000N	10.0000N	20.0000N	30.0000	200.0000	100.0000	20.0000N	5.0000N	20.0000L	150.0000
141537	1.0000N	10.0000N	20.0000N	15.0000	150.0000	50.0000	20.0000N	5.0000N	20.0000L	50.0000
141538	1.0000N	10.0000N	20.0000N	5.0000	150.0000	70.0000	20.0000N	5.0000N	20.0000L	50.0000
141539	1.5000	10.0000N	20.0000N	50.0000	70.0000	100.0000	20.0000N	5.0000N	20.0000L	150.0000
141540	1.0000N	10.0000N	20.0000N	30.0000	150.0000	20.0000	200.0000	5.0000L	20.0000L	100.0000
141541	1.0000N	10.0000N	20.0000N	30.0000	300.0000	70.0000	200.0000	5.0000N	20.0000L	70.0000
141542	1.0000L	10.0000N	20.0000N	50.0000	70.0000	200.0000	30.0000	5.0000N	20.0000L	100.0000
141544	1.0000N	10.0000N	20.0000N	20.0000	100.0000	100.0000	20.0000N	5.0000L	20.0000L	70.0000
141553	1.0000N	10.0000N	20.0000N	30.0000	100.0000	200.0000	20.0000N	5.0000N	20.0000L	100.0000
141554	1.0000N	10.0000N	20.0000N	50.0000	100.0000	70.0000	20.0000N	5.0000N	20.0000L	150.0000
141555	1.0000N	10.0000N	20.0000N	15.0000	150.0000	30.0000	20.0000N	5.0000L	20.0000L	30.0000
141556	1.0000L	10.0000N	20.0000N	15.0000	100.0000	150.0000	20.0000	5.0000N	70.0000	70.0000
141557	1.0000L	10.0000N	20.0000N	30.0000	70.0000	100.0000	20.0000	5.0000N	50.0000	100.0000
141558	1.0000N	10.0000N	20.0000N	20.0000	50.0000	70.0000	30.0000	5.0000N	50.0000	70.0000
141559	1.0000L	10.0000N	20.0000N	10.0000	100.0000	70.0000	50.0000	5.0000N	20.0000	30.0000
141560	1.0000N	10.0000N	20.0000N	15.0000	30.0000	50.0000	30.0000	5.0000N	20.0000	50.0000
141561	1.0000L	10.0000N	20.0000N	15.0000	30.0000	70.0000	20.0000N	5.0000N	20.0000L	30.0000
141562	1.0000L	10.0000N	20.0000N	15.0000	70.0000	100.0000	20.0000L	5.0000N	20.0000	70.0000
141563	1.0000L	10.0000N	20.0000N	30.0000	100.0000	100.0000	20.0000N	5.0000N	30.0000	70.0000
141564	1.5000	10.0000N	20.0000N	20.0000	70.0C00	150.0000	30.0000	5.0000N	70.0000	70.0000
141565	1.5000	10.0000N	20.0000N	20.0000	70.0000	100.0000	20.0000N	5.0000N	30.0000	70.0000

Table 3.--Semiquantitative spectrographic and atomic absorption assay values for samples from cherty iron-manganese formations, B-29 anomaly area, Wadi Bidah-Continued

SAMPLE	S-PB	S-SB	S-SC	S-SN	S-SR	S-V	S-W	S-Y	S-ZN	S-ZR
141521	10.0000L	100.0000N	30.0000	10.0000N	100.0000N	300.0000	50.0000N	20.0000	200.0000L	70.0000
141522	30.0000	100.0000N	5.0000	10.0000N	100.0000L	300.0000	50.0000N	20.0000	200.0000L	30.0000
141523	70.0000	100.0000N	7.0000	10.0000N	100.0000L	500.0000	50.0000N	20.0000	300.0000	100.0000
141524	10.0000L	100.0000N	5.0000	10.0000N	100.0000L	300.0000	50.0000N	20.0000	200.0000L	100.0000
141525	10.0000L	100.0000N	5.0000L	10.0000N	100.0000L	700.0000	50.0000N	50.0000	200.0000L	30.0000
141526	100.0000	100.0000N	5.0000L	10.0000N	700.0000	300.0000	50.0000N	20.0000	200.0000L	30.0000
141527	20.0000	100.0000N	5.0000L	10.0000N	100.0000L	500.0000	50.0000N	20.0000	200.0000L	50.0000
141528	50.0000	100.0000N	7.0000	10.0000N	100.0000L	200.0000	50.0000N	50.0000	200.0000L	10.0000
141529	70.0000	100.0000N	5.0000L	10.0000N	200.0000	300.0000	50.0000N	30.0000	200.0000L	10.0000
141530	50.0000	100.0000N	5.0000L	10.0000N	500.0000	300.0000	50.0000N	30.0000	200.0000L	50.0000
141531	50.0000	100.0000N	5.0000L	10.0000N	150.0000	200.0000	50.0000N	20.0000	200.0000L	10.0000
141532	30.0000	100.0000N	10.0000	10.0000N	150.0000	300.0000	50.0000N	50.0000	200.0000N	100.0000
141533	70.0000	100.0000N	5.0000L	10.0000N	300.0000	200.0000	50.0000N	50.0000	200.0000N	30.0000
141534	30.0000	100.0000N	5.0000L	10.0000N	150.0000	200.0000	50.0000N	30.0000	200.0000N	20.0000
141535	30.0000	100.0000N	5.0000L	10.0000N	150.0000	200.0000	50.0000N	30.0000	200.0000N	15.0000
141536	20.0000	100.0000N	5.0000L	10.0000N	500.0000	150.0000	50.0000N	30.0000	200.0000N	20.0000
141537	30.0000	100.0000N	5.0000L	10.0000N	100.0000	100.0000	50.0000N	20.0000	200.0000N	20.0000
141538	10.0000L	100.0000N	7.0000	10.0000N	100.0000L	100.0000	50.0000N	30.0000	200.0000N	70.0000
141539	10.0000N	100.0000N	5.0000L	10.0000N	150.0000	70.0000	50.0000N	20.0000	200.0000N	20.0000
141540	10.0000L	100.0000N	5.0000L	10.0000N	700.0000	150.0000	50.0000N	30.0000	200.0000N	30.0000
141541	30.0000	100.0000N	5.0000	10.0000N	200.0000	100.0000	50.0000N	20.0000	200.0000N	50.0000
141542	30.0000	100.0000N	5.0000	10.0000N	1500.0000	100.0000	50.0000N	50.0000	200.0000N	50.0000
141544	20.0000	100.0000N	5.0000L	10.0000N	200.0000	100.0000	50.0000N	30.0000	200.0000N	30.0000
141553	30.0000	100.0000N	5.0000	10.0000N	300.0000	150.0000	50.0000N	30.0000	200.0000N	30.0000
141554	30.0000	100.0000N	5.0000	10.0000N	300.0000	200.0000	50.0000N	30.0000	200.0000N	30.0000
141555	10.0000N	100.0000N	5.0000L	10.0000N	150.0000	50.0000	50.0000N	15.0000	200.0000N	10.0000
141556	50.0000	100.0000N	5.0000	10.0000N	200.0000	200.0000	50.0000N	50.0000	200.0000N	50.0000
141557	30.0000	100.0000N	5.0000	10.0000N	500.0000	200.0000	50.0000N	30.0000	200.0000N	50.0000
141558	50.0000	100.0000N	7.0000	10.0000N	100.0000	200.0000	50.0000N	10.0000L	200.0000N	70.0000
141559	70.0000	100.0000N	5.0000	10.0000N	150.0000	150.0000	50.0000N	50.0000	200.0000N	30.0000
141560	20.0000	100.0000N	5.0000	10.0000N	150.0000	100.0000	50.0000N	30.0000	200.0000N	30.0000
141561	30.0000	100.0000N	7.0000	10.0000N	200.0000	100.0000	50.0000N	20.0000	200.0000N	30.0000
141562	15.0000	100.0000N	7.0000	10.0000N	150.0000	100.0000	50.0000N	20.0000	200.0000N	30.0000
141563	20.0000	100.0000N	5.0000	10.0000N	200.0000	100.0000	50.0000N	15.0000	200.0000N	20.0000
141564	20.0000	100.0000N	7.0000	10.0000N	150.0000	150.0000	50.0000N	30.0000	200.0000N	100.0000
141565	30.0000	100.0000N	5.0000	10.0000N	300.0000	150.0000	50.0000N	30.0000	200.0000N	50.0000

Table 3.--Semiquantitative spectrographic and atomic absorption assay values for samples from cherty iron-manganese formations, B-29 anomaly area, Wadi Bidah-Continued

SAMPLE	AA-AU-T	AA-AG-T	AA-CU-P	AA-PB-P	AA-ZN-P
141521	0.0600	1.2000	20.0000	35.0000	250.0000
141522	0.0600	1.4000	180.0000	60.0000	130.0000
141523	0.0600	1.3000	300.0000	80.0000	200.0000
141524	0.0600	1.3000	200.0000	35.0000	130.0000
141525	0.0600	1.7000	250.0000	25.0000	45.0000
141526	0.0600	1.3000	125.0000	75.0000	125.0000
141527	0.0600	1.2000	125.0000	35.0000	105.0000
141528	0.0600	1.7000	85.0000	75.0000	95.0000
141529	0.0600	1.5000	125.0000	75.0000	100.0000
141530	0.1200	1.4000	85.0000	40.0000	210.0000
141531	0.0600	4.8000	170.0000	65.0000	130.0000
141532	0.0500L	1.8000	275.0000	80.0000	80.0000
141533	0.0500L	1.4000	100.0000	80.0000	65.0000
141534	0.0500L	1.5000	105.0000	50.0000	50.0000
141535	0.0500L	1.5000	55.0000	50.0000	25.0000
141536	0.0600	1.5000	110.0000	30.0000	45.0000
141537	0.0600	1.6000	45.0000	50.0000	50.0000
141538	0.0600	1.3000	60.0000	20.0000	70.0000
141539	0.0600	2.4000	110.0000	20.0000	180.0000
141540	0.0500L	1.7000	215.0000	15.0000	80.0000
141541	0.0500L	1.1000	45.0000	60.0000	90.0000
141542	0.0600	1.4000	125.0000	30.0000	140.0000
141544	0.0600	1.4000	90.0000	20.0000	45.0000
141553	0.0800	2.3000	185.0000	35.0000	70.0000
141554	0.0600	1.8000	30.0000	25.0000	40.0000
141555	0.0500L	0.5000L	25.0000	20.0000	20.0000
141556	0.0500L	1.6000	85.0000	30.0000	55.0000
141557	0.0500L	2.3000	75.0000	25.0000	260.0000
141558	0.0600	1.7000	60.0000	80.0000	160.0000
141559	0.0800	1.0000	55.0000	70.0000	25.0000
141560	0.0600	1.5000	50.0000	20.0000	120.0000
141561	0.0500L	1.5000	110.0000	35.0000	45.0000
141562	0.0500L	1.0000	140.0000	20.0000	85.0000
141563	0.0500L	1.2000	95.0000	25.0000	45.0000
141564	0.0800	1.8000	130.0000	20.0000	70.0000
141565	0.0800	2.1000	120.0000	80.0000	100.0000

significant mineralization. In most circumstances, zinc migrates farther than copper during weathering and creates large halos around all deposits except those in very calcareous rocks. The lack of such halos in this area suggests that zinc is not abundant, a conclusion confirmed by the low zinc values obtained by analysis of Rabathan drill-core intersections from the sulfide zone (Kiilsgaard and others, 1978).

Comments

Rock geochemical studies in the B-29 anomaly area indicate that primary dispersion of metals around known massive sulfide deposits is very limited. Consequently, the effectiveness of rock-chip sample surveys is low, and it is doubtful if more detailed surveys would be worthwhile. Although hydrous iron and manganese as well as carbonaceous material are scavengers of many elements including gold, silver, copper, lead, and zinc, there are conflicting reports concerning their effectiveness in adsorbing metal ions (Saxby, 1976). Because these adsorption reactions are complex and so many variables enter into the problem, few conclusions may be drawn concerning concentrations of various metals in any particular carbonaceous or cherty iron-manganese formation. In the B-29 area, the rock-chip sampling program succeeded only in defining zones of cherty iron-manganese or carbonaceous formations containing moderate to high copper, lead, and zinc values. Negative results from the drilling of some of these formations indicate that these zones are probably not generally associated with base metal sulfide deposits, and the low gold and silver contents of all of the samples from the area support a negative assessment of the mineral resource potential.

Results of drilling in the B-29 anomaly area

Three drill targets were selected on the basis of geophysical and geochemical survey results and geologic mapping. All drill holes were inclined at -45° (for detailed drill logs, see plate 3).

Drill hole RAB-1

Drill hole RAB-1 was positioned to undercut the northern end of a -300 mV self-potential anomaly that coincides with the western edge of an in-phase electromagnetic gradient ranging from 100 to 50 percent; to intersect the downward projection of a cherty iron-manganese formation at a depth of about 60 m (plate 2); and to test the zone below moderately high copper values obtained by grid sampling east of and adjacent to the cherty iron-manganese outcrop (plate 1).

The drill hole intersected a series of layered rocks including mudstone, chert, and finely laminated cherty tuff and carbonaceous material (plate 3). Much of the drill hole intersected zones of kink and drag folding that grade into shear zones, some of which are brecciated, mylonitized, and sealed by quartz. Pyrite is distributed along laminations in the siliceous-carbonaceous rock. The drill hole did not intersect cherty iron-manganese formation or other sulfides, and it is proposed that the cherty lens either pinches out or is folded as depicted in plate 2.

Drill hole RAB-2

Drill hole RAB-2 was positioned to test a -400 mV self-potential anomaly that coincides with a -30 percent out-of-phase electromagnetic anomaly and to test a coincident geochemical copper anomaly (plate 1).

The drill hole began in calcareous quartz schist and then intersected a wide zone of interbedded argillite and chert. Between 99.0 and 112.55 m depth, the drill hole intersected a tightly folded and sheared zone composed of about 80 percent carbonaceous material and sparse pyrite (plate 3). The bottom of the drill hole is in epidotized fine-grained graywacke.

Flanigan and others (1982) believe that the drill hole sufficiently tested the geophysical anomalies, which were apparently caused by the carbonaceous shear zone. In addition, rock chips from the coincident copper-anomalous zone were partially carbonaceous.

Drill hole RAB-3

Drill hole RAB-3 was positioned to test the southern end of a -200 mV self-potential anomaly; to intersect the downward projection of a cherty iron-manganese formation; and to test the northern end of a 40 percent in-phase electromagnetic anomaly (plate 1). In addition, moderate copper values were obtained on sample line 1300 N, which passes a short distance to the north of the drill-hole location (plate 1).

No core was recovered between the surface and 29.1 m depth (plate 3). Below 29.1 m, the drill hole intersected alternating layers of slightly brecciated cherty zones bearing disseminated to massive pyrite; these zones are thought to be unoxidized cherty iron-manganese formations. Finely laminated carbonaceous material and siliceous calcareous tuff, both interlayered with massive gray dolomite, compose most of the drill core. Two to three percent disseminated pyrite is associated with the laminated tuff and carbonaceous schist.

Discussion of drilling results

Drill holes RAB-1, -2, and -3 were positioned to test several combinations of conditions in the Rabathan area: 1) coincident self-potential and electromagnetic anomalies and 2) cherty iron-manganese formations, some of which are slightly to moderately anomalous in copper and zinc and some of which coincide with geophysical anomalies.

Drill holes RAB-1, -2, and -3 did not intersect significant amounts of base or precious metals, and it must be concluded either that there are no near-surface sulfide-bearing bodies in the area or that the exploration techniques lacked the necessary sophistication to locate such sulfide bodies. If the latter is the reason, then a more complete geophysical and geochemical study combined with more detailed geologic mapping would be in order. Such a study should include closer spacing of the geophysical and geochemical lines and a careful evaluation of all of the drilling results in combination with detailed surface studies including geology, geophysics, and geochemistry. For instance, Earhart and Mawad (1970) drilled five cherty iron-manganese lenses in the northern part of the Rabathan area, and, although the results from four holes (R-5, -6, -7, and -8) were negative, the fifth (R-3) undercut a very similar lens and intersected a massive sulfide body. Very detailed studies of these drill sites may explain the difference in results.

Flanigan and others (1982, p. 16) conducted detailed electromagnetic and self-potential surveys over the Rabathan deposit. Results of the surveys are so complex that the authors stated, "Using geophysical data alone it would be impossible to identify the massive sulfide had its location not been known."

The complex geophysical results, very limited primary dispersion zones, and very complex geology complicated by a general lack of marker horizons all contribute to the ineffectiveness of standard exploration procedures in this part of the Wadi Bidah valley. Kiilsgaard and others (1978, p. 65) stated that "additional exploration work was not recommended in the Wadi Bidah area because any sulfides found were apt to be of the same size and grade as those previously discovered in the Wadi Bidah area." The present authors agree with this recommendation in regard to the metasedimentary-metavolcanic complex of layered rocks in the Wadi Bidah valley bottom and believe that, although continued effort and expense might find sulfide deposits in this environment, the probably size and grade of the deposits do not warrant the effort.

B-13 ANOMALY AREA, NORTHERN WADI BIDAH

by

B. C. Waters

The B-13 anomaly in the northern part of the Wadi Bidah district is extremely elongate (plate 4), and the B-29 anomaly to the south and exposures in the basalt plateau to the north extend this ribbonlike band of rocks to a total length of approximately 50 km.

Although horizons are extremely persistent and uniform in thickness in a north-south direction, they are narrow in the east-west direction and exhibit notable depositional facies changes within units across strike. This geological style, as well as the absence of coarse-grained volcanic rocks, suggests that the sediments and lavas were deposited in a fairly stable shallow-water trough-and-ridge marine environment as a product of volcanism. Later deformation resulted in north-trending horizontal fold axes.

Direct evidence of folding proved to be of little use in the development of the present geological model. Although much small-scale folding was seen in the thinner and more competent beds, strong subvertical cleavage was produced by isoclinal deformation so that larger scale structures can be implied only by stratigraphic repetition. Sedimentary layering is generally subparallel to cleavage, dips are nearly vertical both east and west, and evidence for the determination of tops and bottoms in the sedimentary section was not found. The north-striking faulting suggested by many workers in the region was not observed in the area. However, on aerial photographs numerous minor faults were observed to strike N. 60° E. and N. 60° W. and probably form a conjugate pair to the north-striking fold axes.

Geological factors that proved to be most obvious in the study include:

1. the lateral persistence of the thicker chert beds in east-west as well as north-south directions,

2. the alternate grading of two rock types,

3. the recognition of facies changes within the main calcareous, carbonaceous shale,

4. the intensity of cleavage development as an index to grain size, and

5. the sloping relations of the diorite intrusive body.

Sharq volcanic stage

The oldest rocks in the belt are the volcanic rocks of the Sharq group, the lowermost unit of which is andesite (plates 4, 5). This andesite unit is composed of variable light- to dark-green or gray-green, fine- to coarse-grained lapilli tuffs and lesser flow rocks; the rocks weather dark brown to yellow brown and retain a uniform texture and composition. The mineral assemblage includes epidote, chlorite, and calcite and represents a combination of alteration and metamorphic products of the original feldspar and ferromagnesian minerals. Especially in the northern part of the area, the andesite contains minor interbeds, several centimeters wide, of feldspathic tuff.

Overlying the lower andesite is a band of hematite chert that ranges from several centimeters to as much as 2 or 3 m thick and is persistent along both sides of the western anticlinal ridge of andesite.

Chert deposition preceded the accumulation of shale, silt, and mudstone of the lower shale unit. The shaly units exhibit a strong slaty cleavage on the eastern side of the western anticline, where they have been quarried. On the western side of the anticline, the shale grades into a thicker, more carbonate-rich series that probably accumulated in a shallow subsiding trough.

Shale deposition was followed by a resumption of volcanic activity of a more intermediate character. The initial eruption of massive andesite-dacite lava in a thick wedge in the northeast was followed in the east by dacitic tuffs and lavas of a less massive character, locally by andesitic tuffs and lavas, and in the west by more distal pyroxene dacite tuffs.

The oldest part of this volcanic pile probably lies far to the east, but within the B-13 anomaly area vitric dacites and andesitic flow rocks are the oldest members. These contain euhedral pyroxene and olivine phenocrysts and quartz- and feldspar-filled vesicles in a fine-grained groundmass. Wedges of coarse-grained agglomerate appear in the sequence toward the easternmost limits of the area.

The transition to deposition of softer, less competent dacitic tuffs and flow rocks was gradual. The intertonguing relation of this member with the finer grained tuffs of the pyroxene dacite unit may be observed because of folding, but clarification was not found in adjacent areas. The pyroxene dacite is a thick unit of variable grain size and clastic euhedral pyroxene content, but its overall composition is homogenous. It is a dark-brown-weathering, green to gray-green tuff containing euhedral pyroxene crystals as large as 0.5 cm in diameter; these crystals are particularly prominent on weathered surfaces. Millimeter-sized grains of pink feldspar are present in most areas. A few thin layers of quartz-feldspar tuff are interbedded with the pyroxene dacite.

The pyroxene dacite shows a gradation in rhythmic interbeds into the upper and lower shales, and the contact with the upper shale is marked locally by interbeds of coarse graywacke 0.5 m thick and by local flows of andesite as thick as 50 m. The upper andesite is not persistent along strike, but it is very similar to the lower andesite.

Bidah group carbonate sedimentation

Sedimentary deposition of Bidah age is represented by the upper shale unit (plates 4, 5). This unit has a gradational contact with the dacites to the east, where interbeds are generally thicker than those in the pyroxene dacite. Initially, a series of fine-grained, greenish-gray shales having a calcareous and locally carbonaceous character accumulated in a quiet-water environment that received a proportion of ash from the waning Sharq volcanoes to the east and west (plate 5). A period of quiescence followed, in which a thick carbonaceous shale containing local disseminated sulfides and only minor carbonate accumulated. Chert deposition, followed closely by precipitation of a 2- or 3-m thick cherty iron-manganese exhalative (chemogenic) layer, probably marked the final waning phase of Sharq basic and intermediate volcanism (plate 5). The chert, which is well-banded, ranges from 1 to 10 m thick but is mostly from 2 to 3 m thick. It is gray to gray black and shows evidence of a primary carbonate content now recrystallized in thin stringers of irregular orientation. The fine-grained, brown or brown-black sedimentary rock is cemented by iron and manganese oxides, has a relatively high specific gravity, and is cut in many places by irregular quartz-hematite stringers.

These horizons are hosted by silty limestones, which were deposited after the shale. The limestones are both calcareous and dolomitic and are generally buff brown where fresh and dark brown to yellow brown where weathered. Stringers of quartz associated with recrystallization are common. The limestones contain layers of calcareous-dolomitic siltstone and in one area in the north-central part of the belt contain a gossan and gossanous chert layer from 0.5 to 2 m thick. Shallow marine conditions allowed the accumulation of silty rocks resulting from rejuvenated erosion to the east contemporaneous with the formation of carbonate precipitates.

Intrusion and tectonism

The oldest intrusive rocks in the area are 1-m-thick dikes of quartz and feldspar porphyry containing inclusions of rhyolite.

A syntectonic, green and white massive hornblende diorite was intruded especially along anticlinal structures within the belt and is a regional feature marking the end of Precambrian volcanism and sedimentation in the Wadi Bidah area (plate 5). Isoclinal deformation of incompetent beds of the Bidah group about north-trending axes was accompanied by folding of longer wavelength in the more competent Sharq and Gharb volcanic rocks.

One of the best pieces of evidence for the relative ages of the volcanic and sedimentary rocks in the area results from this intrusion and deformation. In the upper part of the main western mass of intrusive diorite, baked slices of deformed and recrystallized shale, limestone, and dacite several meters wide are found as roof pendants in the diorite and confirm the position of Bidah sedimentary rocks as a younger sequence than the Sharq volcanic rocks, which are deformed against the intrusive rocks (plate 4, 360 S to 380 N). Faulting about directions 60° east and west of the north-trending fold axes is common, but displacement is no more than several tens of meters.

Recent history

Flat plateau basalts immediately north of the area were probably extruded in Quaternary time, and the north-flowing drainage pattern of Wadi Bidah, a pattern which exploits the easily erodable Bidah group, was probably well established by that time.

Recent sedimentary rocks and unconsolidated alluvium were deposited during periods of torrential rainfall. These deposits are unbedded and from 3 to 5 m thick. They consist of very poorly sorted material including large and generally rounded boulders that appear to be only slightly related to the present wadi drainage pattern.

River-terrace deposits are near the present valley floor of Wadi Bidah and in some places are 10 to 15 m above the wadi base.

Targets within the area

One target that has emerged as a result of this study is a thin cherty gossan, which crops out intermittently over a strike length of 3 km and is from 0.5 to 1 m thick. A zone of copper-enriched shale adjacent to this gossan was mined locally by the ancients (plate 4).

Previous workers have studied other features in the area. Earhart and Mawad (1970) drilled three holes in the region (R-5, R-7, and R-8). Drill hole R-5 tested an "iron formation" (chert) and a cherty iron-manganese formation but failed to intersect major sulfides. Drill hole R-7 was drilled to test a cherty iron-manganese lens, and, although minor pyrite and chalcopyrite were encountered in the graphitic shales, major amounts of sulfide were not located. Drill hole R-8 is located close to R-7 and was drilled to test limonite-rich zones in dolomite. A thin zone of malachitic, dolomitic silt was intersected, but no analytical results were published.

Geochemistry

The present geochemical data from incomplete lines across the anomaly area, commonly spaced more than 200 m apart, are not regarded as sufficient to evaluate the anomaly (plate 4). However, the high spot values were useful in locating shows of malachite in several areas.

Associated areas

C. W. Smith kindly provided comments on a comparison of the B-13 area with the B-29 area to the south, an area that is very similar in lithology and includes the Rabathan orebody. The gossan-cherty gossan possibly is the lateral facies expression of the Rabathan mineralizing event and as such might display mineralized facies equivalents to both the north and the south.

Although very little work has been done north of the B-13 belt, a small chert layer, possibly containing some gossanous material, was located about 20 km north of the B-13 area on a direct strike continuity with the zone.

Conclusions and recommendations

One target has emerged from the present study in the B-13 anomaly area. It is a thin horizon that in most areas has considerable potential for stratigraphic thickening along the unexposed parts of its 3-km strike length. It is the best target to emerge from the current stage of fieldwork in Wadi Bidah. A detailed paleogeographic interpretation of Bidah group sedimentation is recommended to trace lateral facies equivalents and locally restricted basins.

Detailed mapping and geochemical sampling at 1:1,000 scale are recommended for a zone 3.5 km long and from 200 to 300 m wide situated across the gossan and cherty gossan, between lines 8400 N and 11600 N, east of the base line.

Geochemical rock-chip sampling is recommended at 5-m intervals along east-west lines spaced 50 m apart, and careful attention should be paid to sample quality and orientation.

B-25 AND B-26 ANOMALY AREA, BILAJIMAH

by

B. C. Waters

Layered rocks

The gossans of Bilajimah are hosted by fine- to medium-grained felsic to intermediate tuffs (plate 6). Underlying units grade into intermediate and basic tuffs and flow rocks, and the gossans are locally related to a very thin basic tuff horizon.

Green-gray tuff

A green-gray, medium- to coarse-grained felsic tuff unit is 50 m thick, weathers brown to dark brown, and contains clasts as large as several centimeters in diameter. It has poorly developed bedding on the scale of centimeters. Cleavage and, locally, pencil cleavage are well developed, and fold axes are strongly emphasized by stretching of the rock fabric.

Lower gossan

A gossan, 1.5 m thick, is at the top of the lowest felsic tuff unit. It is a dark-brownish-green, very fine grained, iron- and manganese-rich chemogenic sedimentary rock having some basic tuff component. True limonitic gossan material is rare, being confined to a few pods and lenses.

Felsic tuff

The felsic tuff unit in the area is well bedded and 100 m thick. The tuff is generally poorly cleaved, greenish yellow, fine grained, and siliceous. It contains finer grained bands, from 1 to 2 mm thick, that are rich in quartz, and it contains similar layers rich in feldspar and sericite.

Felsic to intermediate tuff

The felsic to intermediate tuff is medium to coarse grained and shows millimeter-scale compositional banding between chlorite-rich (intermediate) and sericite-rich (felsic) layers. In most places the rock is altered to quartz-sericite-chlorite-carbonate schist, and in many places pronounced lineation and elongation along fold axes are present.

Main gossan

The main gossan is a zone from 2 to 3 m thick within the felsic cream-brown tuff. It is composed of dark-green to brown chemogenic iron-manganese sediments. The zone contains pods, lenses, and bands of limonitic gossan as thick as 0.5 m, and layers of limonite-stained tuff and sediments are common.

Rhyolite flow rocks

A 1-m-thick, irregular band of rhyolitic flow rocks locally overlies the main gossan zone; in places it is separated from the gossan by slightly to moderately calcareous tuff. The flow rocks are vitric, well banded, and blue to black, and they weather to gray or dark brown with an associated devitrified crust (now sucrosic quartz). Blebs of hematite are distributed throughout, and biotite is locally present as very fine grained crystal inclusions. In addition, there are a few very fine grained anhedral blebs of chalcopyrite. Flattened vesicles as long as 4 cm are lined with iron-manganese oxides. Bands of grayish-yellow micritic limestone, 1 m thick, are present above the rhyolite, especially in the area of the north gossan (not shown in stratigraphic column).

Felsic cream-brown tuff

The felsic cream-brown tuff unit hosts the main gossan and rhyolitic flow rocks. It is 50 m thick, greenish yellow, and medium grained. It is very similar to the felsic tuff unit except for its compositional variation into more intermediate types and its millimeter-scale laminations.

Quartz crystal tuff

The most marked change in the tuffs overlying the main gossan horizon is the introduction of anhedral blue quartz crystals into tuffs that are otherwise very similar or identical in composition to those previously described. The quartz crystal tuff is 150 m thick, greenish yellow to greenish gray, fine to medium grained, felsic to intermediate in composition, and very similar in parts to the felsic to intermediate tuff, felsic tuff, and felsic cream-brown tuff units. The anhedral blue quartz crystal clasts that differentiate this tuff from the others compose from 1 to 30 percent of the rock and are generally from 2 to 5 mm in diameter. Lamination in this tuff is very similar to that in underlying units except that it is more pronounced because of varying concentrations of quartz clasts. The unit weathers from brown to light brown.

An upper andesite unit (not shown on plate 6) is approximately 100 m thick and consists of medium- to fine-grained tuffs and vesicular flow rocks. The andesite shows an irregular development of quartz-epidote veining that in places bears chalcopyrite, and it forms an upper marker useful in mapping the folded sequence because of its continuity and easy identification on aerial photographs.

Intrusive rocks

Dacitic and andesitic dikes and sills

Highly deformed dikes and sills of dacite and andesite mark the earliest stage of intrusive activity. They are mainly andesitic in composition and have a medium- to fine-grained, equigranular-felted texture. Calcite-filled vesicles are common.

Hornblende granodiorite

Posttectonic hornblende granodiorite dikes are approximately 10 percent biotite, 20 percent anhedral green hornblende, 25 percent quartz, and 45 percent feldspar. The granodiorite is equigranular and anhedral and has a weakly defined fabric resulting from orientation parallel to flow structure. Fresh rock is grayish white, weathered rock is brownish white. Related hornblende rhyodacite dikes occur locally; they are medium to coarse grained and gray green and contain quartz, feldspar, and variable amounts of hornblende and biotite.

Structure

Folding

Folding on shallowly north-plunging axes has produced large-scale anticlines and synclines about 1 km wide. Parasitic folding, especially in the less competent rocks, is intensely developed down to the centimeter scale. The gossan horizons are extensively folded about north-plunging axes on a scale of tens of meters, and this folding has exaggerated the thickness of the gossans in most areas.

Stretching along fold axes has accompanied folding and produced rodding of clasts within some of the tuffaceous units and large-scale boudinage of the very competent rhyolite flow rocks that overlie the main gossan along its entire strike length. Hornblende granodiorite sills and dikes are clearly folded and strongly thickened in anticlinal and synclinal fold noses.

Most porphyritic rhyodacite dikes trend at an angle of 20° to the regional fold axes and are nearly vertical. They are believed to be unrelated to folding and possibly were intruded posttectonically along with the hornblende granodiorite.

Faulting

The area is bounded by pronounced north- and northwest-trending sinistral faults having displacements of several hundreds of meters, as mapped by Earhart and Mawad (1970), Jackaman (1972), and Riofinex Geological Mission (1979). The main body of intrusive hornblende granodiorite in the western part of the mapped area may have exploited a weak (shear?) zone generated by this faulting. In addition to this main fault set, dextral northeast- and east-northeast-trending oblique faults within the area (plate 6) have displacements on the order of tens of meters only.

Metamorphism and alteration

Basic rocks in the area exhibit a low-grade greenschist assemblage (chlorite, epidote, actinolite), whereas felsic rocks have almost universally been converted to quartz-sericite-calcite schist with chlorite development in intermediate layers.

Contact metamorphism of the calcite-rich dacite against the hornblende granodiorite has produced calcite-siderite-hematite rock. Massive specular hematite has developed in areas where extrusive rhyolite is in direct contact with the gossan horizon.

Zones of intense silicification adjacent to hematite-filled fractures are widespread in the tuff units that lie between the lower and main gossans near hornblende granodiorite intrusive rocks. It is not known if the intrusive event was the direct cause of the silicification.

Geologic interpretation

Both the homogeneous texture and composition of the tuffs over tens of meters stratigraphically and the absence of a significant proportion of debris coarser than millimeter size, together with fine millimeter-scale lamination and overall felsic composition, suggest that the tuff sequence was deposited as a conformable stack of ash-fall or shallow-water tuffs at a great distance from the source of felsic volcanism. This interpretation is confirmed by the general absence of rhyolite or rhyodacite flow rocks in the area, in contrast to a belt farther to the north in which such flow rocks are common (Riofinex Geological Mission, 1979). It has yet to be determined if the tuffs display the internal shardic features of a nuee ardente or if they are simply ash-fall tuffs.

Quartz-feldspar porphyritic rocks and granodioritic intrusive rocks are probably related to a center of activity, but little is known of this relationship except that hornblende granodiorite tends to be associated with the axis of the main western anticlinorium (Greenwood, 1975; Greene and Gonzalez, 1980). The intrusive rocks are probably somehow related to the major granitic center to the north. Two potassium-argon ages on the hornblende granodiorite average 800 Ma (Brown, 1960).

Comparison with geology of other local gossans

The Sha'ab at Tare, Wadi Leif, Gehab, Mulgatah, and Mulhal gossans to the north of the Bilajimah area are developed over sulfide horizons associated with limonite-stained sediments, and chert and quartzite are locally present. The mineralized rocks are at the contact between a lower unit of andesitic agglomerate and tuff and an upper unit of altered sericite-quartz-chlorite schist and may be interpreted as a more proximal and possibly deeper water version of the lower gossan horizon at Bilajimah. Because the B-24 anomaly area to the south of the Bilajimah area contains many small gossans and ancient workings that are related to a graphitic schist belt, the two areas are not directly comparable.

Geochemical studies

Rock-chip samples were gathered at 25-m intervals along lines spaced 100 m apart. The geochemical response of copper is very limited, and gossan outcrops are responsible for a few moderately high values (plate 6). Within that part of the area mapped in detail, higher copper values correlate with gossan outcrops. This correlation is also true of the unmapped area to the east, where a zone of north-trending gossans correlates with a few copper values of about 300 ppm.

The geochemical response of zinc is similar to that of copper, and zinc values of from 200 to 700 ppm correlate with gossan outcrops. The highest silver value recorded was 5 ppm (plate 6). A few isolated values of from 3 to 5 ppm correlate with gossan outcrops.

Base and precious metal contents of rock-chip samples are uniformly low. Subsequent drilling results confirm geochemical data and stress the importance of the strong correlation between gossan outcrops and the underlying sulfide geochemistry in the Wadi Bidah district.

Results of drilling in the Bilajimah area

by

C. W. Smith

Two drill holes were positioned according to Waters' recommendations and drilled at an angle designed to intersect the projection of surface gossans (plate 6, figs. 4, 5; drill logs, plate 3). At a depth of about 20 m, drill hole BJ-1 cut a gossanous-carbonaceous zone that consists of approximately 70 percent carbonaceous material and 30 percent limonite. This zone is undoubtedly an extension of the gossan mapped at the surface, although surface mapping did not identify carbonaceous material. Weathering characteristics of carbonaceous rocks at Bilajimah are similar to those of carbonaceous rocks mapped in the Wadi Bidah valley bottom; that is, they do not readily disclose their carbonaceous nature because they have been altered to iron-stained sericite and clay. If vestigial carbonaceous rocks are present, they are completely masked by iron staining.

Drill hole BJ-1 cut an anticlinal structure and intersected two distinct sulfide zones in which pyrrhotite is associated with carbonaceous rocks. The sulfides apparently were deposited in fine layers, but small-scale folding and shearing have transformed the pyrrhotite into a fine, wispy filigree that composes about 10-15 percent of the rock. Pyrrhotite is replaced locally by fine wisps of chalcopyrite, but zinc minerals were not seen. Drill hole BJ-2 intersected a similar carbonaceous-sulfide zone. The presence in both drill holes of only minor amounts of base and precious metals explains very well their appearance at the surface, their slightly anomalous character as shown in geochemical studies, and their tendency to appear as anomalous zones in airborne electromagnetic, ground electromagnetic, self-potential, and magnetic surveys (Flanigan and others, 1981). The low-grade assay results are shown in figures 4 and 5. Two gossanous-carbonaceous rock samples from the oxidized zone intersected in BJ-1 contained 8.1 and 8.8 grams per ton silver. Silver appears to be slightly enriched in the oxidized zone because in both drill holes consistently lower silver values were found throughout the sulfide zone.

The folded stratigraphic section intersected by drill holes BJ-1 and -2 consists of tuffs that are mostly dacitic but range from felsic to intermediate and grade to mafic with minor andesite flows. Carbonaceous material is interlayered with the tuffs and ranges in volume from a few thin partings to sections that are almost pure carbon. Chert and glauconitic argillite are also interlayered but are less abundant

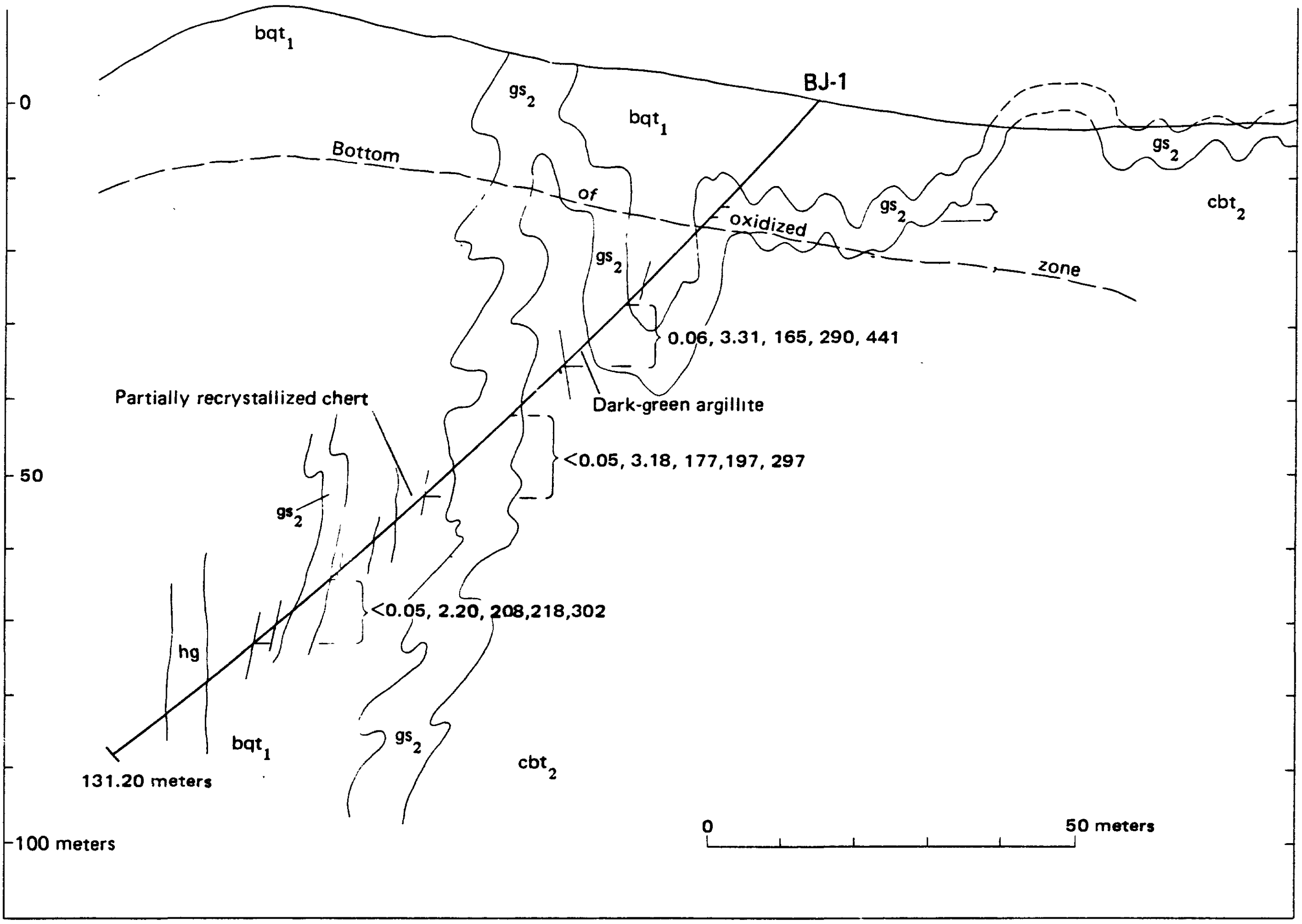

Geology by B. C. Waters, 1979.

EXPLANATION

hg — Hornblende granodiorite, fine-to medium-grained. Occurs as posttectonic dikes

bqt_1 — Quartz crystal tuff, grayish-white, medium-grained. Contains blue-gray quartz crystals

cbt_2 — Felsic cream-brown tuff, medium-grained, finely banded

gs_2 — Main gossan. Sulfide equivalent is carbonaceous schist containing ~15 percent pyrrhotite

Contact

Drill intersection
0.06, 3.31, 165, 290, 441--Weighted average of drill core assays over interval, in parts per million, for gold, silver, copper, lead, and zinc

Layering and foliation in drill core

Figure 4.--Geologic cross section along drill hole BJ-1, looking north, Bilajimah.

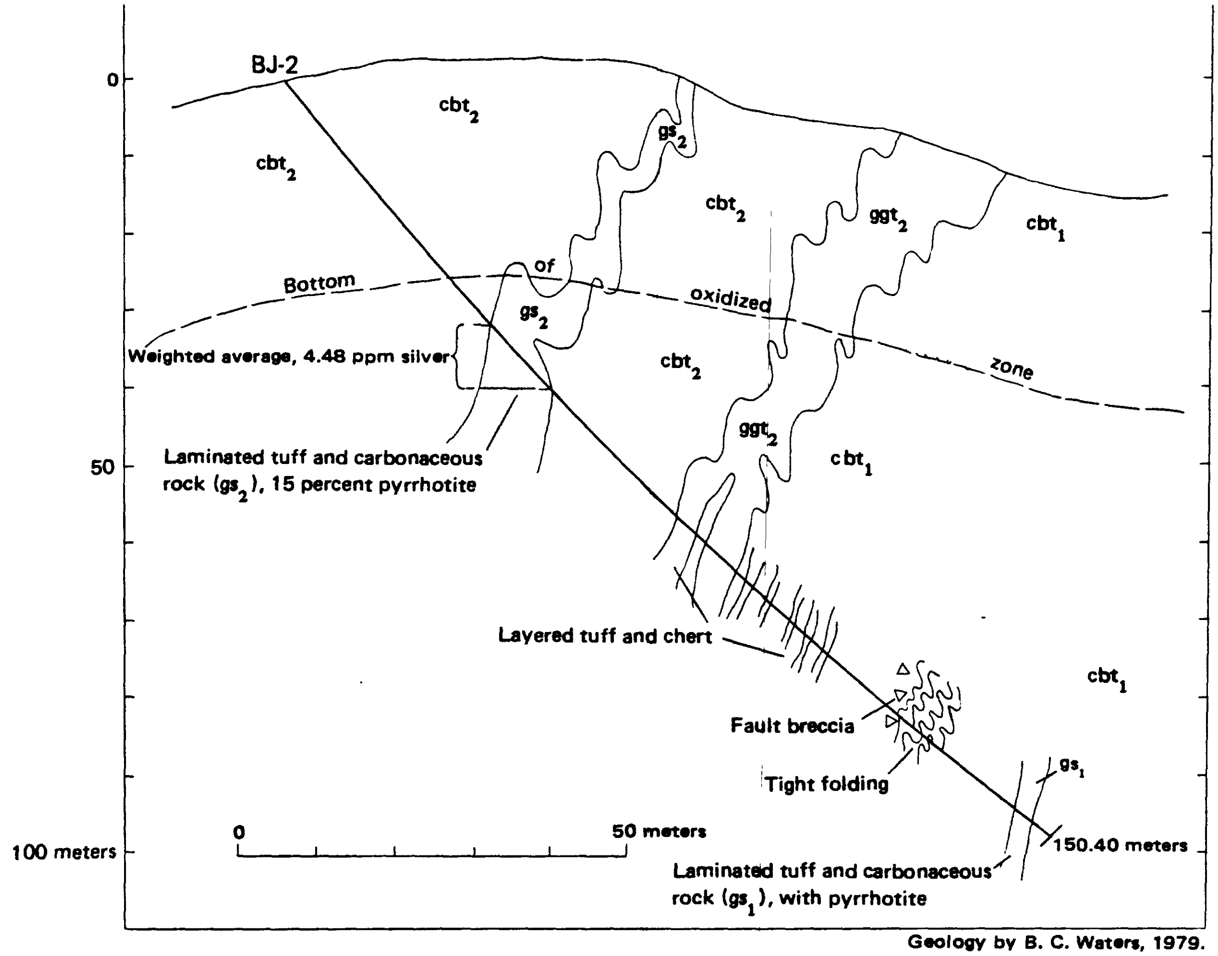

EXPLANATION

cbt_2	Felsic cream-brown tuff, medium-grained, finely banded	cbt_1	Felsic tuff, fine-grained, greenish-yellow
gs_2	Main gossan. Sulfide equivalent is carbonaceous schist containing ~15 percent pyrrhotite	gs_1	Lower gossan. Sulfide equivalent is carbonaceous schist laced with pyrrhotite
ggt_2	Felsic to intermediate tuff, medium- to coarse-grained, brown-weathering	——	Contact

Figure 5.--Geologic cross section along drill hole BJ-2, looking north, Bilajimah.

than carbonaceous material. This geologic setting indicates intermittent volcanic activity some distance away from the volcanic center. Pillow basalts on the surface and glauconitic argillite in the drill core suggest a marine environment. Sulfides interlayered with carbonaceous material also suggest that the marine conditions were shallow and provided a chemically reducing environment.

NORTHERN PART OF THE B-24 ANOMALY AREA, KHAYAL AL MASNA'AH ANCIENT MINE

Geology

The Khayal al Masna'ah (As Sut) ancient workings are located west of Wadi Bidah at the northern end of a long, north-trending AEM anomaly designated B-24 (figs. 2, 3, 6). The small workings, about 35 m long and as deep as 5 m, are on a north-trending quartz vein and parallel shear zone. The vein is almost vertical and is as thick as 35 cm; in places it contains barite. The workings are centered on a shear zone that extends both north and south and consists of quartz-sericite schist containing disseminated hematite pseudomorphs after pyrite. Copper staining is present in both the vein and shear zone, and a light-green chromium mica is sparsely distributed within the zone.

Rocks in the area are tightly folded about almost horizontal north-trending axes and are highly schistose and in places slaty. They consist of pyroclastic andesite, volcanic wacke, chert, carbonaceous schist, and felsic tuff (fig. 7). Worl and Greenwood (Greenwood, 1975, p. 14) described the Asut (Khayal al Masna'ah) ancient mine area: an "extensive area of alteration along major north-trending shear zone; minor copper stain and numerous small gossans. Several quartz veins, 30 cm to 3 m wide and as much as 800 m long. Some veins contain white to pink carbonate." Figure 7 shows a sketch map of the Khayal al Masna'ah mine area and gives analytical data for several chip samples.

The study area lies on the northeastern edge of the B-24 AEM anomaly. After evaluating both airborne and ground surveys, Flanigan and others (1982, p. 41) stated, "It may be sufficient to note that there is no electrical expression at either [Khayal al Masna'ah and Mahawiyah] mine site."

Geochemistry

Two geochemical rock-chip sample lines were run 500 m east and west of the Asut ancient mine (fig. 7). Rock samples were collected at 25-m intervals; one line was positioned through the ancient mine and another 100 m to the south. Electromagnetic and self-potential geophysical measurements were made at the sample locations. Analytical

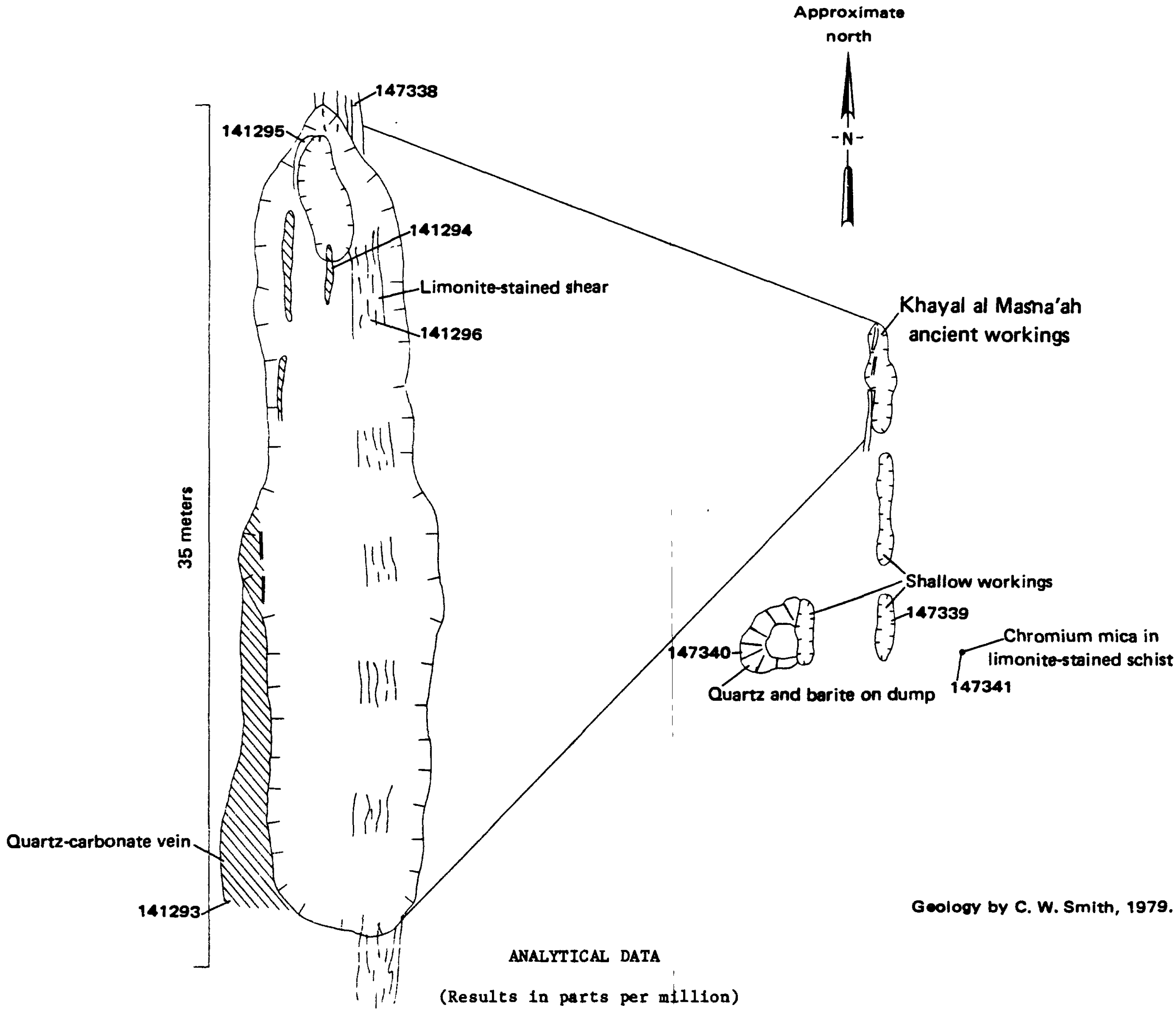

ANALYTICAL DATA

(Results in parts per million)

Sample number	Width (meters)	Au	Ag	Cu	Pb	Zn	Description
141293	0.35	6.19	37.0	15,000	2,300	52,500	Quartz-carbonate, copper stained
141294	.15	0.82	16.0	550	650	3,500	Iron-stained shear
141295	.20	<.05	1.6	300	60	200	Iron-stained shear
141296	1.50	.28	6.5	800	2,600	3,000	Iron-stained shear
147338	2.00	1.96	17.7	3,500	2,850	25,000	Quartz-sericite limonite schist, copper-stained
147339	2.50	6.38	23.4	950	2,050	800	Quartz-sericite-limonite schist
147340	*	1.96	9.1	5,000	1,950	2,500	Dump sample - 15 percent limonite
147341	6.00	.14	1.4	185	65	55	Iron-stained shear

*Width not known.

Figure 6.--Sketch map of the Khayal al Masna'ah (As Sut) ancient workings (not drawn to scale) and table showing geochemical results.

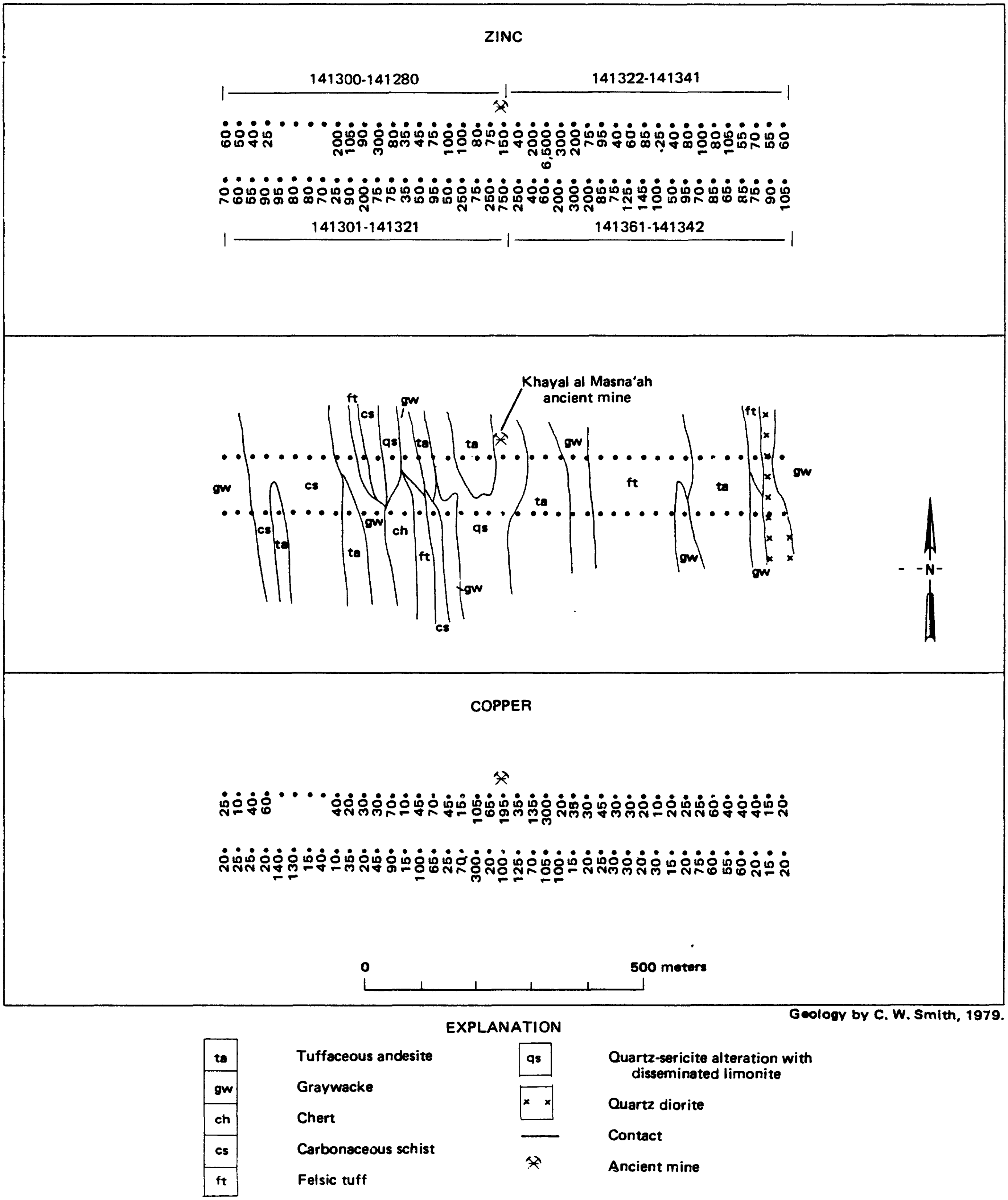

Figure 7.—Geologic and geochemical maps of the northern part of the B-24 anomaly area, Khayal al Masna'ah ancient workings. Dots on geochemical maps represent sample localities; geochemical values, in parts per million, are next to dots.

results indicate a subtle positive zinc anomaly extending erratically east and west of the workings. Zinc values of from 200 to 300 ppm probably indicate an area slightly anomalous in zinc. Although statistical studies were not conducted, these values appear to be above the mean for the district. Two samples from within the zone had much higher zinc contents than the other samples (6,500 and 750 ppm). Copper values were not as high as zinc values, and apparently copper is confined to a zone associated with quartz-carbonate veins in the ancient workings. A few erratic and probably anomalous lead, gold, and silver values were in samples from the same general zone near the ancient workings. Values as high as 1.07 ppm gold, 6.8 ppm silver, and 2,900 ppm lead were obtained.

Conclusions and recommendations

This area is of interest primarily because of the moderate gold and silver values obtained in sampling. As observed by Worl and Greenwood (Greenwood, 1975), the area of shearing, alteration, gossanous zones, and quartz-carbonate veins is extensive. Further study of the relationship between precious metals and the presence of chromium-bearing mica in limonite-stained and altered shear zones may be valuable. On a scale of one to ten, this area could be given a priority of five.

SOUTHERN PART OF THE B-24 ANOMALY AREA, MAHAWIYAH ANCIENT MINE

Geology

The Mahawiyah ancient mine area (fig. 8) has been mapped previously as part of a Master of Science thesis for the University of London by A. R. Abo-Rashid (1971). It has also been mapped and sampled in detail by Al Koulak (unpub. data). Both of these authors described the zone as being composed of metamorphosed felsic volcanic rocks that in places are sheared, hydrothermally altered, and intruded by rhyolite and andesite dikes or sills. As in most of the Wadi Bidah district, the layered rocks have been tightly folded about north-trending axes and the attitude of bedding is now almost vertical. Hydrothermal alteration affects large areas in the district, and, according to Al Koulak (unpub. data), these areas are distinguished by varying degrees of chloritization, silicification, sericitization, and pyritization. The Mahawiyah mine workings are centered on one of these altered zones, which extends from far south to far north of the mine area. Three diamond drill holes undercut the workings (Allcott, 1970). The holes intersected rocks containing moderate to low amounts of zinc and lesser amounts of copper and lead. Gold values ranged from nil to 1.03 ppm, and silver values ranged from less than 1.37 ppm to 13.1 ppm. Allcott recommended

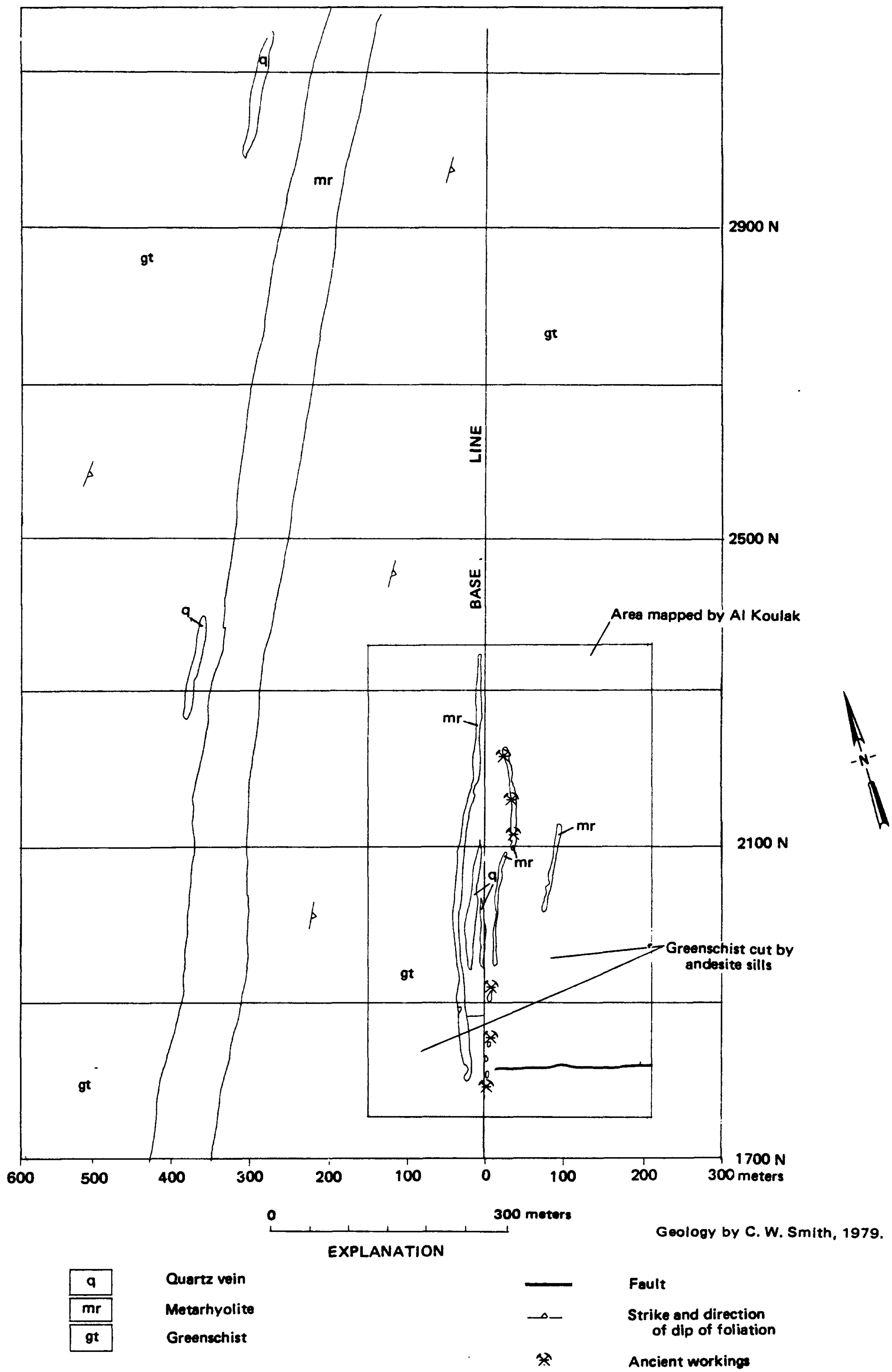

Figure 8.--Geologic sketch map of the southern part of the B-24 anomaly area, Mahawiyah ancient mine. Geology from Abo-Rashid (1971; entire area, 1:15,000 scale) and Al Koulak (unpub. data; area enclosed in box, 1:1,000 scale).

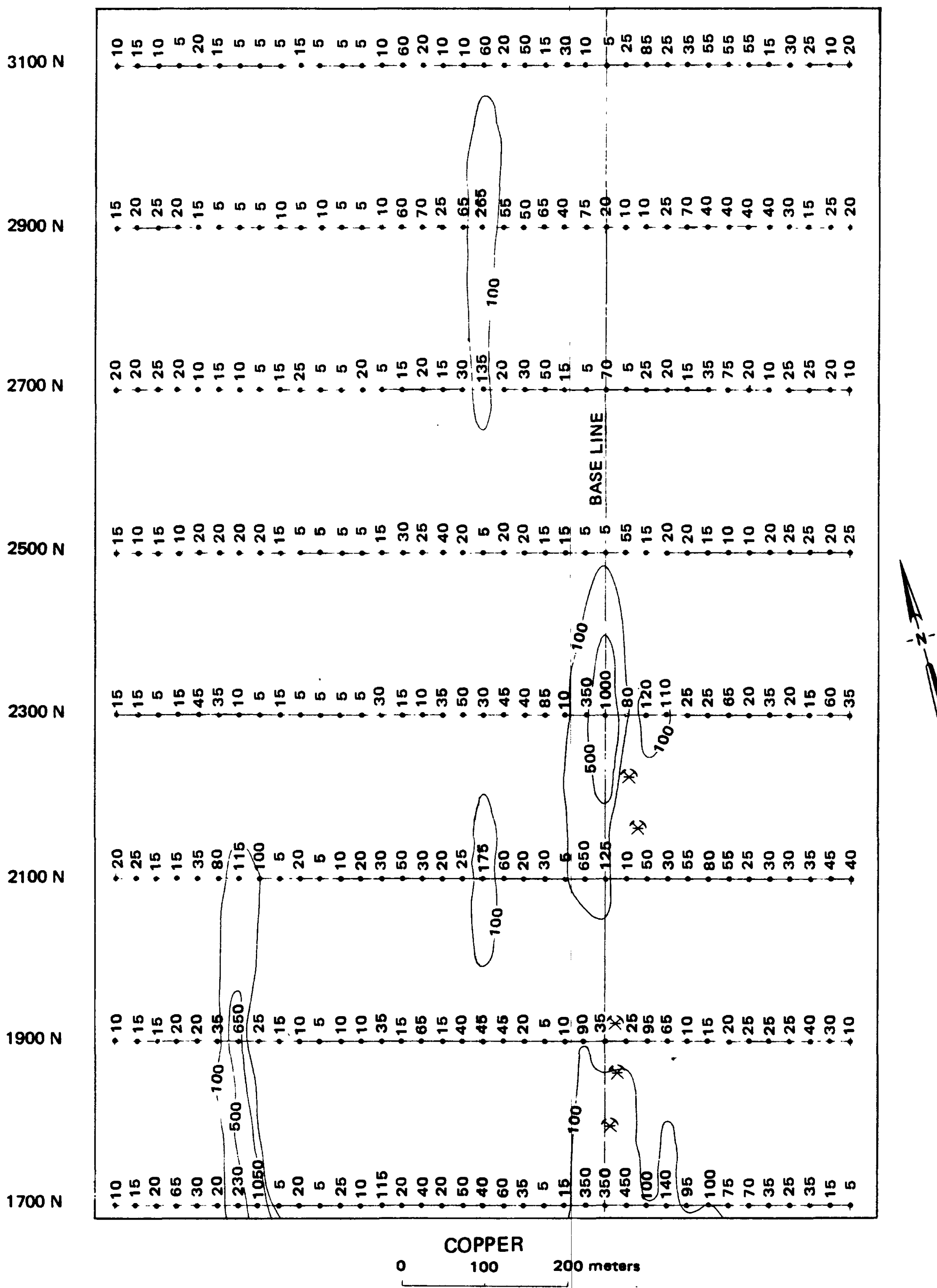

Figure 9.--Geochemical maps showing the distribution of copper and zinc in the southern part of the B-24 anomaly area, Mahawiyah ancient mine. Dots along traverse lines indicate rock sample localities and either zinc or copper content, in parts per million. Geochemical data contoured at 100, 500, 1000, 2000 and 5000 parts per million zinc and 100 and 500 parts per million copper.

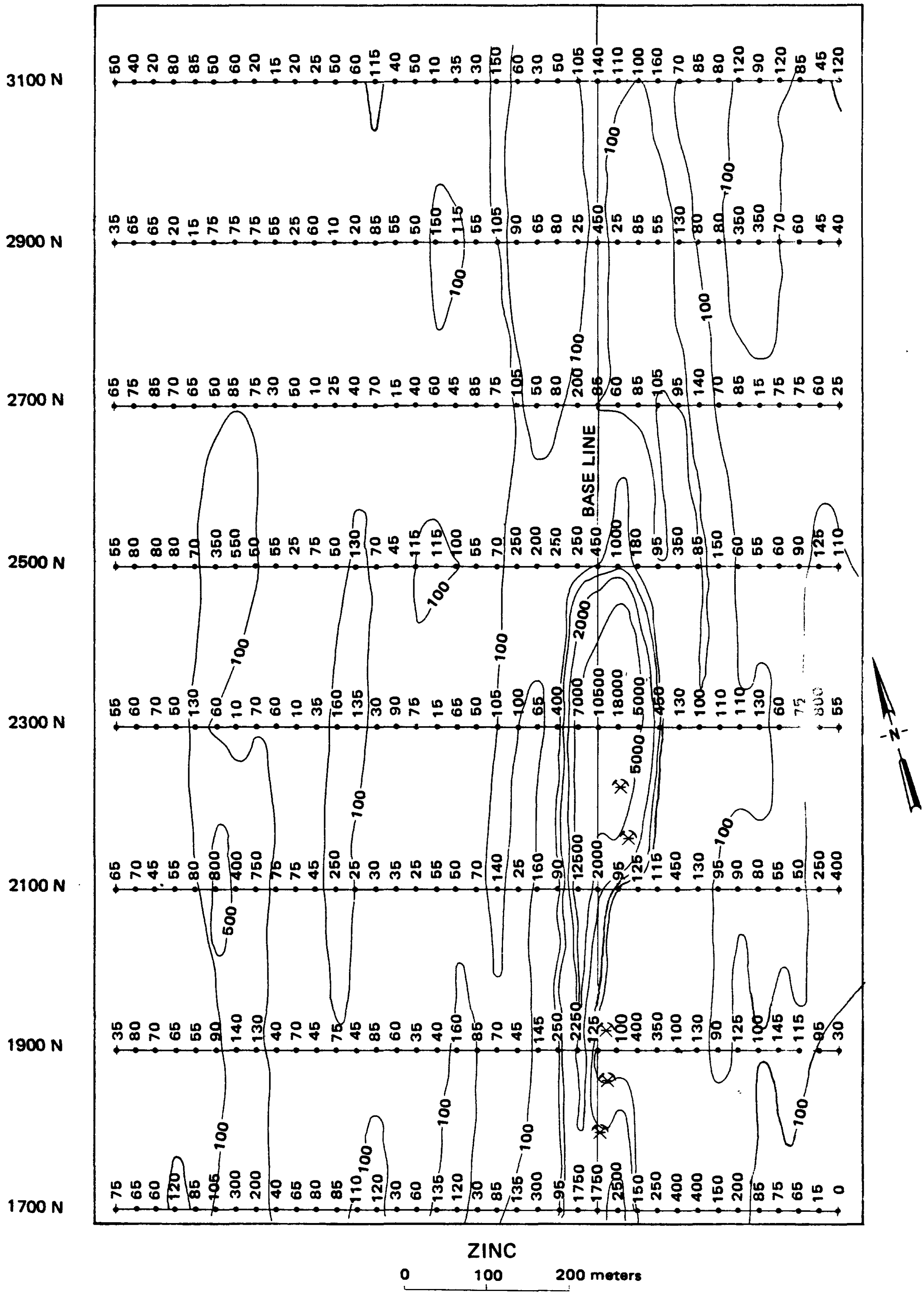

Figure 9.--Continued

that a geochemical survey be conducted to cover an area 2 to 3 km north of the ancient workings.

Geochemistry

Rock-chip sampling along lines spaced at 200-m intervals delineated an area including the ancient mine workings as being anomalous in zinc and copper (fig. 9). Anomalous zinc values were higher and more widespread than anomalous copper values. Anomalous zinc and copper values along the southern sample line suggest that this zone may continue to the south. A small copper and zinc anomaly found 430 m west of the base line includes copper values as high as 1,050 ppm copper and zinc values as high as 500 ppm. The cause of this anomaly is not known.

Conclusions and recommendations

Rock-chip sampling disclosed anomalous zinc and copper zones including one in the ancient mine area. The area just north of the mine did not contain anomalous amounts of copper and zinc. Although a small copper-zinc anomaly was found 430 m west of the base line, we believe that the mine area has been explored sufficiently and that further exploration would not be rewarding.

B-42A AND B-44A ANOMALY AREAS, ASSIFAR AREA

by

M. Naqvi

The Assifar area (fig. 2) derives its name from a small ancient gold mine located at the center of the area; the area is nearly 30 km northwest of the town of Al Bahah or about 10 km west of the At Taif-Al Bahah highway. The Assifar area is in mountainous terrain; the northern part is accessible by road, but the very rugged southern part is accessible only by foot or helicopter. Much of the northern part is under cultivation in terraced fields and most of the southern part is covered by juniper forests.

The ancient workings of Assifar have been cursorily sampled at various times, and although Greenwood (1975) mapped the geology of the Jabal Ibrahim quadrangle (20/41 C), in which the study area is located, the present report describes the first detailed work to be undertaken in this part of the Wadi Bidah district.

Nearly 1,000 rock-chip samples were collected along grid lines along which geophysical measurements had previously been made. Sample locations and geological data were plotted on enlarged aerial photographs at 1:10,000 scale.

Geology

The rocks of the Assifar area include mostly fine clastic sedimentary rocks; calcareous rocks are notably absent (figs. 10, 11). Andesitic volcanic rocks are present in minor amounts. This rock assemblage and numerous thin cherty iron-manganese lenses and thicker chert layers indicate a stable marine environment that is in contrast to a volcanic environment a few kilometers to the east in which felsic pyroclastic rocks abound. Carbonaceous rocks were noted along the northwestern edge of anomaly area B-44A but do not appear to be present elsewhere within the zone. All of the rocks in the Assifar area have been metamorphosed to greenschist facies.

Layered rocks were separated into stratigraphic units (figs. 10, 11) and are briefly described below, from oldest to youngest. The total thickness of each of the units described is less than a few hundred meters.

Stratigraphy

Siltstone.--Siltstone in the Assifar area is slightly foliated and ranges from light tan to light gray. Compositional layering is present only locally and most siltstone is almost featureless. Although the siltstone contains minor visible silica grains, it was classified separately from argillite only on the basis of its slightly foliated appearance. Siltstone in the area grades into both chert and argillite.

Cherty iron-manganese lenses.--Cherty iron-manganese lenses are present throughout the mapped area; they are interlayered with siltstone or chert and parallel to major faults and shear zones, although not necessarily conformable to the layered rocks. The lenses range in composition from mainly manganese and iron oxide staining to nearly pure oxide. In most places they consist of black manganese oxide-bearing chert with small amounts of iron oxide on weathered surfaces. Fresh surfaces generally display finely disseminated pyrite.

All of the oxide-bearing cherts appear to have the same general composition irrespective of the nature of the enclosing rocks, and, in places, where interlayered with siltstone, they evidently served as a locus for major faulting. Manganese-iron oxide cherts found in shear zones that crosscut rock layering are probably remnants of conformable lenses that were sheared into their present position.

Chert.--Chert is extensive in the mapped area and locally grades into argillite. In most places it is medium to dark gray; weathered surfaces are generally iron oxide stained, and fresh rocks contain finely disseminated pyrite. The chert is massive, and layering resulting from the differing

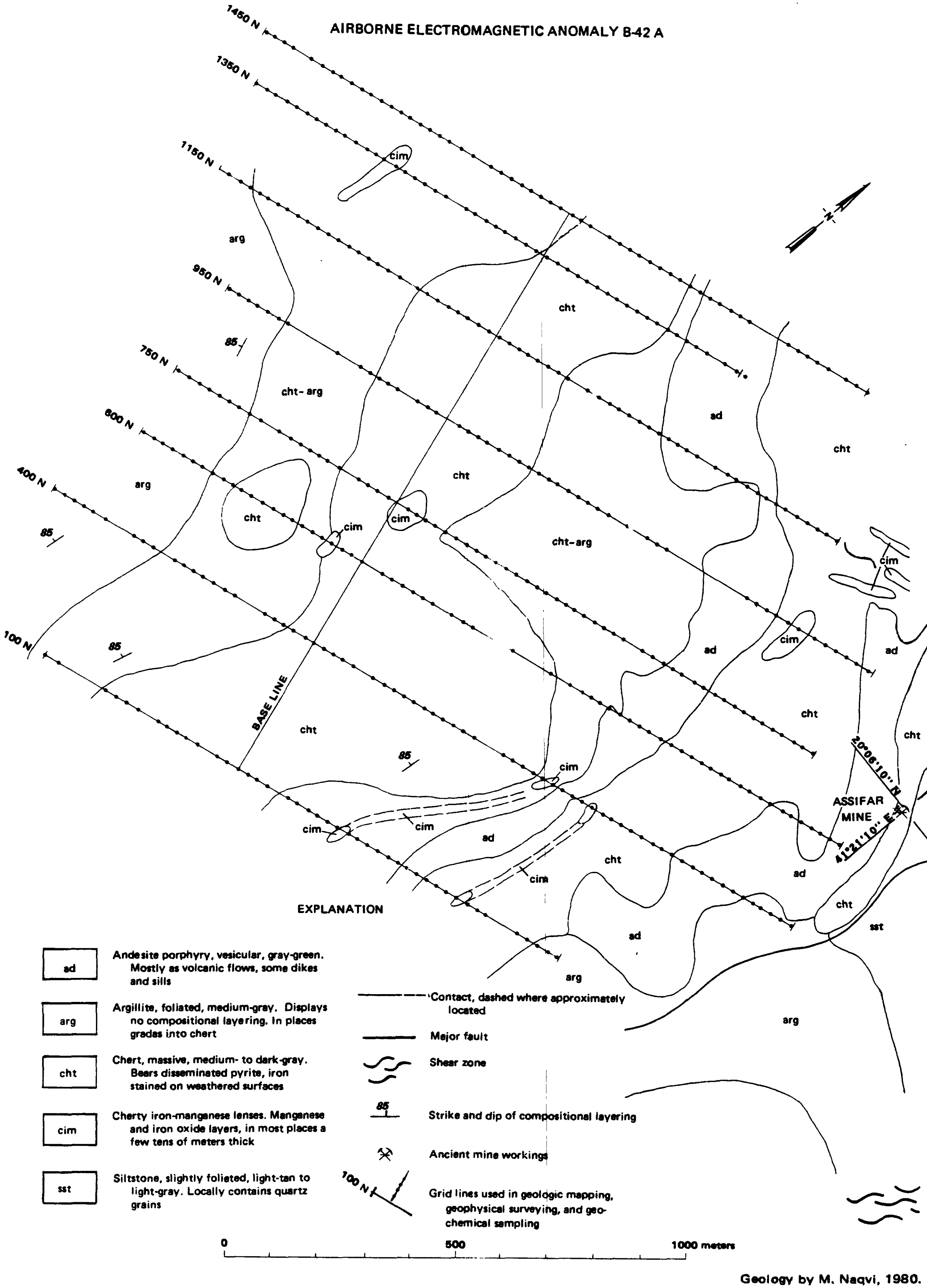

Figure 10.--Geologic and geochemical maps of the B-42A anomaly area, Assifar ancient mine.

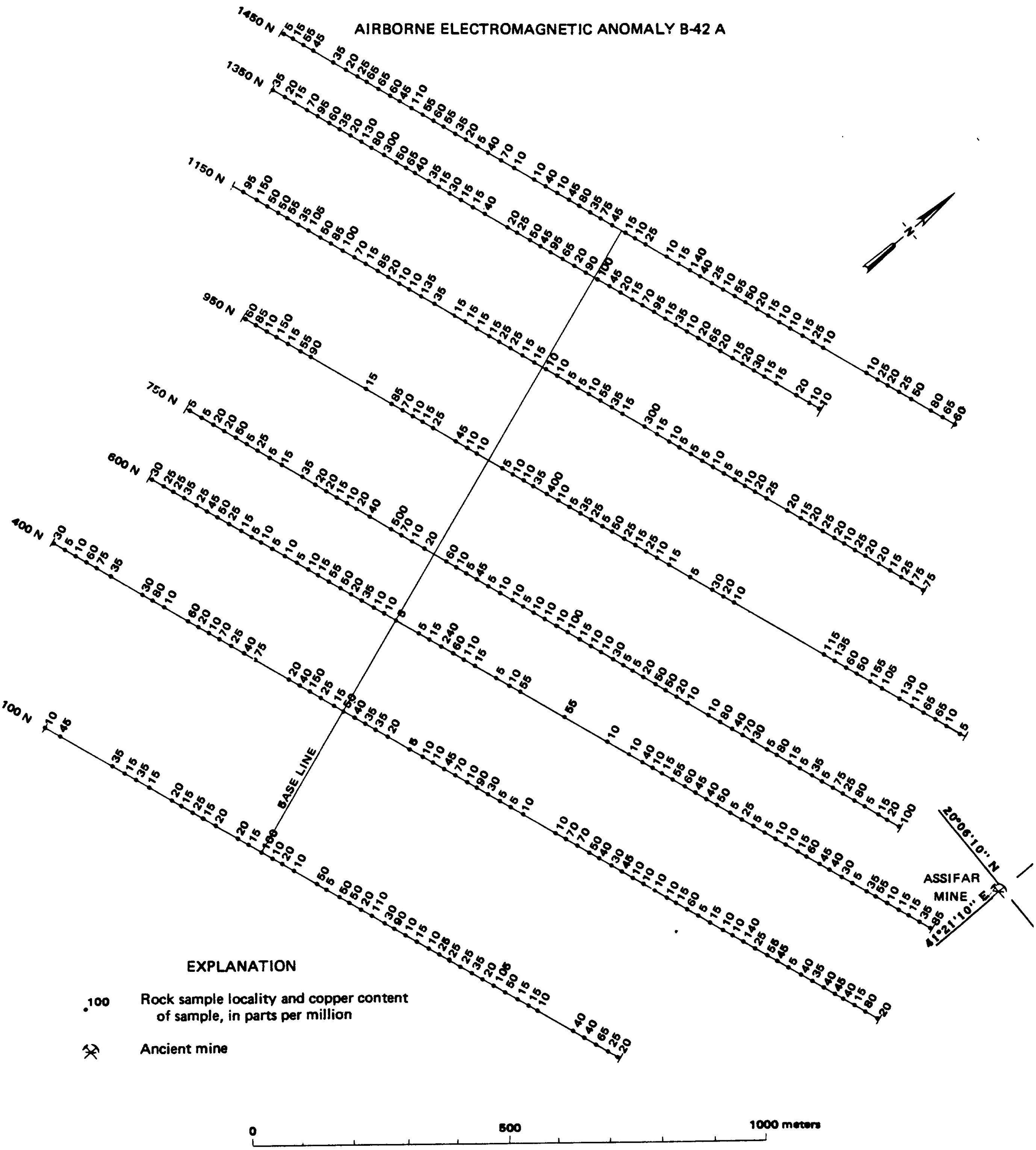

Figure 10.--Continued

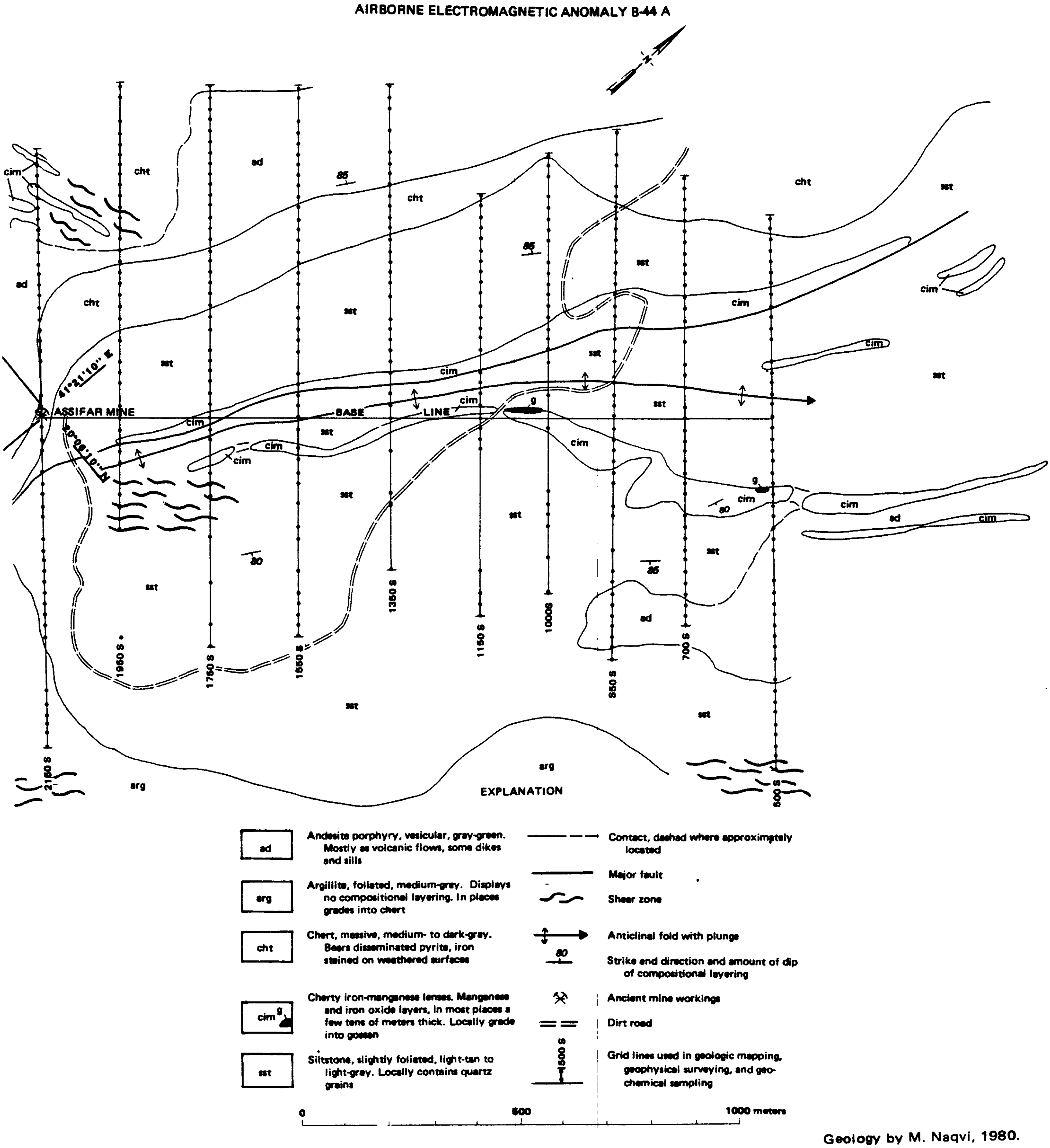

Figure 11.--Geologic and geochemical maps of the B-44A anomaly area, Assifar ancient mine.

AIRBORNE ELECTROMAGNETIC ANOMALY B-44 A

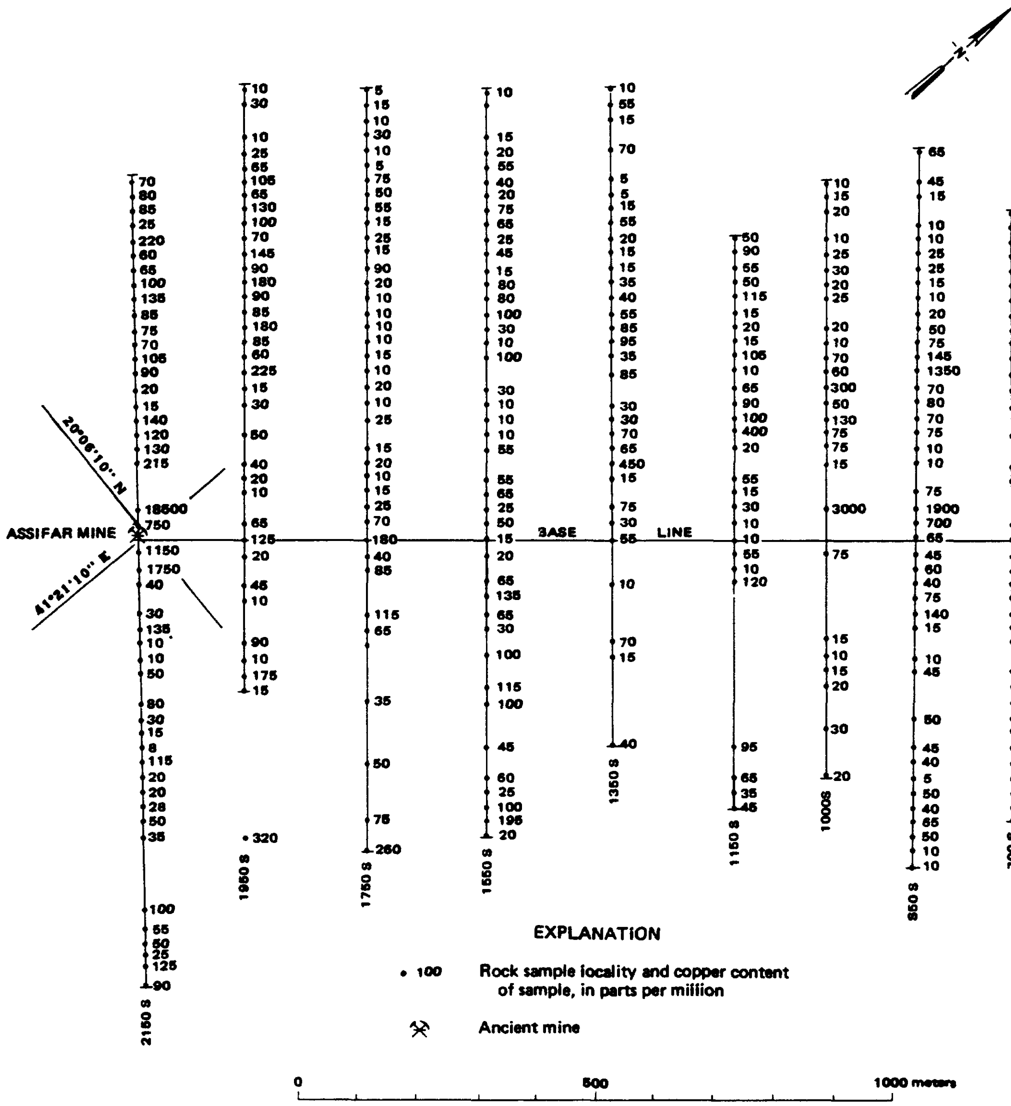

Figure 11.--Continued

densities of disseminated pyrite is locally evident. Quartz veinlets, some of which have minor malachite staining, intersect chert layers in some areas. The veinlets probably formed by solution of silica and redeposition during folding and metamorphism.

Argillite.--Because of its very fine grained nature, argillite in the area tends to be more schistose than siltstone. It is medium gray on weathered surfaces and displays no compositional layering. The argillite is probably gradational into both chert and siltstone, and, in places in the B-42A area, relationships between the chert and argillite are so complex that they were mapped as an undivided unit.

Andesite porphyry.--Volcanic to subvolcanic rocks in the area include andesite porphyry flow rocks, dikes, and sills. Flow rocks are vesicular and in places display flow banding. They weather medium gray green and are interlayered with chert and siltstone.

Structure

The most outstanding structural feature in the area is the difference in trends of the layered rocks between the B-42A and B-44A areas. Rocks west of the Assifar ancient mine (B-42A area) trend a few degrees west of north, but those in the mine area and to the east of it (B-44A area) trend approximately 20° NE. (figs. 10, 11). The northeast-trending rocks have clearly been faulted into their present position. On aerial photographs northeast-trending rocks appear to cut across the fabric of the general northwest trend in this region. The faulted zone appears to be less than 1 km wide and is centered approximately on the B-44A survey area. A major fault crosses the surveyed area (figs. 10, 11), but mapping outside the area is necessary to fully understand this large structural feature.

Generally, the layered rocks dip steeply both east and west, and, although complex folding on a scale of centimeters was noted in many places, no large-scale folding was measured. There is a strong possibility that a north-plunging anticlinal fold extends across the B-44A survey area and that the fold has been faulted semiparallel to the fold plane (fig. 11). Shear zones, many of which contain quartz stringers, indicate the complex nature of the relationship between shearing and stratigraphy. For example, the major fault mapped in the study area is generally parallel with layering, but the broad shear zones mapped along the southern extension of lines 1950 S and 2150 S and at the eastern end of line 1150 N are almost perpendicular to bedding.

Economic geology

Two small and slightly malachite-stained gossans were identified in the B-44A area (fig. 11). One gossan, located almost 150 m east of the base line along line 500 S, has an outcrop length of 30 m and a width of as much as 4 m. Part of the gossan may be covered with soil at its southern end. The iron oxides of the gossan vary from bright orange red and maroon to tan and light brown to dark brown. In most places the gossan has a fine siliceous cellular structure containing pulverulent limonite, but in places it is dense and siliceous and displays brecciation. A second gossan is adjacent to a dirt road passing through the area, and its main outcrop is between lines 1000 S and 1150 S, just west of the base line. This outcrop is exposed for a distance of 100 m but appears to be lenticular and discontinuous. It is similar in composition to the gossan just described. Both gossans grade into a cherty iron-manganese lens and are believed to be directly related to this formation.

Part of the same iron-manganese-rich formation is probably exposed in the western part of the B-42A area as a segment of the western flank of a north-plunging anticlinal fold. Within this segment, small pockets of iron-manganese oxide, interlayered mostly with chert, contained moderate to high copper values (fig. 10), but no notable gossans were mapped.

Geochemistry

In general, both the B-42A and B-44A areas were found to contain only minor anomalous zones, and only copper values were plotted (figs. 10, 11).

In the B-44A area, rock-chip sampling identified narrow copper- and zinc-anomalous zones coincident with gossans and cherty iron-manganese lenses (fig. 11), but otherwise metal values were generally very low. High copper values and relatively high gold values were found on line 2150 S where it crosses the Assifar ancient mine area. The geochemical study disclosed no previously unknown mineralized zones.

Flanigan and Sadek (1983) stated that ground geophysical studies in the Assifar ancient mine area indicate moderate to low potential for economic mineralized rocks. A zone of possible interest, as delineated by geochemical and self-potential geophysical surveys, is beneath and immediately south of the Assifar ancient mine.

The B-42A area contains only minor, randomly scattered zones of economically insignificant base metal concentrations.

Conclusions and recommendations

The results of this study indicate that further work is not justified. Small gossans, found associated with cherty iron-manganese lenses, are most likely the products of chemical precipitation onto a sea floor. Other iron-manganese cherts found in the area, however, are barren of base or precious metals. The ancient workings at Assifar are at the center of a copper-stained silicified breccia zone containing small, lenticular gossans. The breccia zone is 200 m long and 50 m wide, and sampling by previous workers disclosed only low gold and moderately high copper values. Because no deposits of economic grade were found despite the intensive nature of the mapping and sampling in the area, no further mineral exploration is recommended.

MULHAL ANCIENT MINE

Earhart and Mawad (1970) mapped the area of the Mulhal ancient mine in detail and recommended no further work; according to their interpretation, the gossans and layered rocks of the deposit are part of a synclinal structure and have no tonnage potential. Earhart and Mawad did, however, indicate anomalous gold values. At about the same time, Allcott (written commun., 1970) conducted a geochemical study of the area and suggested that the gold in this and other deposits in the area is associated with barite. Because of the recent rise in gold prices, a mapping and sampling program to evaluate the gold potential of the Mulhal ancient mine area was considered worthwhile, and 5 days were spent in plane-table geologic mapping and sampling.

The mine, which is inaccessible by road, is located in an isolated area in the hills west of Wadi Bidah (fig. 3). Ancient ruins of dwellings are numerous, and grinding wheels scattered about the mine area attest to the probability that gold was one of the commodities recovered by the ancients. Small slag piles indicate that copper and perhaps zinc were also recovered. Kufic inscriptions on rocks in the mine area suggest that the mines were worked at least once after Islam has become well established.

Geology

Most rocks in the Mulhal ancient mine area are pyroclastic, ranging from andesite to dacite; minor basaltic flows and perhaps dikes or sills are also present (fig. 12). Most rocks have been hydrothermally altered and sheared, and identification is difficult. Extensive hydrothermally altered shear zones extend approximately 1.8 km north of the ancient mine and terminate, possibly as a result of faulting, at the southern end of the workings. Many contacts are gradational, and layering is only locally present.

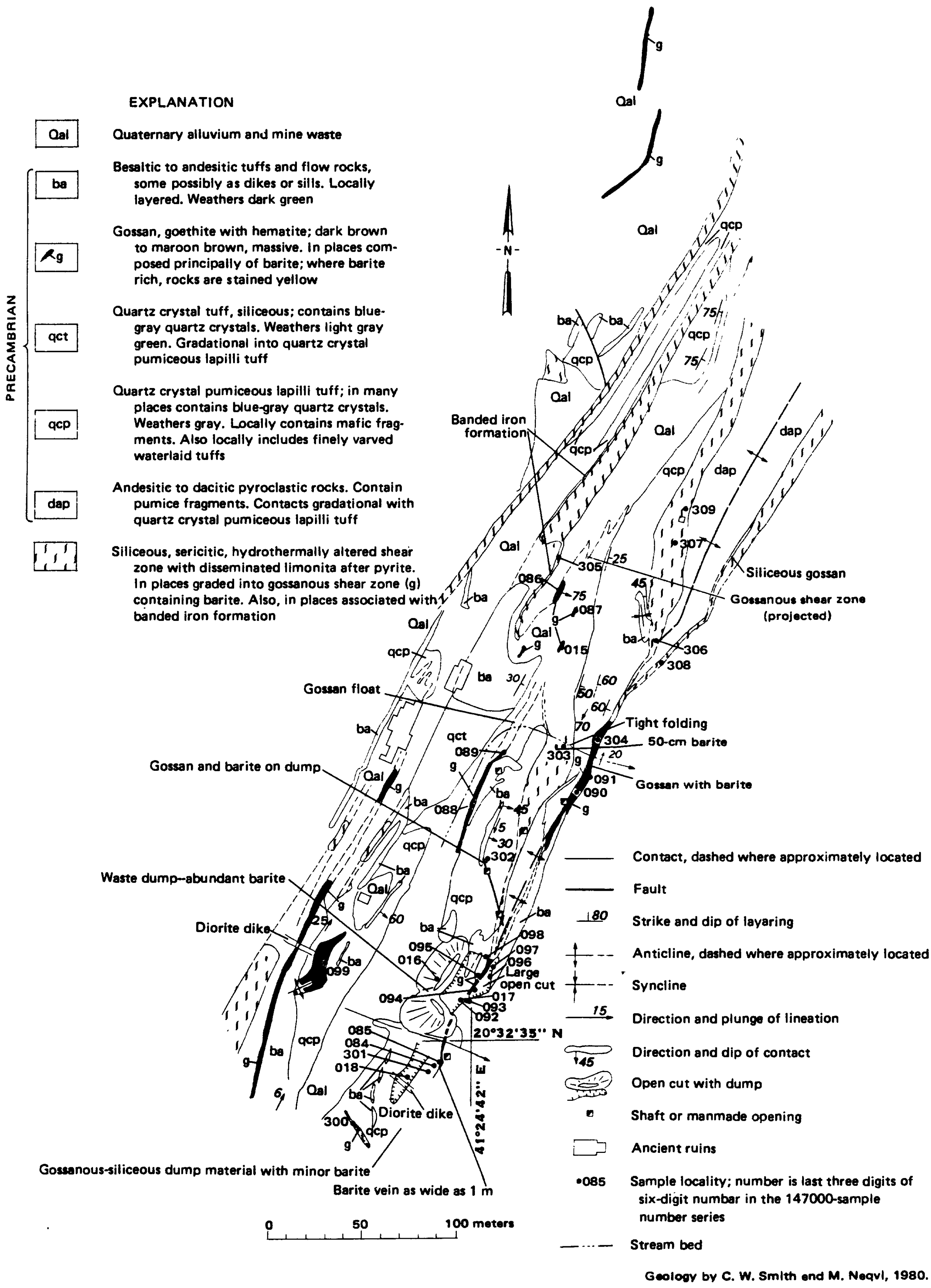

Figure 12.--Geologic map of the Mulhal ancient mine.

Andesitic to dacitic pyroclastic rocks

The andesitic to dacitic pyroclastic rocks are dark gray green and grade into quartz crystal pumice tuff. They are only slightly foliated and weather to a hackly surface texture. They generally contain pumice fragments and in places contain mafic fragments. These rocks were found only in the northeastern corner of the mine area, where they crop out as a thin layer exposed along an anticlinal ridge.

Quartz crystal pumiceous lapilli tuff

This quartz crystal pumiceous lapilli tuff is now quartz-sericite-chlorite schist and contains pumice fragments that have been flattened and smeared along folium planes. Blue-gray quartz crystals are present in many places, and mafic fragments may be observed locally. Finely varved waterlaid tuff is also present locally and grades into pumiceous tuff.

Quartz crystal tuff

Quartz crystal tuff is siliceous and contains blue-gray quartz crystals. It is a well-foliated quartz-sericite-chlorite schist, which, except for the blue quartz crystals, has no particular distinguishing characteristics. It grades laterally into rocks bearing pumice fragments.

Gossan

Siliceous, copper-stained, dark-brown to maroon-brown goethite with hematite gossans are sheared in most places and contain barite. Where barite is abundant, the gossans are stained yellow and yield a sulfurous odor on fresh surfaces. At the southern end of the mine area, gossanous material was observed lying flat between contacts of basalt with pumiceous tuff, and, although no direct measurements of thickness could be made, the gossan is probably no more than 2 m thick. Banded iron formation is locally associated with the gossans.

Basaltic to andesitic tuffs and flow rocks

Although some of the rocks included in the basaltic to andesitic tuffs and flow rocks unit are definitely waterlaid tuffs that locally display fine layering, most rocks of the unit are fine grained and show no internal structure. Much of the basalt appears to be in thin layers overlying the more siliceous rocks, but some may be in the form of dikes or sills. The rocks are locally epidotized, and the presence of amygdules in places suggests that some of the basalts are flow rocks.

Structure

Although rocks in the Mulhal ancient mine area appear to dip generally east, folding is intense and tight folds around north-trending axes have amplitudes of only a few meters. Both north and south plunges are indicated by mineral streaking, and attitudes change within a distance of a few meters. Shearing is the most important structural feature in the area, and large areas of mostly siliceous rocks have been sheared. Gossans have been especially subjected to shearing, and in places baritic gossans grade laterally into sheared siliceous rocks. In many places it impossible to measure attitudes because much of the mine area is covered with alluvium and mine waste, but it is believed that the larger shears flatten and terminate toward the southern end of the mine area.

Economic geology

One large open cut, approximately 30 m long and 7 m deep, and numerous smaller workings were mapped within an area 400 m long and 100 m wide. The workings are concentrated in gossanous zones, usually at contacts with basaltic rock, and they were probably mined for both gold and copper (fig. 12). The gossans are partly layered and partly in faults and shears. This deposit originally formed by volcanic action that precipitated metals, probably on a sea floor. The resulting stratiform deposit and enclosing rocks were then subjected to a period of intense folding, shearing, and hydrothermal alteration in which precious metals and barite may have been leached and redeposited in fractures and shears. This history has resulted in two forms of gossans: stratiform deposits at the contacts between quartz crystal pumiceous tuff and basalt and discordant deposits in shears, faults, and fractures. At one locality in the large open cut, pyrite and barite are exposed in an extremely silicified, almost vertical zone. South of the open cut, an almost vertical barite vein approximately 1 m wide crops out. North of the open cut, two workings are located on a fault that is diagonal to foliation and layering. The presence of both gossanous material and barite in dumps adjacent to the workings indicates that sulfides and barite were remobilized and concentrated in the fracture.

Shears that pass through the mine area are part of a major north-trending fault zone. In most places the shears are moderately silicified and moderately to highly sericitized and contain disseminated limonite after pyrite and a light-green chromium mica. In places the shears merge into gossan and in one place into banded iron formation.

Geochemistry

Thirty samples were collected across gossan, barite, hydrothermally altered shears and veins, and gold, silver, copper, lead, and zinc contents were determined by use of atomic absorption methods (fig. 12, table 4). Gold was present in all samples; values ranged from less than 0.05 to 29.60 ppm, with a mean value of 4.01 ppm. Silver values ranged from less than 0.5 to 112.00 ppm, with a mean value of 16.55 ppm. Mean values for copper, lead, and zinc were 499 ppm, 1,575 ppm, and 409 ppm, respectively. Semiquantitative spectrographic analysis of the 30 samples shows that two samples contained more than 200 ppm arsenic, numerous samples contained more than 5,000 ppm barium, and numerous samples contained between 5 and 30 ppm molybdenum.

Conclusions and recommendations

Results of geochemical sampling indicate that the higher gold and silver values are in barite. Barite apparently is distributed, perhaps unevenly, throughout shear zones because many shear zone samples contained more than 5,000 ppm barium. Petrographic examination of a barite sample from a vein indicated a small amount of galena but no gold or silver.

The Mulhal deposit is polymetallic and the mineral suite includes chalcopyrite, sphalerite, galena, and tetrahedrite, a suite similar to those of numerous deposits in the Arabian Shield. In such deposits, gold and silver are probably the economically important metals and the tonnage potential of the base metals is probably too low for economic consideration. Because of the extensive hydrothermally altered shear systems at these deposits, mineralized shear zones and faults are likely to have more economic potential than the stratiform deposits. The significance of the chromium mica that is distributed throughout the shear zones is not known, but it should be noted that such micas are associated with numerous gold deposits elsewhere in the world. Whitmore and others (1946, p. 1) stated that, "Chrome micas, classed variously as fuchsite, mariposite and chromiferous muscovite, are of wide distribution throughout gold-bearing districts in the Canadian Shield." After a review of information concerning various Canadian gold deposits and related chromium mica occurrences, they concluded that the chromium micas were derived from siliceous magmas rather than from mafic or ultramafic magmas and that the chromium micas are associated with ankerite, quartz, sulfides, and gold in most of the Canadian gold deposits studied. Leo and others (1965, p. 393) observed that quartzite and conglomerate of the Serra de Jacobina gold deposits in Brazil are green because of finely disseminated chromium muscovite. They stated, "Green mica is present in gold-bearing conglomerate layers, but it cannot be stated with certainty that the mica is restricted to such layers.

Table 4.--Trace metal analyses of vein, gossan, and shear zone samples from the Mulhal ancient mine area
[Results in parts per million. All elements by atomic absorption analysis. Leaders indicate not detected]

Sample number	Width (meters)	Gold	Silver	Copper	Lead	Zinc	Remarks
147015	0.50	1.40	3.10	350	695	950	Gossan, maroon brown
147016	--	2.40	37.00	550	4,250	80	Dump sample, siliceous gossan
147017	.30	1.40	23.00	350	870	20	Siliceous with pyrite
147018	--	<0.05	0.40	30	45	25	Quartz vein
147084	.40	.06	5.4	550	280	700	FeO-stained qtz-sericite at contact with basalt
147085	.50	10.24	112.0	135	1,045	150	Barite wth strong oxidized sulfate odor
147086	2.00	2.54	5.0	450	580	800	Gossan, dense, massive, goethite with hematite
147087	3.00	6.60	14.3	650	8.,00	550	Gossan, hematite with goethite, massive
147088	2.00	2.96	13.6	1,150	4,700	600	Gossan, hematite, sparse goethite
147089	2.00	2.54	2.7	1,100	4,000	3,000	FeO-stained shear, quartz-sericite
147090	2.50	4.80	32.2	850	2,450	400	Gossan, massive, goethite with qtz-sericite
147091	2.00	1.88	14.2	550	1,400	200	Siliceous quartz crystal tuff-barite(?)
147092	.20	29.60	18.2	35	430	30	Barite, with yellow oxide, qtz crystal pumiceous tuff
147093	.30	1.50	20.2	90	675	15	Small adit-quartz, FeO, pyrite
147094	.40	1.50	25.2	3,000	2,450	550	FeO-stained quartz-sericite
147095	.40	2.34	1.1	550	850	200	FeO-stained quartz-sericite
147096	.50	3.04	3.4	450	925	350	FeO-stained quartz-sericite, sparse copper stain
147097	1.50	2.68	8.0	1,900	3,050	1,200	Shear zone, maroon FeO with barite(?)
147098	.50	4.00	1.5	155	20	400	Quartz with maroon FeO
147099	4.00	.80	5.2	400	2,250	300	Gossan, maroon-brown
147300	2.50	.22	< .5	20	190	150	Quartz-sericite with FeO stain
147301	4.00	.06	< .5	15	10	350	Sericite with minor quartz
147302	--	7.62	43.0	350	1,850	200	Dump, mostly iron-stained barite
147303	.50	1.88	12.2	205	1,250	300	Gossan, mostly goethite
147304	2.00	4.96	70.0	300	945	25	Gossan, goethitic, siliceous
147305	2.50	4.80	5.5	150	2,900	90	Gossan, goethitic, siliceous
147306	2.00	8.28	4.0	190	335	450	Shear zone with abundant goethite
147307	4.00	1.64	3.0	100	25	15	Siliceous gossan-shear
147308	3.00	6.22	10.3	220	375	130	Shear, maroon FeO, siliceous sinter
147309	3.00	2.42	2.8	125	50	35	Shear, maroon FeO, siliceous sinter
Range*		.06-29.60	<.5-112	15-3000	40-8400	15-3000	
Mean*		4.01	16.55	499	1,575	409	

* Range and mean for gold exclude three samples for which gold not detected.

In other words, the relationship, if any, between gold-uranium mineralization and distribution of chromium muscovite is not known." Boyle (1979, p. 182) indicated that chromium muscovite is a common mineral in the gold-bearing Rand quartz-pebble conglomerates of South Africa. Chen and Lee (1974) reported on fuchsite, a chromium-bearing mica, associated with an ankerite-quartz-sulfide lens in a pelitic schist in Hualien, Taiwan; this ankerite-quartz-pyrite rock contained 2 ppm gold. In a description of gold mineralization of the Mother Lode, California, Lindgren (1932, p. 551) stated, "In serpentine the alteration to a coarse aggregate of ankerite and bright-green chromium mica (mariposite) is characteristic."

The Mulhal deposit is definitely anomalous in gold and silver, and additional studies including detailed geochemistry, self-potential, and electromagnetic surveys should be made to further assess the importance of these metals. Further laboratory studies may also help identify the ore controls and the minerals in which gold and silver occur. In many gold deposits of the world, chromium mica is associated with ankerite, quartz, sulfides, and gold, and petrographic studies may determine similar associations in this deposit.

HYDROTHERMALLY ALTERED SHEAR ZONE EXTENDING NORTH OF THE MULHAL DEPOSIT

An intensely sheared and hydrothermally altered zone extends approximately 1.8 km north of the Mulhal ancient mine (fig. 13). The shear zone is almost vertical and is from a few meters to tens of meters wide. It may be traced over an altitude difference of some 200 m. The shear zone is a continuation of the shear system described at the Mulhal mine and is fairly uniform in composition and texture except for extensive zones of silicification. Within silicified areas, the original schistose and folded structure of rocks has been preserved. In unsilicified areas, the rocks have been completely sericitized and pyritized and contain pods of bright-green chromium mica.

Geochemistry

Atomic absorption analyses of rock-chip samples collected along the entire shear zone are somewhat inconclusive (table 5). A mean gold value of 0.42 ppm and generally low silver, copper, lead, and zinc values indicate that the zone is subeconomic. Higher gold values, in the 2 ppm range, are concentrated in the easternmost part of the shear zone, which leads into the Mulhal mine area.

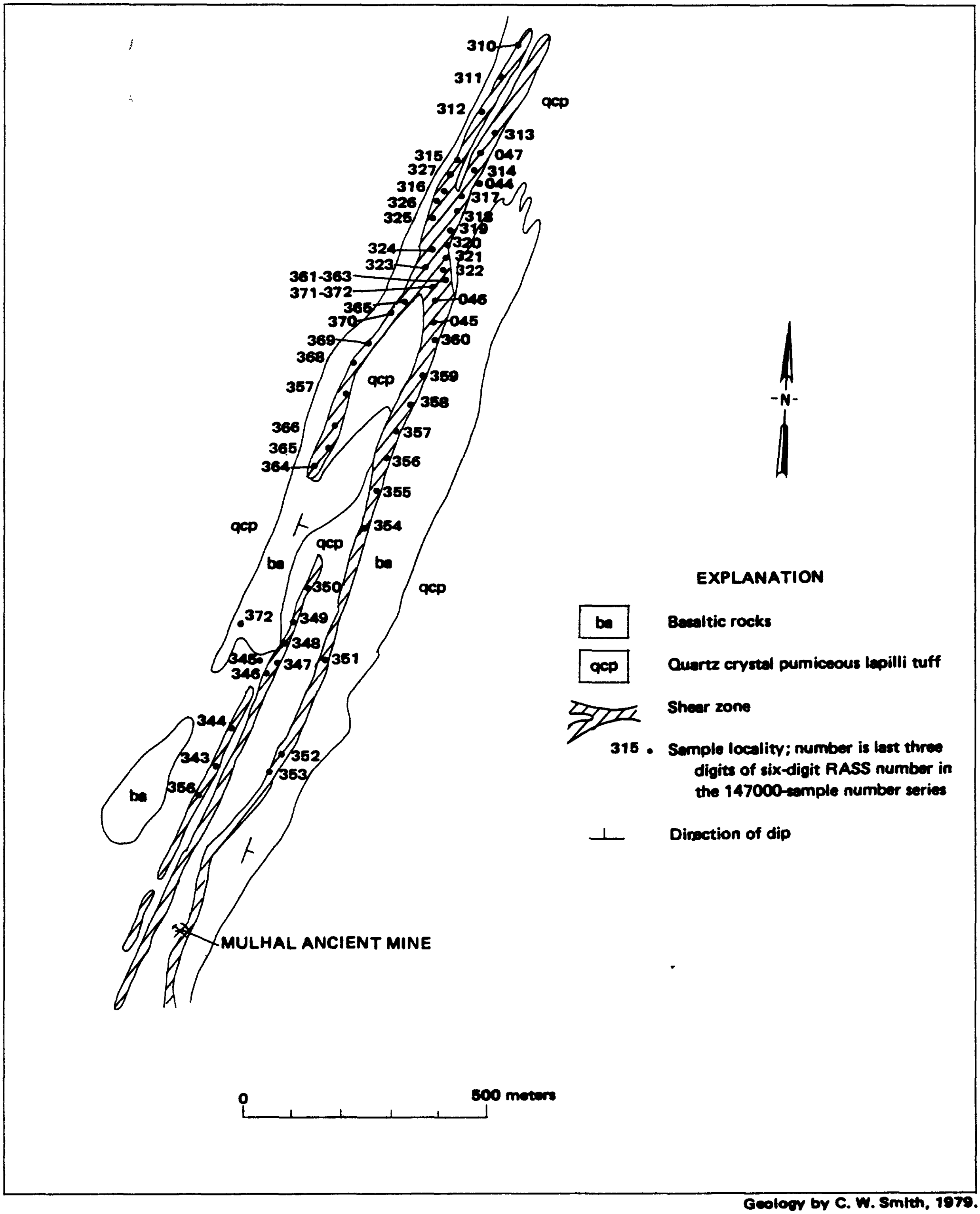

Figure 13.--Geologic map of an area extending north of the Mulhal ancient mine, showing shear zones and sample localities.

Table 5.--Trace metal analyses of rock-chip samples from a hydrothermally altered zone extending 1.8 km north of Mulhal ancient mine

[Results in parts per million. All elements by atomic absorption analysis]

Sample number	Gold	Silver	Copper	Lead	Zinc	Remarks
147043	0.07	<0.5	30	15	30	Chromium mica with brown limonite
147044	.07	1.2	350	40	650	Chromium mica with brown limonite
147045	.07	.7	20	25	250	Siliceous, brown FeO with chrome mica
147046	.36	1.0	40	95	30	Strong quartz-sericite
147047	1.52	1.3	75	45	200	Strong quartz-sericite
147310	.12	< .5	15	<10	70	Quartz-sericite, FeO-stained
147311	.16	1.6	1,200	5	3,500	Shear in mafic rock, FeO-stained
147312	.22	1.0	60	50	1,100	Shear with maroon FeO stain
147313	.22	.7	300	25	450	Quartz-sericite shear
147314	.28	.7	75	25	25	Quartz-sericite with chromium mica
147315	.16	11.2	245	100	550	Quartz-sericite with chromium mica
147316	.90	1.2	130	195	150	Quartz-sericite
147317	.22	1.1	85	20	250	Qtz-sericite shear, 10 m wide, abundant chromium mica
147318	2.14	1.4	10	80	10	Qtz-sericite shear, 10 m wide, abundant chromium mica
147319	.06	.8	15	<10	350	Quartz-sericite, FeO-stained
147320	.16	< .5	10	30	Nil	Quartz-sericite, FeO-stained
147321	.68	.7	25	245	40	Very siliceous
147322	.22	.7	40	135	35	Quartz-sericite, FeO-stained
147323	.28	1.5	35	175	5	Quartz-sericite, with chromium mica
147324	.12	.6	160	35	200	Siliceous shear zone
147325	.16	.7	35	60	5	Strong shear-quartz-sericite, chromium mica
147326	.62	.9	215	55	95	Strong shear-quartz-sericite, chromium mica
147327	.06	.5	40	<10	60	Abundant chromium mica in shear
147343	.76	2.5	120	305	25	Quartz sericite with veinlets of gossan
147344	.06	< .5	30	<10	105	Quartz, chromium mica, sparse FeO
147345	< .05	< .5	10	<10	50	Quartz-sericite
147346	.06	.8	15	15	5	Quartz sericite with abundant chromium mica
147347	.06	.5	15	20	200	Quartz-sericite with chromium mica

Table 5.--Trace metal analyses of rock chip samples from a hydrothermally altered zone extending 1.8 km north of Mulhal ancient mine-Continued

Sample number	Gold	Silver	Copper	Lead	Zinc	Remarks
147348	0.30	0.5	10	20	60	Quartz-sericite with maroon FeO
147349	.40	1.6	20	175	5	Very siliceous shear, 5 m wide
147350	.20	Nil	15	180	5	Very siliceous shear, 5 m wide
147351	2.30	.8	35	20	15	Mostly siliceous zone with chromium mica, 6 m wide
147352	.10	.5	90	10	35	Quartz-sericite with moderate FeO
147353	2.68	3.0	110	355	40	Siliceous, cellular, limonite zone, 5 m wide
147354	2.44	3.7	35	225	20	Very siliceous zone, minor FeO
147355	.10	< .5	10	20	5	Very siliceous zone, minor FeO, intruded by aplite dikes
147356	.66	5.2	65	205	60	Very siliceous zone, 6 m wide
147357	.06	< .5	25	100	35	Shear, quartz-sericite
147358	.50	.6	20	550	20	Zones of nearly 100 percent silica
147359	.72	1.0	50	195	85	Siliceous with goethite stringers
147360	.12	< .5	50	25	25	Sericite with hematite
147361	.06	Nil	10	20	5	Sericite with hematite
147362	.36	< .5	25	30	15	Hematite, silica, goethite, chromium mica
147363	.22	< .5	180	20	55	Siliceous, hematitic
147364	.06	< .5	145	10	95	Siliceous, hematitic
147365	.20	.8	150	100	200	Quartz-chromium mica, with goethite stringers
147366	.10	< .5	30	50	200	Silica 95 percent, with chromium mica
147367	.08	.5	20	10	300	Sericite, chromium mica
147368	.08	< .5	25	10	20	Quartz-sericite with chromium mica
147369	.08	< .5	25	10	80	Siliceous with chromium mica, sparse FeO
147370	.08	< .5	25	10	35	Siliceous with chromium mica, sparse FeO
147371	.20	.6	110	20	55	Siliceous with chromium mica, sparse FeO
147372	.12	1.4	400	60	300	Gossan, siliceous
Range	<.5 - 2.68	<.5-11.2	10-1,200	<10-550	5-3,500	
Mean	0.42	1.09	96	81	193	

Conclusions and recommendations

Results of geochemical sampling demonstrate that most of this sheared and altered zone is subeconomic. However, detailed sampling and mapping in the easternmost part of the shear zone may help delineate subzones containing 2 ppm or more gold. X-ray fluorescence analysis of some samples from the shear zone indicated high barium, rubidium, strontium, zirconium, vanadium, and potassium values. Semiquantitative spectrographic analysis indicated high barium contents for all samples, a molybdenum content between nil and 75 ppm, a strontium content between nil and 700 ppm, no detectable arsenic, and an antimony content between nil and 150 ppm.

RECONNAISSANCE SAMPLING IN HYDROTHERMALLY ALTERED ZONES, NORTHERN WADI BIDAH

Several areas in the vicinity of the Sha'ab at Tare deposit in northern Wadi Bidah (fig. 3) show intense hydrothermal alteration. These areas were sampled in reconnaissance fashion, and one sample (147382, table 6) contained a notable trace metal content of 750 ppm copper. The remainder of the samples had low metal contents (table 6). Semiquantitative spectrographic analysis of the 25 samples collected showed that one (147391) contained 700 ppm arsenic; the remaining 24 samples displayed low values for all 30 elements measured.

JABAL MOHR GOSSAN

The Riofinex Geological Mission (1979) reported that of 14 composite chip samples collected along three traverses across the Jabal Mohr gossan two samples contained 0.11 percent and 0.31 percent copper and no sample contained more than 1.6 ppm gold and 2.2 ppm silver.

A detailed plane-table map of the Jabal Mohr gossan was prepared to provide a more complete picture of the sulfide deposits in the Wadi Bidah district. Ground electromagnetic and self-potential geophysical surveys were performed concurrent with the mapping.

Geology

The Jabal Mohr gossan crops out along a distance of approximately 500 m; either a remnant of the same gossan or part of another is exposed in a limited zone 250 m to the south (fig. 14). The full width of the gossan is not known because of alluvial cover; in some places exposures are as wide as 20 m, and the average width is 12 m. The gossan

Table 6.--Trace metal analyses of reconnaissance samples collected from hydrothermally altered zones, northern Wadi Bidah district

[Results in parts per million. All elements by atomic absorption analysis. Leaders indicate not detected]

Sample number	Gold	Silver	Copper	Lead	Zinc
147374	<0.05	--	5	5	--
147375	< .05	<0.5	15	10	35
147376	.06	< .5	25	10	10
147377	.06	< .5	5	5	--
147378	.06	< .5	15	10	15
147379	.06	< .5	20	10	60
147380	.08	< .5	65	10	10
148381	.06	< .5	35	20	105
147382	.06	< .5	750	20	60
147383	.10	1.0	20	10	10
147384	< .05	.8	--	<10	15
147385	.40	.6	--	<10	20
147386	< .05	< .5	--	10	25
147387	< .05	< .5	--	<10	10
147389	< .05	.5	10	--	20
147390	< .05	1.4	75	<10	500
147391	.12	.5	15	--	15
147432	< .05	1.2	20	25	5
147433	< .05	.8	55	15	5
147434	< .05	< .5	--	--	15
147435	< .05	.8	65	10	10
147436	< .05	< .5	10	10	5
147437	< .05	< .5	135	10	10
147438	< .05	< .5	10	10	10
147439	< .05	< .5	25	10	5

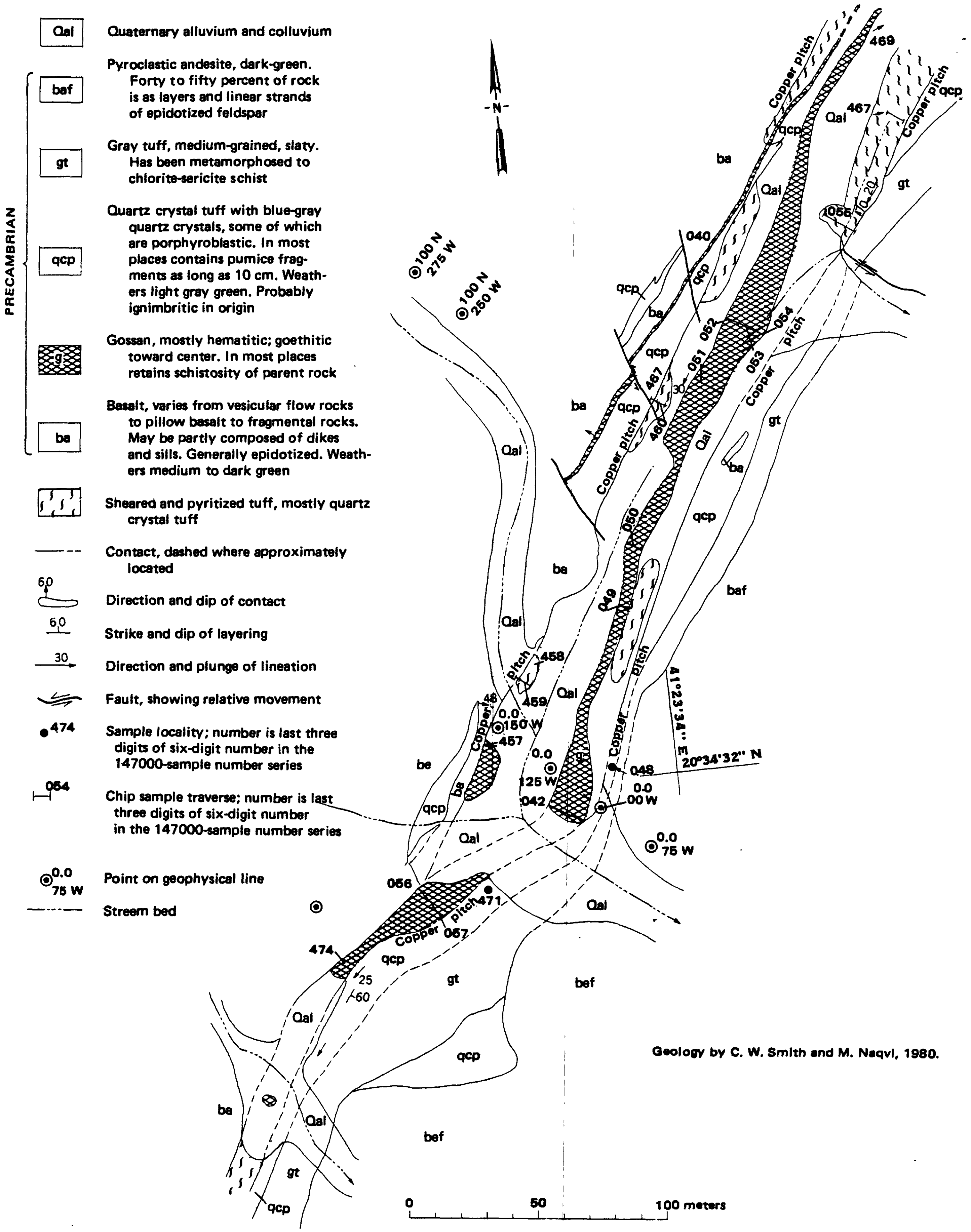

Figure 14.--Geologic map of the Jabal Mohr gossan and table showing geochemical results.

ANALYTICAL DATA

(Results in parts per million)

Sample number	Width (meters)	Au	Ag	Cu	Pb	Zn	Description
147040	10	0.92	3.9	700	3,900	250	Gossan
147042	20	.07	2.1	195	5	95	Gossan, hematitic, siliceous
147048	2	<.05	1.2	2,000	45	850	qcp, stained with copper pitch
147049	3	.17	1.2	115	40	5	Maroon gossan
147050	7	.07	1.3	35	15	5	Massive hematitic gossan
147051	2	.20	3.5	80	90	5	Hematite with goethite
147052	6	.10	2.0	95	55	5	Hematite gossan
147053	6	.07	1.6	105	10	25	Goethitic gossan
147054	5	.07	1.6	105	10	25	Hematite gossan
147055	14	.07	0.2	1,250	15	250	Tuff with moderate disseminated limon-ite
147056	8	.22	2.7	275	55	200	Hematitic, goethitic gossan
147057	7	<.05	2.0	800	45	600	Hematitic, goethitic gossan
147457	3	.16	1.9	50,000	35	65	Siliceous, hematitic gossan with copper pitch
147458	5	.10	1.1	1,000	40	650	Sericitic, hematite-altered tuff
147459	1	.10	1.6	2,650	35	3,500	Mafic tuff
147460	4	.10	1.3	175	355	80	Siliceous hematitic, argillaceous, sericitic tuff
147461	1	0.10	0.6	140	25	600	Sericitized quartz crystal tuff
147467	7	.10	.5	2,450	10	250	Quartz crystal tuff with sparse copper pitch
147469	3	.10	<.5	500	10	5,000	Quartz crystal tuff, chloritic, sericitic, siliceous
147471	1	.06	1.3	2,600	20	4,500	Copper pitch in dacite tuff
147474	0.5	.21	.6	300	30	55	Red-brown limonite

Figure 14.--Continued

appears to be tabular in shape and probably dips steeply east parallel with enclosing rocks. Both field and laboratory studies indicate that the iron oxide content of the gossan is between 70 and 80 percent and that hematite is the predominant iron mineral. Goethite and jarosite are also prominent toward the center of the lens. Much of the gossan retains original schistosity, but local zones contain slump breccias formed by mass removal of iron and other constituents.

The gossan formed through the weathering of a sheared quartz crystal tuff that contained layers of very fine pyrite; the average sulfide content of the tuff was probably about 70 percent. Iron oxide pseudomorphs of no minerals other than pyrite and no recognizable secondary zinc minerals were identified in the gossan. There is minor copper staining in the gossan, but selvages of sheared, iron-stained quartz crystal tuff bear a black or brown-black secondary copper mineral, probably tenorite (CuO). Malachite is present only very locally in the selvages.

A semiparallel gossan, from 1 to 2 m thick, lies on the contact between quartz crystal tuff and basalt. It is similar to the large gossan except that it dips steeply west and exhibits more secondary copper staining.

The structure of the Jabal Mohr area is complex, and rocks immediately west of the gossan are tightly folded, partly as a result of drag folding previous to major shearing on both sides of the gossan. Rocks west of the gossan generally dip west at the northern end, and rocks east of the gossan dip east near the southern end. If the easterly dip of the gossan and enclosing volcanic rocks is not a result of overturned folds, then the rock sequence from oldest to youngest is basalt, quartz crystal tuff, gossan, quartz crystal tuff, gray tuff, and pyroclastic andesite. Mineral streaking in layered rocks enclosing the gossan indicates a southerly plunge ranging from 20° to 30°.

Basalt

Basalt at the western contact of the gossan on the southern end is light olive and locally epidotized. In some areas the rock is a volcanic breccia, and in others it shows pillow structure; however, it is mostly featureless and moderately massive. The structural relationship of the basalt to the more siliceous rocks is complex, and some of the basalt may be sills or dikes.

Gossan

The large gossan is a tabular body enclosed by quartz crystal tuff in the northern part and contained between quartz crystal tuff and basalt in the southern part of the

Table 7.--X-ray fluorescence analyses of gossan samples from Jabal Mohr and Mulhal No. 2
[K_2O and FeO in percent; all other results in parts per million. Leaders indicate not detected]

Sample number	K_2O	FeO	Cu	Zn	Ba	As	Rb	Sr	Y	Zr	Nb	Mo	Pb
JABAL MOHR													
147466	3	26	138	63	27	138	7	25	2	29	3	1	39
147470	6	60	263	41	59	126	17	59	4	37	4	131	91
147157	6	63	196	54	33	195	22	41	2	16	2	5	63
147473	7	42	415	224	33	39	12	161	6	13	3	4	123
147462	0.4	4	24	8	12	14	-	55	2	32	-	4	24
147463	2	26	82	43	15	65	3	31	1	24	1	3	11
147465	2	23	114	39	20	13	6	38	1	27	3	25	22
147490	2	50	85	-	9	38	8	20	2	9	1	8	72
Mean	3.5	37	164	59	26	78	9	53	2	23	2	22	55
MULHAL NO. 2													
147491	-	34	213	36	-	4	4	15	1	4	2	1	30
147477	1	28	189	63	-	31	-	18	2	4	1	1	13
147478	-	17	396	114	3	4	-	7	1	3	1	1	8
147476	1	37	1,095	96	3	-	6	343	3	-	-	2	179
Mean	.5	29	468	77	1	10	2	95	2	3	1	1	57

mapped area. It is not clear if the change in host rock was caused by depositional differences or resulted from later shearing.

Quartz crystal tuff

Quartz crystal tuff encloses the gossan throughout much of the gossan's length. In gossan selvages the tuff is sheared and pyritized to such an extent that only the blue-gray quartz crystals are recognizable. Within the shear zone the tuff is a quartz-sericite schist containing disseminated hematitic psuedomorphs after pyrite. At least part of the tuff contains pumice fragments, and the amount of quartz crystals varies from place to place. Locally the pumice fragments, which have been flattened parallel with schistosity, are aligned in layers and are as long as 10 cm. This rock, which was probably an ignimbrite, is now a quartz-sericite-chlorite schist.

Gray tuff

Gray tuff is in contact with quartz crystal tuff and pyroclastic andesite. It is medium grained and has been chloritized to such an extent that only the ghosts of mineral outlines are present. It is platy and has a gross slaty structure, but layering is not evident. This rock was probably a volcanic ash.

Pyroclastic andesite

The original texture of the pyroclastic andesite has been completely recrystallized. The rock is dark green and fine grained and contains what are probably clasts, smeared out parallel with foliation, of a very light green, epidotized material. The clasts are as long as 10 cm and 5 mm thick. The clasts perhaps originally consisted of feldspathic material and presently compose approximately 40 percent of the rock. The rock is composed of chlorite, epidote, and quartz and represents medium-grade greenschist-facies metamorphism.

Geochemistry

Continuous chip samples were collected across the gossan in several places, and the gossan was also sampled at various points (fig. 14). Atomic absorption assay results are as follows (in ppm):

Number of samples		Gold	Silver	Copper	Lead	Zinc
Range	11	0.03-0.22	0.6-3.5	35-800	10-90	5-600
Mean	11	0.11	1.65	190	32	93

One sample (147457) was not included in the above because it contained an anomalously high amount of secondary copper, assaying 5 percent copper.

Sampling of gossan selvages gave the following results (in ppm):

Number of samples		Gold	Silver	Copper	Lead	Zinc
Range	9	<0.05-0.21	<0.5-1.6	35-2650	10-355	65-5000
Mean	9	.08	1.01	1,418	61	1,742

Values for K_2O, FeO, and 11 other elements are listed in table 7. Especially noteworthy are the mean arsenic and molybdenum values of 78 and 22 ppm, respectively. Results of semiquantitative spectrographic analysis indicate that most gossan samples contained more than 5,000 ppm barium and had a mean molybdenum content of 30 ppm.

One sample was collected from a gossanous outcrop approximately 250 m south of and on strike with the Jabal Mohr gossan. It contained 0.22 ppm gold, 1.1 ppm silver, 160 ppm copper, 30 ppm lead, and 75 ppm zinc.

Conclusions and recommendations

Base and precious metal assay contents of gossan samples from Jabal Mohr are low, and the results are not encouraging. The gossan is probably the oxidized remnant of finely crystallized pyrite that contained only trace amounts of base and precious metals. Gossans at Mulgatah, Gehab, Sha'ab at Tare, and Rabathan have been sampled by the USGS and Riofinex Geological Mission (1970-1979), and all were found to have much higher metal contents than the Jabal Mohr gossan. Although a black secondary copper mineral (tenorite?) may be present in gossan selvages, the copper accumulation probably resulted from oxidation of pyrite that contained very small amounts of base and precious metal.

Notwithstanding the low assay values obtained from gossan sampling, two or three core holes should be drilled for documentation and scientific studies. Comparative data on gossans and underlying sulfide-mineralized rocks would be useful in further exploration within the Wadi Bidah district and in other similar districts. Studies of drill core could provide information concerning genesis, mineral form, and structure of the sulfides, amounts of various metals, and the structure of the enclosing rocks, including contact configurations. In addition, electromagnetic and self-potential ground geophysical surveys have disclosed moderately anomalous zones, which in most of the area correlate with the position of the gossan zone (Flanigan and others, 1982). Drilling could also provide data for a more thorough interpretation of the geophysical responses.

MULHAL NO. 2 GOSSAN

The Mulhal No. 2 gossan (fig. 3, 15) is located on a very steep, isolated hillside. Most outcrops of the gossan are in two places where drainages are incised, and they indicate that the gossan is covered partly by alluvium and partly perhaps by bedrock. The longitudinal section (fig. 15) emphasizes this relationship and suggests that perhaps that the top of a sulfide lens is now being exposed.

Geology

Gossan exposures as wide as 17 m crop out intermittently along a distance of 375 m. The Mulhal No. 2 gossan is composed mainly of hematite, goethite, and jarosite, and it bears some resemblance to the Jabal Mohr gossan, although the former appears more massive and contains a larger proportion of goethite. In places the Mulhal No. 2 gossan is composed of a soft, pulverulent hematite enclosing pods of goethite; it also contains siliceous ribs and patches of jarosite. Collapse breccias formed by the oxidation of sulfides and the removal of iron are locally evident. The enclosing rocks are primarily quartz crystal ignimbritic tuff interlayered with thin basalt-andesite layers. Tuff layers dip very steeply east, and presumably the gossan and related sulfide layers are conformable and have the same attitude. The felsic rocks closely resemble those at Jabal Mohr and are probably ignimbritic in origin. The contacts of the gossan are sheared, as is the case with most sulfide deposits in the Arabian Shield, because of the contrasting competency of sulfide-bearing and tuffaceous rocks. The sheared rock is an iron-stained quartz-sericite schist, which in places contains secondary copper (tenorite?) in a manner similar to the Jabal Mohr gossan selvages. A syntectonic felsic intrusive body is located 1 km west of the gossan, and aplite dikes extending out from the main intrusive body are present in the gossan zone.

Geochemistry

Five continuous chip samples of various lengths were collected across the gossan. Atomic absorption assay results are as follows (in ppm):

	Gold	Silver	Copper	Lead	Zinc
Range	0.03-1.26	2.0-20.0	275-4,000	120-2,000	50-1,450
Mean	0.51	6.54	1,245	720	487

Four additional gossan samples were assayed by use of X-ray fluorescence techniques, and the mean values for copper, lead, and zinc were 468, 57, and 77 ppm, respectively (table 7). These values are from three to ten times less than those obtained by use of atomic absorption analysis. However, an examination of semiquantitative spectrographic analysis results for the same gossan samples assayed by use of atomic absorption analysis indicates that the results for copper, lead, and zinc are in the same general range.

Two samples from the sheared gossan selvages contained 1,600 and 3,000 ppm copper and 250 and 200 ppm zinc. Semiquantitative spectrographic analysis of the five continuous-chip gossan samples indicated more than 5,000 ppm barium and as much as 2,000 ppm strontium.

Mulhal No. 2 gossan--Northern extension

Approximately 1 km north of the Mulhal No. 2 gossan and apparently on strike with it, a gossanous zone is exposed on the steep north wall of a deeply incised, west-trending wadi. The gossanous material is composed of approximately 70 percent hematitic, cubic pseudomorphs after pyrite and very much resembles material from the Jabal Mohr gossan. The gossan is as wide as 15 m at the wadi bottom and is hosted by quartz crystal pumiceous rocks. It appears to be nearly vertical and parallel with the enclosing rocks but was not examined in detail throughout. Analysis of two continuous-chip samples of approximately 15 m length gave the following results (in ppm):

Sample number	Gold	Silver	Copper	Lead	Zinc
147478	0.06	0.5	300	10	20
147479	.06	1.3	400	10	20

Sparse secondary copper oxide (tenorite?) in gossan selvages was noted but not sampled. A copper-stained gossan approxi-

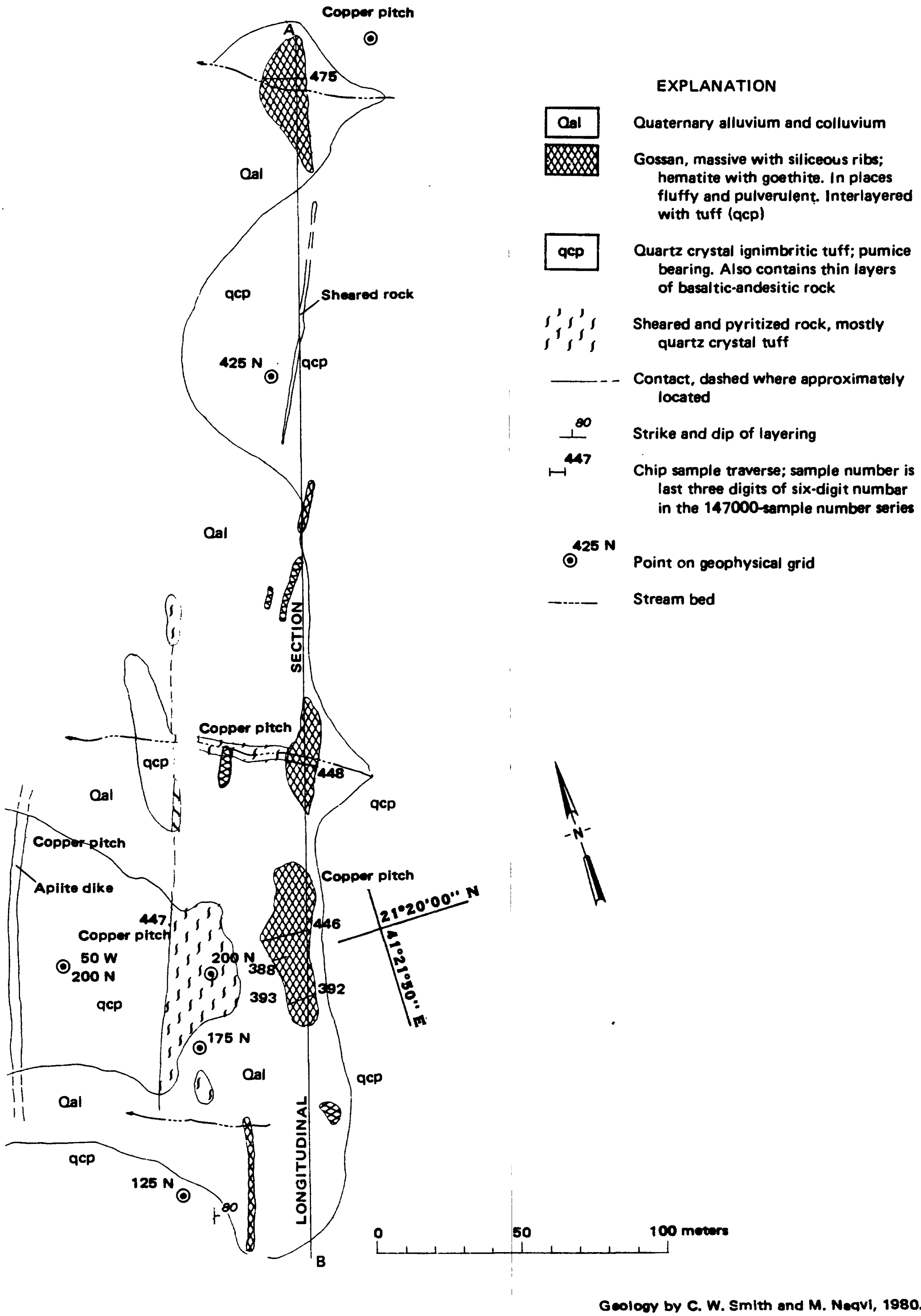

Figure 15.--Geologic map of the Mulhal No. 2 gossan, longitudinal section, and table showing geochemical results.

ANALYTICAL DATA

(Results in parts per million)

Sample number	Width	Au	Ag	Cu	Pb	Zn	Description
147388	6 m	0.16	2.6	650	220	95	Massive, hematitic gossan
147392	8 m	1.26	2.5	275	160	50	Hematitic, goethitic gossan
147393	2 m	.08	2.0	1,600	25	250	Disseminated hematite
147394	40 cm	.08	<0.5	400	35	90	Goethitic gossan, 200 m on strike to south of 147393
147446	17 m	<.05	2.0	750	120	140	Gossan, pulverulent to silicic, with few bands of goethite
147447	-	<.05	.6	3,000	15	200	Copper pitch in pyrite-free tuff
147448	11 m	.88	5.6	550	1,100	700	Soft, fluffy hematite and goethite
147475	15 m	.21	20.0	4,000	2,000	1,450	Siliceous, hematitic, goethitic, jarositic

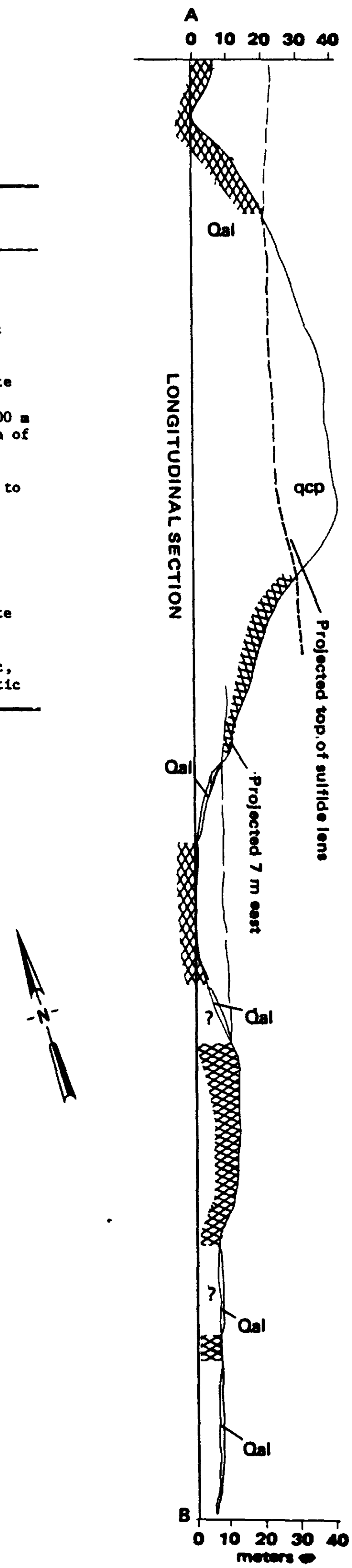

Figure 15.--Continued

mately 1 m thick was found on the south wall of the wadi, although wadi alluvium obscures the intervening rocks. Analysis of this gossan gave the following results:

Sample number	Gold	Silver	Copper	Lead	Zinc
147480	0.06	<0.5	2,300	15	15

Copper staining by both tenorite(?) and malachite was observed in many places in rocks in the general area surrounding both the Mulhal No. 2 gossan and its northern extension. The secondary copper minerals are erratically distributed in small amounts, and some of the staining may be associated with quartz veinlets. Iron staining is not ordinarily present.

Conclusions and recommendations

The Mulhal No. 2 gossan appears to have some potential as a base or precious metal deposit. If the top of a sulfide body is now being exposed by stream cutting, as depicted on the longitudinal section (fig. 15), then it is possible that the sulfide lens continues with depth and contains moderate tonnages of sulfides.

A self-potential geophysical survey across the strike of the gossan conducted at 25-m intervals and with a line spacing of 125 m also indicates a moderate tonnage potential. The survey found a -80 mV anomaly approximately 35 m south of the northern gossan exposure (Flanigan and Sadek, 1983). In addition, a -70 mV anomalous zone continues for 70 m to the north in an area where the gossan is not exposed. To the south, the two exposed gossans are marked by -30 to -40 mV anomalies, and contouring of the data shows a definite linearity coincident with that of the gossan lenses. Flanigan and Sadek (1983) stated that geophysical surveys over the Mulhal No. 2 gossan indicate a sulfide zone approximately 500 m long.

The Mulhal No. 2 gossan does not resemble any of the gossans in the Bilajimah area, approximately 2 km to the southeast, which were mapped, sampled, geophysically surveyed, and drilled as part of the present program and found to contain low amounts of base and precious metals.

Two or three diamond drill holes beneath gossan exposures are warranted for investigation of metal potential. Further detailed mapping should also be done, especially in the area north of Mulhal No. 2 where other gossanous zones are exposed.

ORIGIN OF WADI BIDAH SULFIDE DEPOSITS

Previous studies

Opinion is divided as to the genesis of the sulfide deposits in the Wadi Bidah area. Earhart and Mawad (1970), Jackaman (1972), Kiilsgaard and others (1978), Moore (1978), and the Riofinex Geological Mission (1979) all have suggested that the deposits formed more or less contemporaneously with the enclosing rocks and are generally related to volcanism. However, Greenwood and others (1974, p. 15) stated that "the main copper deposits are replacement bodies in both sedimentary and intrusive host rocks. The recognition of massive sulfide deposits of similar character in intrusive as well as sedimentary rocks makes the hypothesis of a syngenetic origin for Wadi Bidah ores untenable." Roberts and others (1975, p. 40-41) stated that "the deposits are of epigenetic origin and were formed in previously deformed rocks," and that they "formed following a complex sequence of events, including 1) regional folding, 2) development of schistosity, 3) metamorphism, 4) intrusion of quartz porphyry sills, and 5) metallization, took place during two stages: an initial replacement of favorable units (calcareous tuff and propylitized intrusive quartz porphyry) by pyrite and pyrrhotite; and a distinctly later replacement of brecciated pyrite and pyrrhotite following an episode of refolding and shearing, by chalcopyrite, sphalerite, barite and quartz." Subsequently, after sulfur isotope studies of Wadi Bidah drill core, including sulfide minerals from Rabathan, Sha'ab at Tare, and Gehab, Rye and others (1979, p. 138) concluded that "sulfur of this composition could have come either from sea water or deep-seated sources depending on the physical chemistry of ore deposition." These findings support neither syngenetic nor epigenetic theories of sulfide deposition.

Present studies

In an explanation of the complexities of determining the origin of massive sulfide deposits associated with volcanism, R. R. Large (1977, p. 554) stated, "The important factor is that mineralization is coeval with volcanism whether it be epigenetic or syngenetic....In reality there is most probably a complete spectrum of deposits from those that are solely subsurface replacement to those that are complete on-surface deposition." In accordance with this concept, the only criterion for the definition of a volcanogenic sulfide deposit would be a general relationship to volcanism, and this criterion almost certainly applies to all of the Wadi Bidah sulfide deposits.

Large's (1977) classification of deposits as "distal" or "proximal" related to their distance from the volcanic vent.

Deposits such as Rabathan, which are enclosed in tuffaceous sedimentary rocks and carbonaceous and calcareous rocks, are in a distal environment, and deposits such as Gehab, Sha'ab at Tare, Jabal Mohr, Mulhal, and Mulhal No. 2, which are in siliceous pyroclastic rocks, are in a proximal environment. Numerous volcanogenic deposits in Japan are relatively unaffected by folding and metamorphism, and a schematic section by Sato (1970) of a typical volcanogenic sulfide deposit shows a lenticular sulfide mass overlain by and grading laterally into mudstone or felsic tuff, a thin barite bed, and ferruginous chert and underlain by felsic tuff breccia. Although the Wadi Bidah sulfide deposits have been greatly modified by folding and shearing, all of these features can be recognized in various deposits in the district. Another feature of Sato's schematic section is the presence of an intrusive rhyolite dome partly underlying the sulfide lens. Moore (1978) suggested that the rhyolite dome adjacent to the sulfide deposits a few kilometers east of the village of Mahawiyah is such a dome and that it was the heat source driving the geothermal cell that caused rock alteration and redistribution of base metals within the volcanic and sedimentary rocks.

In areas of less extreme folding, such as Bilajimah, sulfide layering may be recognized. In the Bilajimah area, geologic mapping has defined a broadly flexured synclinorium, but all scales of folding ranging down to kink folds are present. The gossans are the oxidized parts of carbonaceous layers that have been impregnated with pyrrhotite and sparse chalcopyrite. They crop out over an area approximately 1 km long and 0.5 km wide and are interlayered with felsic tuffs. The gossan layer at the Mulhal ancient mine appears to have formed in felsic pumiceous tuffs and is capped by andesitic pumiceous tuffs.

Sulfide layers in the Bilajimah area formed in a shallow sea bottom where organic life proliferated. Sulfides in the Mulhal area may also have formed on the sea bottom, but the coarser nature of the tuffaceous rocks suggests they probably formed closer to a volcanic vent. The tabular and conformable shapes of the Jabal Mohr and Mulhal No. 2 gossans, one at the contact between siliceous pumiceous quartz crystal tuff and basalts, some of which have pillow structure, and the other within pumiceous felsic tuffs interlayered with very thin, tabular mafic rocks, suggest that the sulfide layers were deposited on the sea floor in a period of alternating felsic-mafic volcanism. It is believed that most if not all of the sulfide deposits in the Wadi Bidah district are contemporaneous with the enclosing layered rocks.

ACKNOWLEDGMENTS AND DATA STORAGE

All work during the present study was performed as part of an agreement between the USGS and the Saudi Arabian Ministry of Petroleum and Mineral Resources. The work described in this report was done in collaboration with the USGS geophysics section, and the reader is referred to the work of Flanigan and others (1982, 1982) and Flanigan and Sadek (1983) for descriptions of these studies. All analytical results were obtained from the USGS-DGMR chemical laboratory under the direction of K. J. Curry (USGS) by use of atomic absorption analysis and semiquantitative spectrography. Mohammed Naqvi and Rashid Samater were plane-table alidade operators for all of the detailed mapping. Wais Essa Assumali (USGS) helped with detailed plane-table surveying and was responsible for core splitting and bagging all drill-core samples. Ali Mohammed Dualeh, Merdi al Mutari, Ali Mohammed Jabarti, Mir Amjad Hussain, and Wais Essa Assumali (all of USGS) assisted in the rock sampling surveys. Numerous mineral identifications were made in the USGS petrographic laboratories under the direction of J. J. Matzko. G. I. Selner (USGS computer section) assisted with the geochemical statistical studies.

Mineral localities referred to in this report are recorded in the Mineral Occurrence Documentation System (MODS) data bank, and each is identified by a unique five-digit locality number. The following localities were entered into the MODS data bank as a result of this study: Rabathan (MODS 002701), Mulhal No. 2 (MODS 002702), Bilajimah (MODS 002703), and Jabal Mohr (MODS 002827). No MODS entries were deleted.

Each geologic sample is identified by a unique six-digit number, and data for all such samples are recorded in the Rock Analysis Storage System (RASS) data bank. Results of all chemical analyses are stored in data file USGS-DF-03-3.

Inquiries regarding either data bank or the data file may be directed to the Office of the Technical Advisor, Saudi Arabian Deputy Ministry for Mineral Resources, Jiddah.

REFERENCES CITED

Abo-Rashid, A. R., 1971, The geology and mineralization of the Mahawiyah area, Hijaz quadrangle, Kingdom of Saudi Arabia: M.S. thesis, University of London, 106 p.; also, 1971, Saudi Arabian Directorate General of Mineral Resources Open-File Report 428.

Allcott, G. H., 1969, Geochemical investigation of the Ma'dan gold-copper mine, in Mineral resources research, 1967-1968: Saudi Arabian Directorate General of Mineral Resources, p. 40-41.

__________ 1970, Diamond drilling at the Ma'dan ancient mine, in Mineral resources research, 1968-69: Saudi Arabian Directorate General of Mineral Resources, p. 34-39.

Arabian Geophysical and Surveying Company, 1978, Wadi Bidah (geophysical report) May-June 1978: Arabian Geophysical and Surveying Company (ARGAS) 78 ARG 10, 28 p.

Brown, G. F., 1960, Geomorphology of western and central Saudi Arabia: International Geological Congress, 21st, Copenhagen, 1960, Proceedings, sec. 9, p. 150-159.

Brown, G. F., Jackson, R. O., Bogue, R. G., and MacLean, W. H., 1963, Geologic map of the southern Hijaz quadrangle, Kingdom of Saudi Arabia: U.S. Geological Survey Miscellaneous Geologic Investigations Map I-210 A, scale 1:500,000.

Boyle, R. W., 1979, The geochemistry of gold and its deposits: Geological Survey of Canada Bulletin 280, 584 p.

Chen, P. -Y., and Lee, C. W., 1974, Fuchsite in gold-bearing rock from Laochi, Hualien: Acta Geologica Taiwanica, (Science reports of the National Taiwan University), no. 17, p. 7-11.

Davis, W. E., and Allen, R. V., 1965, Geophysical exploration in the southern Hijaz, Saudi Arabia: U.S. Geological Survey Saudi Arabian Project Technical Letter 27, 6 p.; also, 1970, U.S. Geological Survey Open-File Report (IR)SA-27.

Earhart, R. L., and Mawad, M. M., 1970, Geology and mineral evaluation of the Wadi Bidah district, Southern Hijaz quadrangle, Kingdom of Saudi Arabia: U.S. Geological Survey Saudi Arabian Project Report 119, 100 p.; also, 1970, U.S. Geological Survey Open-File Report (IR)SA-119.

Flanigan, V. J., 1970, Geophysical reconnaissance of sites in the Precambrian shield, Kingdom of Saudi Arabia--Pt. 1, Evaluation of an electromagnetic anomaly in the Suk al Khamis area; Pt. 2, Electromagnetic reconnaissance of the Wadi Fig and Mahawiyah areas: U.S. Geological Survey Saudi Arabian Project Report 115, 15 p.; also, 1970, U.S. Geological Survey Open-File Report (IR)SA-115.

Flanigan, V. J., Wynn, J. C., Worl, R. G., and Smith, C. W., 1981, Preliminary report on geophysics ground follow-up of the 1977 airborne survey in the Wadi Bidah district, Kingdom of Saudi Arabia: U.S. Geological Survey Saudi Arabian Mission Technical Record 9 (Interagency Report 348), 54 p.; also, 1982, U.S. Geological Survey Open-File Report 82-202.

Flanigan, V. J., and Sadek, Hamdy, 1982, Ground-followup studies of the 1977 airborne electromagnetic survey in the Assifar and Mulhal areas, Wadi Bidah district, Kingdom of Saudi Arabia: Saudi Arabian Deputy Ministry for Mineral Resources Open-File Report USGS-OF-03-9, 46 p.; also, U.S. Geological Survey Open-File Report 83-367.

Flanigan, V. J., Sadek, Hamdy, and Smith, C. W., 1982, Phase 3 geophysical studies in the Wadi Bidah district, Kingdom of Saudi Arabia: Saudi Arabian Deputy Ministry for Mineral Resources Open-File Report USGS-OF-02-45, 44 p.; also, 1982, U.S. Geological Survey Open-File Report 82-597.

Gonzalez, Louis, 1966, Report on field trip to Wadi Bidah and Ablah areas, Saudi Arabia: U.S. Geological Survey Saudi Arabian Project Technical Letter 85, 9 p.; also, 1970, U.S. Geological Survey Open-File Report (IR)SA-85.

Goldsmith, R., 1971, Mineral resources of the Southern Hijaz quadrangle, Kingdom of Saudi Arabian: Saudi Arabian Directorate General of Mineral Resources Bulletin 5, 62 p.

Greene, R. C., and Gonzalez, L., 1980, Reconnaissance geology of the Wadi Shuqub quadrangle, sheet 20/41 A, Kingdom of Saudi Arabia: Saudi Arabian Directorate General of Mineral Resources Geologic Map GM-54, 15 p., scale 1:100,000.

Greenwood, W. R., 1975, Geology of the Jabal Ibrahim quadrangle, sheet 20/41 C, Kingdom of Saudi Arabia, with a section on Economic geology, by R. G. Worl and W. R. Greenwood: Saudi Arabian Directorate General of Mineral Resources Geologic Map GM-22, 18 p., scale 1:100,000.

Greenwood, W. R., Roberts, R. J., Kiilsgaard, T. H., Puffet, Willard, and Naqvi, I. M., 1974, Massive sulfide deposits in the Wadi Bidah mining district, Kingdom of Saudi Arabia: Arab Conference on Mineral Deposits, 2nd, Jiddah, Conference Documents, Background Papers, Copper, p. 86-89.

Hase, D. H., 1970, Qualitative analysis of airborne magnetometer data--the Arabian Shield, Kingdom of Saudi Arabia: U.S. Geological Survey Saudi Arabian Project Report 110, 44 p.; also, 1970, U.S. Geological Survey Open-File Report (IR)SA-110.

Imai, Hideki, 1978, Geological studies of the mineral deposits of Japan and East Asia: Tokyo, University of Tokyo Press, 392 p.

Jackaman, B., 1972, Genetic and environmental factors controlling the formation of massive sulfide deposits of Wadi Bidah and Wadi Wassat, Saudi Arabia: Saudi Arabian Directorate General of Mineral Resources Technical Record TR-1972-1, 244 p.

Kazzaz, H. H., 1969, Geophysical survey in Wadi Bidah district: Saudi Arabian Directorate General of Mineral Resources Open-File Report 332, 11 p.

Kiilsgaard, T. H., 1981, Geology of areas marked by geophysical anomalies (B-35 and B-34), Wadi Bidah district, Kingdom of Saudi Arabia: Saudi Arabian Deputy Ministry for Mineral Resources Technical Record USGS-TR-01-1, 34 p.; also, 1982, U.S. Geological Survey Open-File Report 82-668.

Kiilsgaard, T. H., Greenwood, W. R., Puffett, W. P., Naqvi, Mohammad, Roberts, R. J., Worl, R. G., Merghelani, Habib, Flanigan, V. J., and Gazzaz, A. R., 1978, Mineral exploration in the Wadi Bidah district, 1971-1976, Kingdom of Saudi Arabia: U.S. Geological Survey Saudi Arabian Project Report 237, 89 p.; also, 1978, U.S. Geological Survey Open-File Report 78-771.

Large, R. R., 1977, Chemical evolution and zonation of massive sulfide deposits in volcanic terrains: Economic Geology, v. 72, no. 4, p. 549-572.

Larken, T. P., 1936, Jabal al Azhar (ancient workings): Saudi Arabian Directorate General of Mineral Resources Open-File Report 6, 8 p.

Leo, G. W., Rose, H. J., Jr., and Ware, J. J., 1965, Chromium muscovite from the Sierra de Jacobina, Bahia, Brazil: American Mineralogist, v. 50, p. 392-402.

Lindgren, Waldemar, 1933, Mineral deposits (4th ed.): New York, McGraw-Hill, 930 p.

MacLean, W. H., 1957, Al Mindahah and Al Mahawiyah (ancient workings): Saudi Arabian Directorate General for Mineral Resources Open-File Report 73, 2 p.

Mawad, M. M., 1980, Evaluation of the Wadi Mandahah ancient mine, Kingdom of Saudi Arabia, with a section on a Geophysical survey, by H. M. Merghelani: U.S. Geological Survey Saudi Arabian Project Report 274, 31 p.; also, 1980, U.S. Geological Survey Open-File Report 80-1262.

Metz, K., Ertl, V., Fehleissen, F., Litscher, H., and Petschnigg, H., 1971, The geology of the Aqiq-Ablah and Wadi Bidah-Mahawiyah area: Saudi Arabian Directorate General of Mineral Resources Technical Record TR-1971-2, 60 p.

Moore, J. McM., 1978, Volcanogenic mineralization and a rhyolite dome in the Arabian Shield: Mineralium Deposita, v. 13, p. 123-129.

Riofinex Geological Mission, 1979, An assessment of the mineral potential of part of the Wadi Bidah district: Riofinex Geological Mission (Saudi Arabia) Report RF-1979-1, 48 p.

Roberts, R. J., 1976, The genesis of disseminated and massive sulfide deposits in Saudi Arabia: U.S. Geological Survey Saudi Arabian Mission Project Report 207, 54 p.; also, 1976, U.S. Geological Survey Open-File Report 76-602.

Roberts, R. J., Greenwood, W. R., Worl, R. G., Dodge, F. C. W., and Kiilsgaard, T. H., 1975, Mineral deposits in western Saudi Arabia: U.S. Geological Survey Saudi Arabian Mission Project Report 201, 60 p.; also, 1975, U.S. Geological Survey Open-File Report 75-654.

Rye, R. O., Roberts, R. J., and Mawad, M. M., 1979, Preliminary sulfur isotope investigations of mineral deposits in the Precambrian shield, Kingdom of Saudi Arabia, in Evolution and mineralization of the Arabian-Nubian Shield: King Abdulaziz University, Institute of Applied Geology Bulletin 3, v. 1: Oxford-New York, Pergamon Press, p. 131-140.

Sato, Takeo, 1970, Geology and ore deposits of the Hokuroko district: International Mineralogical Association, International Association on the genesis of ore deposits, 7th general meeting, Tokyo-Kyoto, 1970, Guidebook 3, Excursion A3, p. 4.

Saxby, J. D., 1976, The significance of organic matter in ore genesis, in Wolf, K. H., ed., Handbook of strata-bound and stratiform ore deposits, v. 2, Geochemical studies: Amsterdam, Elsevier, p. 111-133.

Smith, C. W., 1963a, Geologic reconnaissance of the Mahawiyah-Mashuka area: Saudi Arabian Directorate General of Mineral Resources Open-File Report 212, 6 p.

__________ 1963b, Geologic report of Mindaha mine: Saudi Arabian Directorate General of Mineral Resources Open-File Report 218, 3 p.

__________ 1964a, Geologic report, Mulha area (Mulha Mehaid): Saudi Arabian Directorate General of Mineral Resources Open-File Report 244, 3 p.

__________ 1964b, Geologic report, Mahawiyah-Mashuka area: Saudi Arabian Directorate General of Mineral Resources Open-File Report 245, 5 p.

Strauss, G. K., Madel, J., and Alonso, F. F., 1977, Exploration practice for strata-bound volcanogenic sulfide deposits in the Spanish-Portuguese pyrite belt: Geology, geophysics and geochemistry, in Klemm, D. D., and Schneider, H. J., eds., Time and strata-bound ore deposits: New York, Springer-Verlag, p. 55-93.

Trent, V. A., and Sultan, G. H., 1966, A geologic and mineral reconnaissance of the Ablah formation and the Kamden anomaly, south Aqiq area, Saudi Arabia: U.S. Geological Survey Saudi Arabian Project Technical Letter 64, 16 p.; also, 1968, U.S. Geological Survey Open-File Report (IR)SA-64.

Whitmore, D. R. E., Berry, L. G., and Hawley, J. E., 1946, Chrome micas: American Mineralogist, v. 31, p. 1-21.

Worl, R. G., 1977, Evaluation of the Umm al Khabath copper prospect, Jabal Ibrahim quadrangle, sheet 20/41 C, Kingdom of Saudi Arabia, with a section on Geophysical investigations, by V. J. Flanigan and H. M. Merghelani: U.S. Geological Survey Saudi Arabian Project Report 213, 42 p.; also, 1978, U.S. Geological Survey Open-File Report 78-521.

Worl, R. G., and Wynn, J. C., 1982, Preliminary exploration report and drilling proposal for the Wadi al Khadra prospect, Wadi Bidah district, Kingdom of Saudi Arabia: Saudi Arabian Deputy Ministry for Mineral Resources Open-File Report USGS-OF-02-9, 18 p.

Wynn, J. C., and Blank, H. R., 1979, A preliminary assessment of the 1977 INPUT survey on the Arabian Shield, Kingdom of Saudi Arabia, with guides for interpretation and ground follow-up: U.S. Geological Survey Saudi Arabian Project Report 268, 32 p.; also, 1979, U.S. Geological Survey Open-File Report 79-1508.